Chair of Reservoir Engineering

Master Thesis

Mature Field Redevelopment: A Case Study of El Badr Oil Field

In
Cooperation
With
OMV Tunisia

In Partial Fulfilment
of the Requirements
for the Degree of
Master of Petroleum Engineering
The Montan University of Leoben, Austria
October, 2016

Written by:

Hichem Fakhfakh, Bsc
1435702

Advisors:

Univ. Prof.Dr. Holger Ott
D.I. Hela Hamdi

EIDESSTATTLICHE ERKLÄRUNG

Ich erkläre an Eides statt, dass ich die vorliegende Diplomarbeit selbständing und ohne fremde Hilfe verfasst, andere als die angegebenen Quellen und Hilfsmittel nicht benutzt und die benutzten Quellen wörtlich und inhaltlich entnommenen Stellen als solche erkenntlich gemacht habe.

AFFIDAVIT

I hereby declare that the content of this work is my own composition and has not been submitted for any higher degree. All extracts have been distinguished using quoted references and all information sources have been acknowledged.

_____ _____

Date Signature

Acknowledgment

I wish to express my sincere appreciation to Prof. Holger Ott and Dr. Siroos Azizmohammadi for their guidance, suggestions and patience. I would like to express special thanks to D.I. Hela Hamdi and D.I. Maher Chraief particularly and to all the Petroleum Engineering Department in OMV Tunisia for their guidance and help in every aspect of this thesis. I wish to acknowledge the moral and technical support of Kappa Engineering Softwares and Prof. Tom A. Blasingame.

I would like to express my deep indebtedness to OMV, without whose support this thesis would have not been possible, especially university network team in Vienna and Mr. Achraf Habachi in Tunisia who provided every possible mean to carry out this study. I am also indebted to my mentor Dr. Wolfgang Posch who shared a lot of knowledge with me.

Special thanks to my fellow students for their friendship and moral support during my Master studies.

I wanted to acknowledge the benefit of studying at the department of Petroleum Engineering at Montan University of Leoben and to thank all the teachers and stuff for providing a truly academic and professional environment.

In the end, I would like express my deep indebtedness and sincere appreciation to my family for their patience, encouragement and moral support.

Kurzfassung

Diese Arbeit beschreibt eine Feldstudie über das El-Badr Öl-Feld, welches sich in Tunesien befindet. Das Verknüpfen der Daten des Petrophysikalischen- und des Lagerstättenverhaltens, sowie der Hintergrundgeschichte des Öl-Feldes, führten zu einem besseren Verständnis und einer Verminderung der technischen Unklarheiten

Durch eine Produktionsanalyse konnte der individuelle Einzugsradius ermittelt werden, um in Folge das Öl vor Ort, pro Quelle, zu ermitteln, sowie um die Lagerstätteneigenschaften wiederzugeben und die Reserven unter aktuellen Bedingungen einzuschätzen.

Mithilfe von diagnostischen Wasser-Öl-Verhältnis Diagrammen wurde der Wasserursprung evaluiert. In Verbindung mit Lagerstättentests und der Schichteigenschaften wurden die verbleibenden Reserven und das Lagerstättenverhalten auf Schichtbasis berechnet. Vorschläge zu Lagerstättenmanagement werden im Detail diskutiert.

Die Ölmengen wurden durch die totale gemessene Produktion zugewiesen. Diese Annäherungen sind druckbasierend und verwenden verschiedene Zuweisungsmethoden um die individuellen Lagerstättenmengen auf Tagesbasis zu bestimmen.
Schlussendlich geben wir Empfehlungen für zukünftige Aktivitäten in Lagerstättenmanagement und Entwicklung.

Abstract

This thesis describes a field study performed on El-Badr oil field located in southern Tunisia. We incorporated petrophysical and reservoir performance data along with well history to better understand and reduce technical uncertainty.

We used production analysis to estimate individual well drainage radius, in order to estimate oil in place per well, replicate reservoir properties and estimate reserves under current conditions.

We evaluated water origin using water oil ratio diagnostic plots. In conjunction with well tests and layers properties, we evaluated the remaining reserves and reservoir performance potential on layer basis. Suggestions for reservoir management are discussed in detail.

We reallocated oil rates within the wells from total measured production. Our approach is pressure based and uses different allocation methods to determine individual well rates on daily basis.

Finally, we give recommendations for future activities in reservoir management and development.

List of Tables

List of Figures

Abbreviations

STOOIP	Stock Tank Originally Oil in Place
STOIP	Stock Tank Oil in Place
EUR	Expected Ultimate Recovery
CPF	Central Processing Facility
IPR	Inflow Performance Relationship
VLP	Vertical Lift Performance
PI	Productivity Index
SSD	Sliding Sleeve Door
PLT	Production Logging Tool
PVT	Pressure Volume Temperature
MDT	Modular Dynamic Tool
ICD/ICV	Inflow Control Devices/ Inflow Control Valves

Table of Contents

1 Introduction

Low oil prices have made efforts to invest in exploration cost prohibitive. Currently, most oil companies are tackling challenges to develop mature fields. Undoubtedly, these fields require lower investment costs as most of them are onshore. Likewise, the discovery rate of new fields is getting lower and lower from year to year which obviously steered the endeavors to seek more reserves from existing fields.

Several methods exist to develop a mature field, however a solid investigation of opportunities must be determined. The first step consists of reducing technical uncertainty with a thorough characterization of the situation, then identify the best solution that can increase reserves and accelerate production. For a mature field, the reservoir management and redevelopment strategies are mainly depending on the field reserves assessment and well performance estimation.

Material balance and simulation can be difficult to apply to a layered reservoir because the depletion rate may be different in each layer. Furthermore, well shut in pressure may not equalize to reservoir pressure in short time which makes this methods more challenging. Large pressure gradient are likely to take place in multilayered reservoirs. This renders the prediction of inflow performance difficult if there is cross flow between layers in the wellbore [1].

Reservoir management practices to develop mature oil fields may include data acquisition and analysis campaigns to evaluate the remaining reserves, reevaluating wells completion and clustered analysis of the wells based on their performances [2]. Therefore, wells production rates constitute the most available data throughout the reservoir life. Additionally, the increase in electronic measurements has made the flowing pressure as readily available as flow rates. Coupled with advances in the science of production data analysis in recent years, Production rates and bottom hole flowing pressures enabled more advanced analysis accompanied with more reliable and detailed results [3].

In this thesis, diagnostic procedures are presented where production data are either plotted on simple production charts or advanced type curves to obtain results such fluid in place, Expected Ultimate Recovery (EUR), drainage area and reservoir properties similar to those inferred from pressure transient analysis like permeability and skin. We extended the production data analysis to back allocate production rates. Rate back

allocation refers to us as determining individual flow rates from each well or layer from commingled production system. Two allocation algorithms along with the pressure based rate estimation of rates are used in order to determine a more suitable allocation procedure for the field.

2 El Badr Field Overview

El Badr field is an onshore field located in southern Tunisia within Cherouq concession as shown in Figure 1. The structure was discovered by the drilling of EBR-1 in 2007 and appraised through the drilling of EBR-2 in 2008. The field was developed and initially operated by Pioneer natural resources Tunisia. In 2011, the field was acquired by OMV and hence the operatorship.

EL Badr structure is the largest structure in Cherouq A concession with oil in place of about 59 MMSTB as P50 volumetric calculations.

Although, the field was producing for long time with respect to other fields in, it still has the most remaining reserves in the concession amongst the others. Therefore a proper reservoir management of the wells in this structure may keep the life of the concession for longer time.

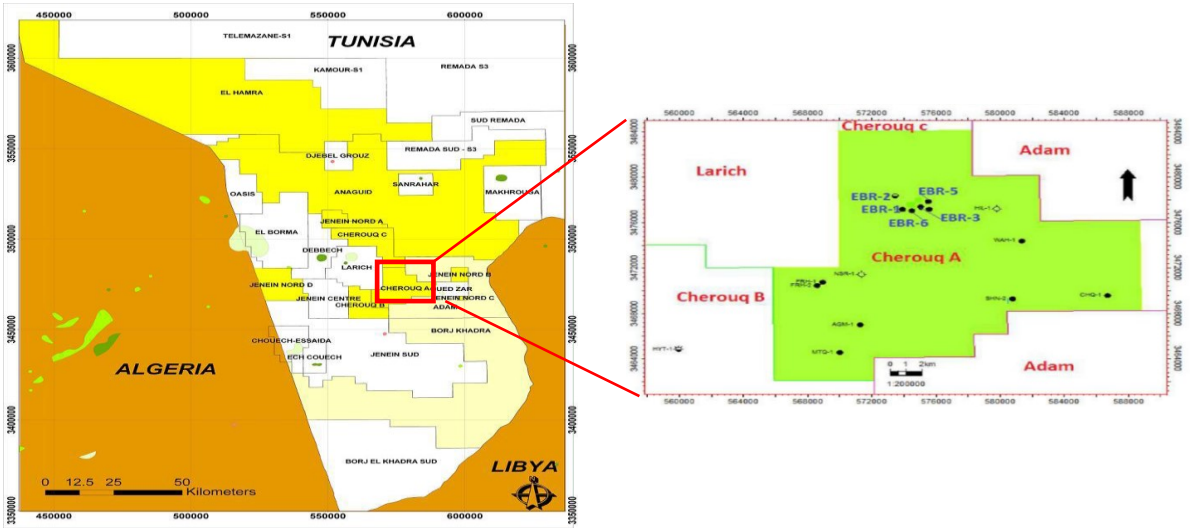

Figure 1: EL Badr Field Location

2.1 Petroleum System Glimpse

El Badr field is located in Ghadames basin (Figure 2). This system is characterized by S-N progradational geometry. The marine shales of the Silurian Tannezuft are rich in organic matter. Particularly, the “Hot Shale” unit at the base of the Silurian constitutes one of the main source rock for the basin and it is found to have sourced the Silurian Tannezuft/ Acacus reservoir under study [4].

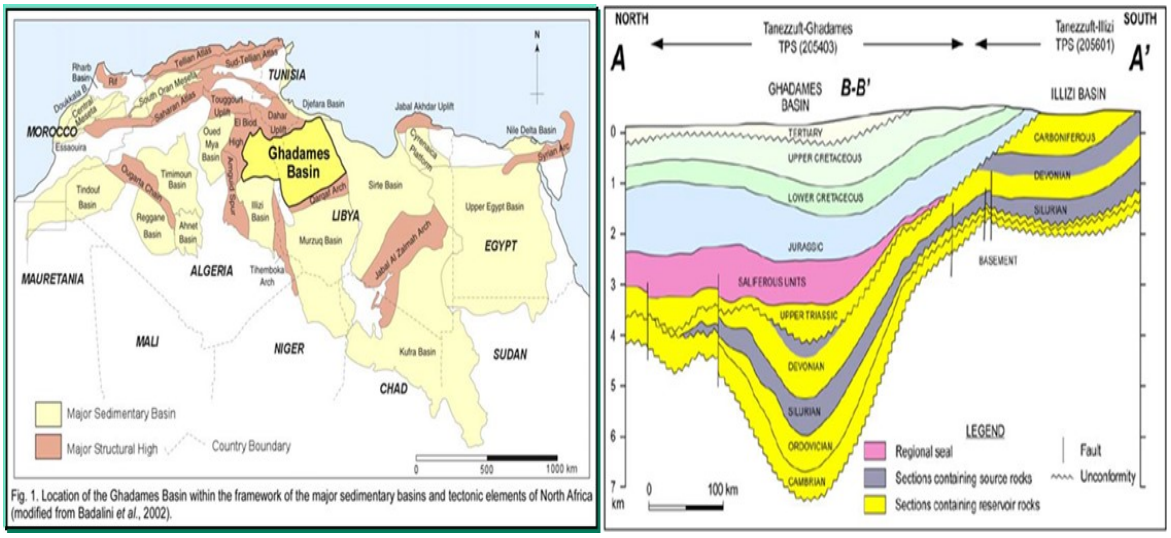

Fig. 1. Location of the Ghadames Basin within the framework of the major sedimentary basins and tectonic elements of North Africa (modified from Badalini *et al.*, 2002).

Figure 2: Ghadames basin Location

The prograding condition during Silurian resulted in a gradual increase to the basin and deposition intercalation of thin sand layers at the Tannezuft. The T-sands (i.e. Tannezuft sands) have been found to be hydrocarbon bearings within the most drilled wells. These layers precede the Acacus marine step positional system. Where productive, the lower Acacus sandstones are typically low resistivity pay sands.

2.2 Petrophysical Properties

Rock properties depend on rock materials basically. Usually in conventional reservoirs, these material can be either sandstones (consolidated or unconsolidated) or limestones (sometimes fractured).
In El Badr field, Acacus and Tannezuft sandstones constitutes the reservoir rock interbedded with shale layers. The latter is considered completely tight, hence, there is no crossflow between productive layers in reservoir. The Figure 3 below represents a cross section Acacus sand reservoir and their fluid distribution accordingly.

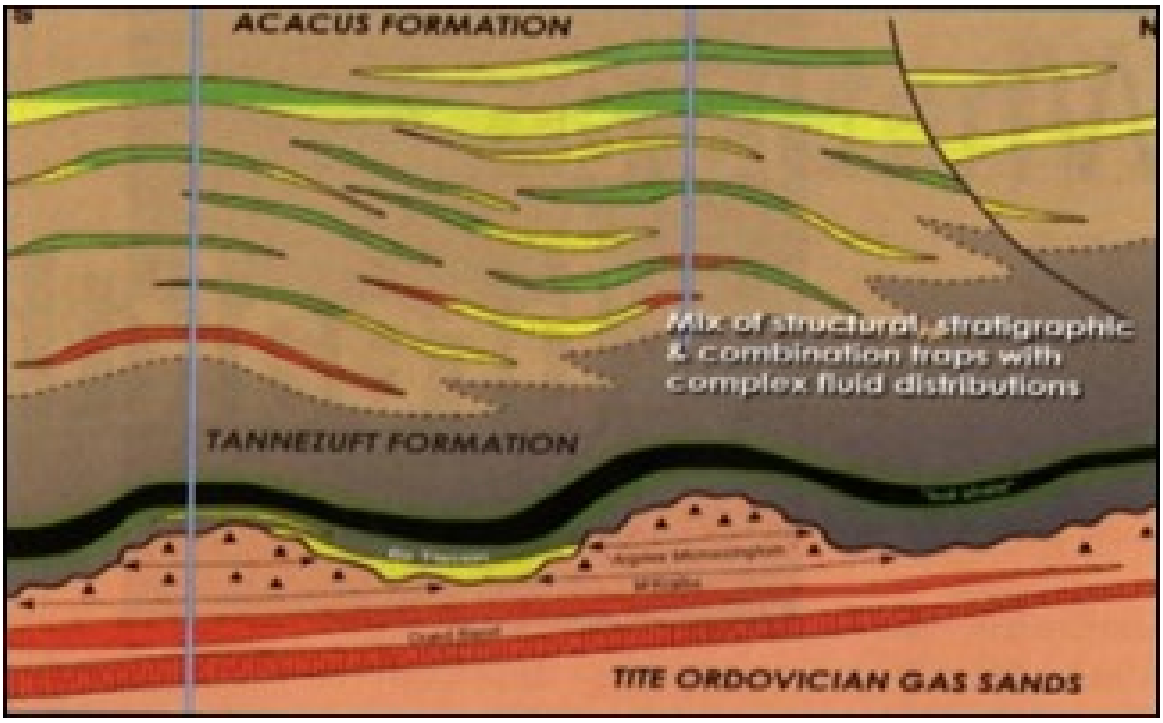

Figure 3: Acacus/ Tannezuft Reservoirs [4]

Rock properties are estimated based on logs of each well and checked with core data taken from EBR-2 (dry well). Due to the presence of chlorite coating around the quartz grains, petrophysical analysis are deemed to be effected by these sandstone mineralogical constituents responsible for abnormal low resistivity readings in the pay zones.

Yet, logs remain the main source for estimating rock properties such layer porosity, permeability and initial water saturation.

Figure 4 shows the calculated oil in place per layer in each well based on the following volumetric formula:

$$\frac{N}{A} = \frac{7758 * h * \Phi * (1 - Sw)}{Bo} \text{ [STB/Acres]} \qquad (1)$$

In equation (22): N=Stock tank oil in place A= area in acres; h=average net thickness in feet; Φ=porosity, fraction; Sw=water saturation, fraction; and

Bo= formation volume factor (FVF) in RB/STB.

The results shown in Figure 4 represent the oil in place distribution between the wells. EBR-1, EBR-3 and EBR-5 illustrates more connected hydrocarbons than EBR-4 and EBR-6.

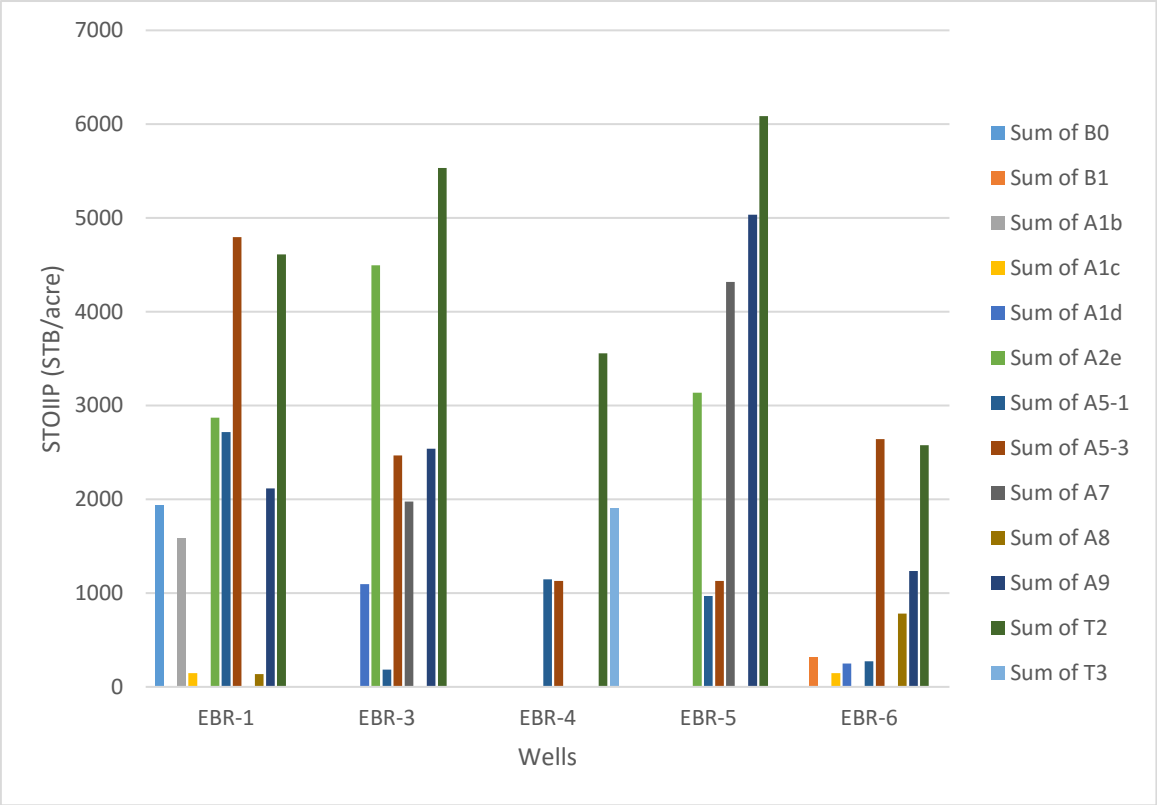

Figure 4. Oil in Place per layer in each well

2.3 Fluid Properties

Fluid samples are taken from the T2 zone at separator level in EBR-1. And subsequent laboratory analysis was carried out on these samples. It should be noted that there is limited amount of PVT data in multilayered reservoir. We believe that no compositional or compartmentalization exist because on the one hand, most of the wells showed small pay zone intervals and on the other hand fluid properties determined from production test do not show significant variance in terms of oil gravity, temperature and gas gravity.

Similarly to rock and completion data, fundamental fluid properties must be entered into the program[1] for estimation of fluid in place, drainage area, permeability and skin factor. Therefore, the PVT report will be used as basis to develop correlations of oil properties.
Plots of the solution gas oil ratio, oil formation volume factor, oil density, oil viscosity and single phase oil compressibility are shown in Figure 5 to

[1] Topaze: A Kappa Engineering Software

Figure 9. These properties were tuned using Glaso-volatile oil correlation while viscosity was tuned using Beggs and Brill correlation.

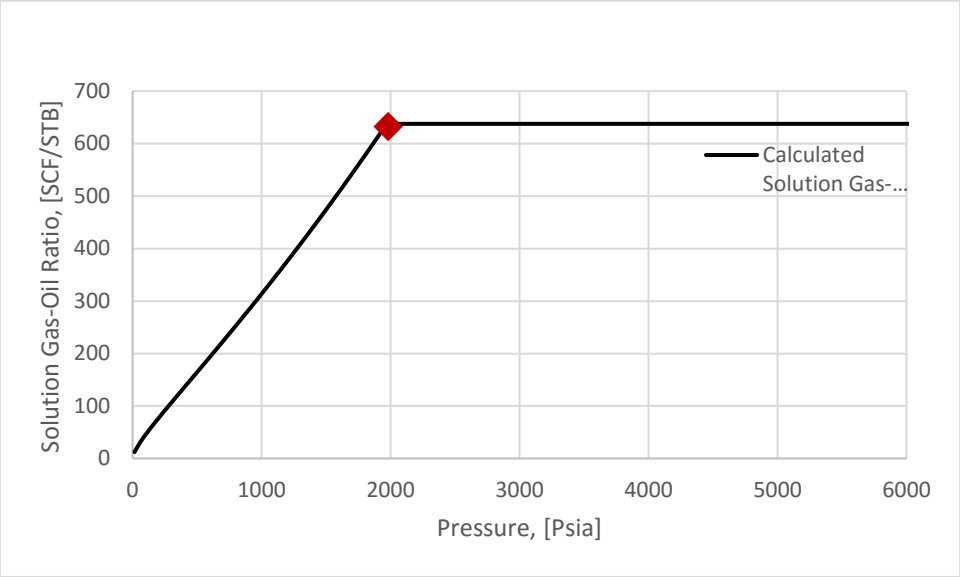

Figure 5: Solution Gas-Oil Ratio

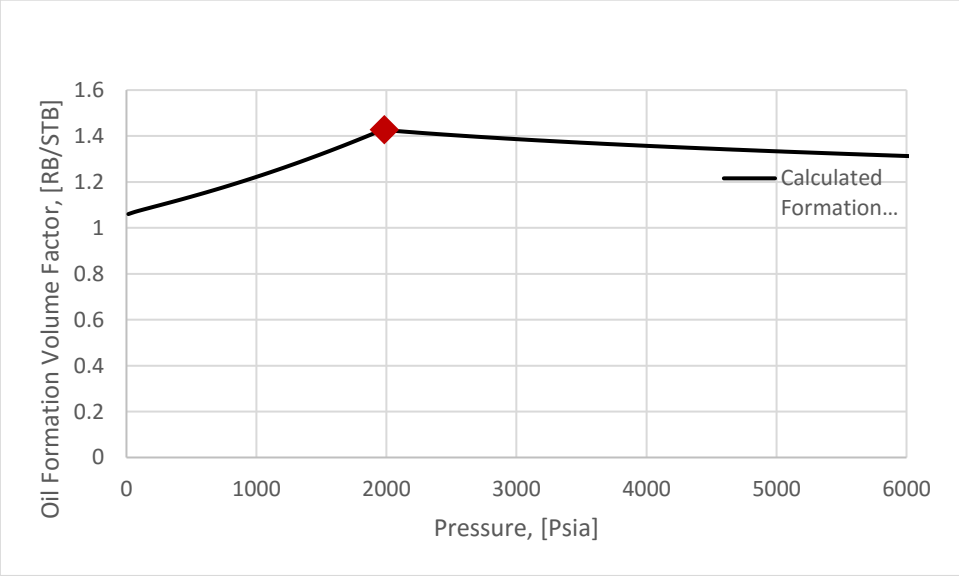

Figure 6. Oil Formation Volume Factor

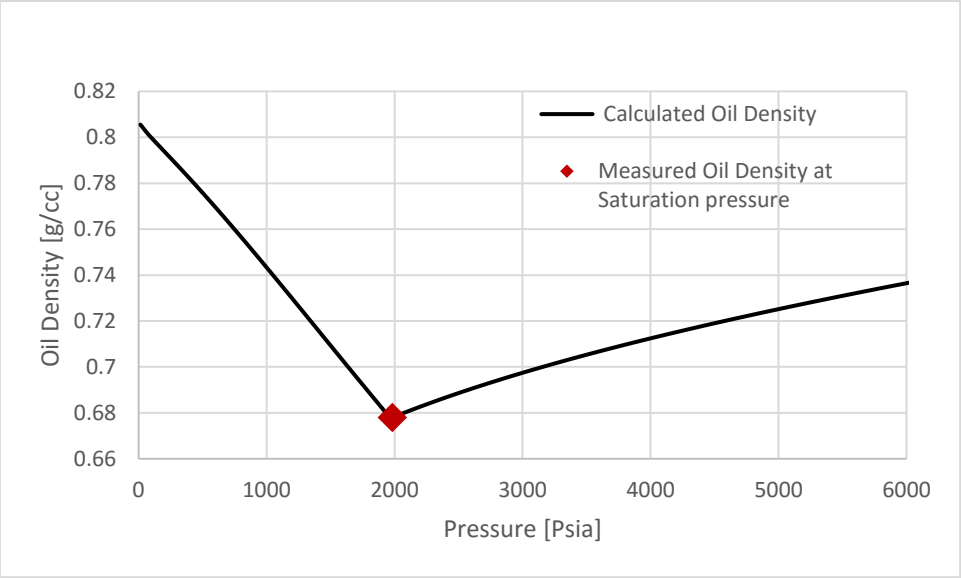

Figure 7: Oil Density

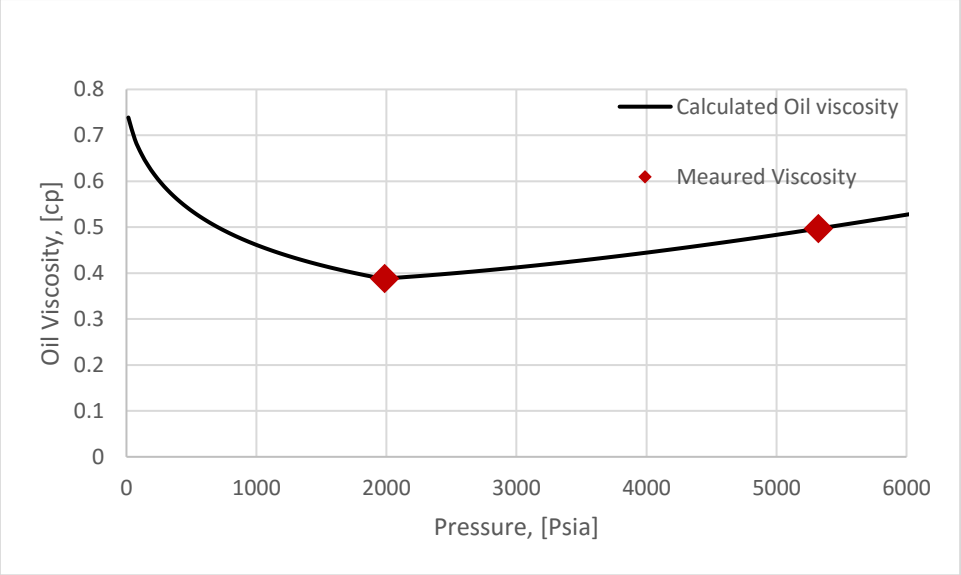

Figure 8. Oil viscosity

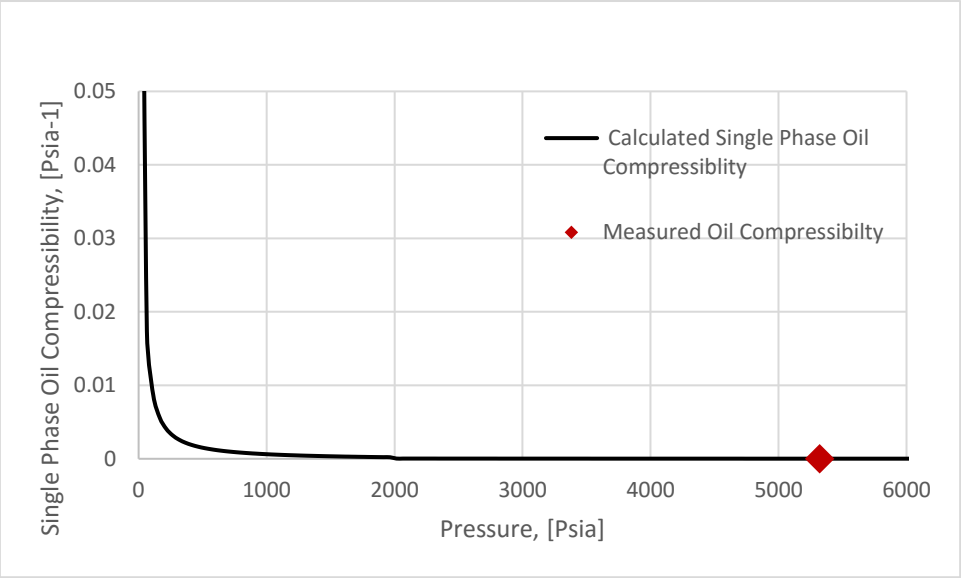

Figure 9. Single Phase Oil Compressibility

The following table presents the laboratory measured data used for regression.

Table 1. Measured Fluid Properties

Reservoir Pressure	5322 psia
Reservoir Temperature	212°F
Reservoir Bubble Pressure	1983.7 psia
Formation Volume Factor at Bubble point	1.427 RB/STB
Oil Viscosity at Reservoir Pressure	0.497 cp
Oil Viscosity at Bubble Point	0.388 cp
Oil Density at Bubble Point	0.678 g/cc
Oil compressibility at Reservoir Pressure	1.279E-5

2.4 RESERVOIR PERFORMANCE

First production from El Badr field was recorded from a single well EBR-1 in January 2008 with an oil rate of 2500 STB/D. In July 2010, EBR-3 was added as a development well and lately EBR-4 and EBR-5 started contributing in February and March 2011. The last development well drilled in the structure was EBR-6 in July 2013. The daily production reached a peak in 2011 about 4700 STB/D.

The daily production from all El Badr wells is gathered near the wells and transported through common pipeline along 7 km to Waha Central Processing Facility (CPF) where it is eventually handled as illustrated in Figure 10. This current schematic of field production facilities makes the counting of hydrocarbon production from each well of the field a challenging exercise because what is measured at Waha CPF is the field

total production. From here comes the need for applying a proper production allocation method in order to get an accurate aggregation of the field production reflecting the real performance of each in the field.

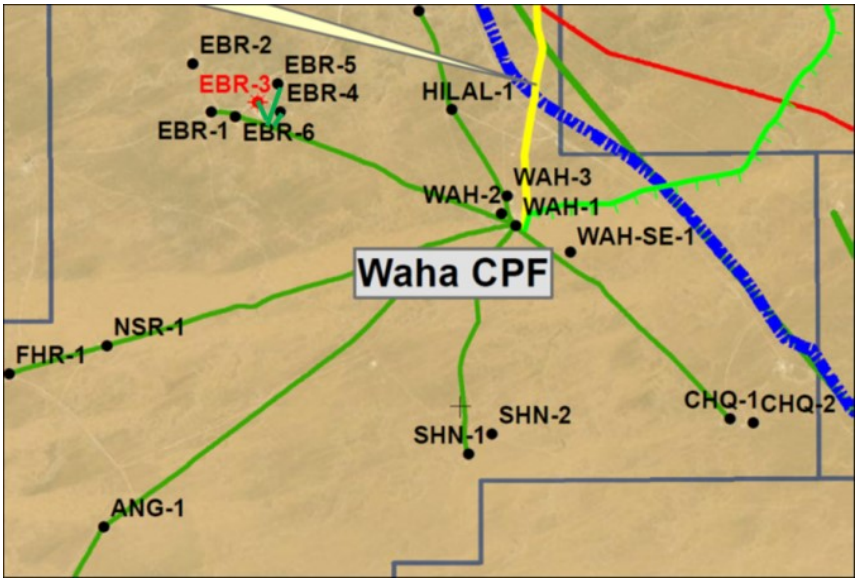

Figure 10: Surface Facility from EL Badr field to WAHA CPF

Under current depletion condition, the cumulative oil production reported to be 5.38 MMSTB or less 10% of the oil in place. Water breakthrough was observed first in EBR-1 after more than a year of production, however, the other wells produced water since the first day of production. The actual cumulative produced water is in the order of 1.6 MMSTB which is 30% of total production.

EBR-5 and EBR-3 found to be watered out in December 2013 and April 2014 respectively. Due to this premature high water production these wells are currently shut in. Cumulative oil production reached 1.32 MMSTB from EBR-5 and 0.63 MMSTB from EBR-3.

Figure 11 illustrates oil production throughout the field life, respective cumulative production of each well which are represented as bubble map and Figure 12 shows relative location of the wells in the structure respectively.

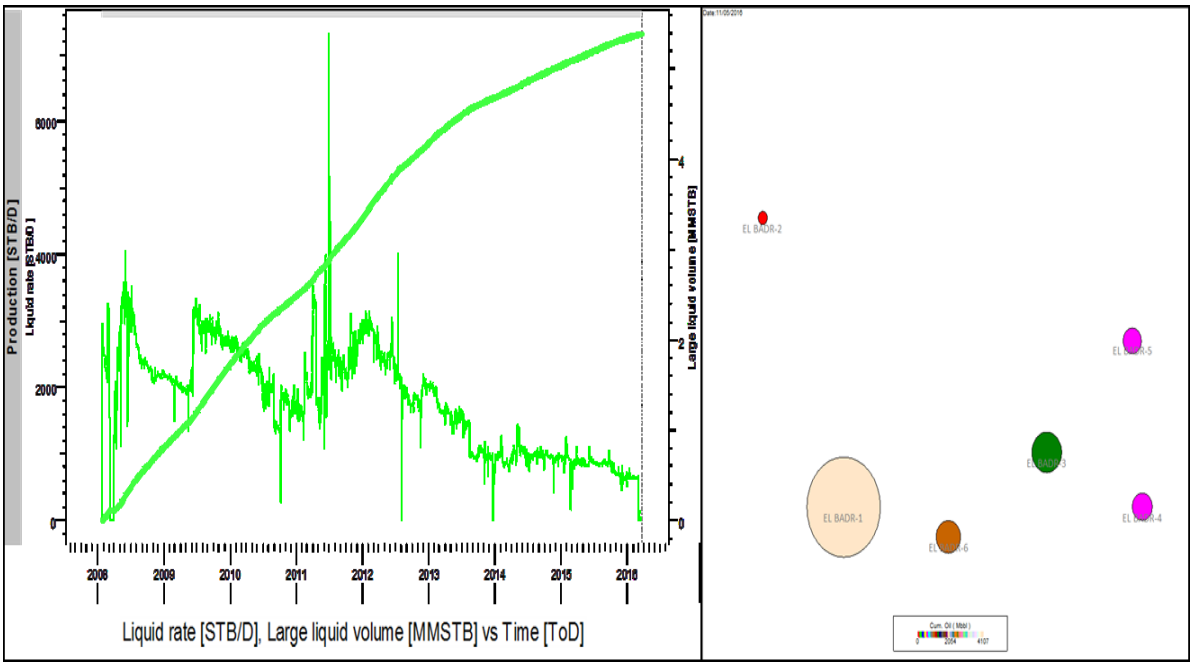

Figure 11: Left: El Badr field Production Right: El Badr wells Oil cumulative Production bubble map

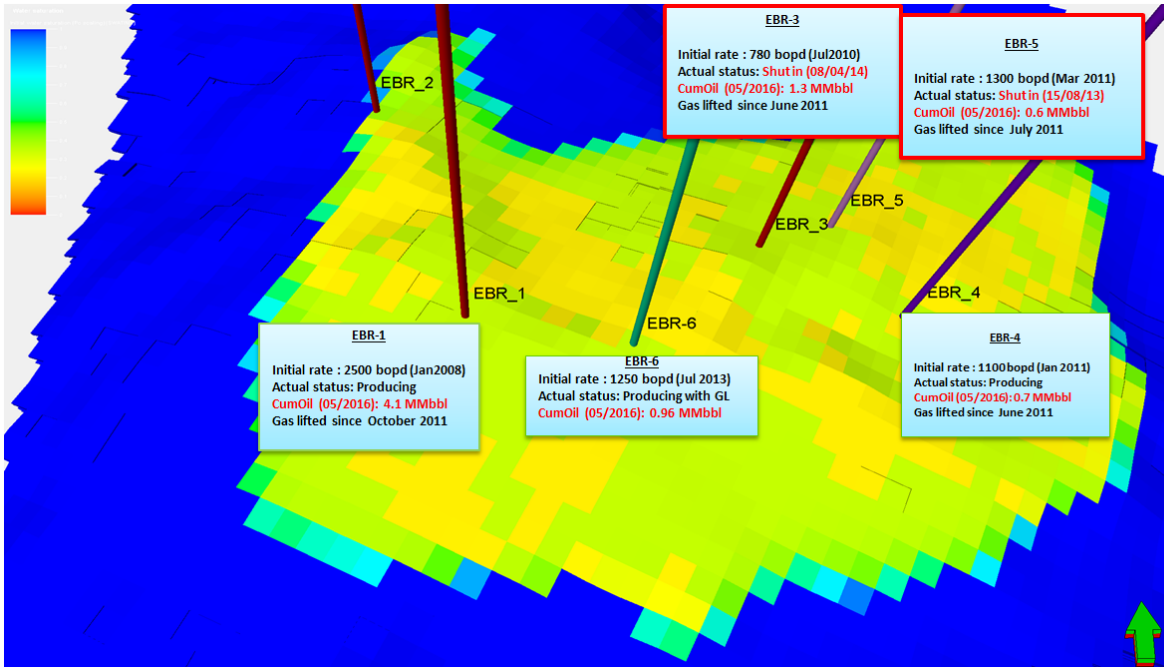

Figure 12: EL Badr Wells Location within the structure

To investigate the performance and the efficiency of each well in El Badr field, we plotted the production history of each well with the separator well test results and PLTs (Production Logging Tools). We analyzed only the oil and water phases in details but not the gas one. GOR was frequently mis-

reported due to inconsistent metering and/or to variance in solution gas ratio used in PLTs to estimate gas rates. Most of the PLT reports claimed that accurate PVT data would be better to match surface conditions.

2.5 EL BADR-1 WELL PRODUCTION PERFORMANCE

EBR-1 is completed in 7 sets of perforations and producing through SSD (A to F). Acacus and Tannezuft Silurian sandstones reflects the net pay zones and have been perforated respectively as shown in Table 2.
The well features 3 ½ “tubing completion string with wireline entry guide at 3568m. The tubing is set in 7” liner with a liner show at 3650m. The open hole section extends to 4162m (Appendix A).
The well exhibited various flow periods where it started producing through a choke before being replaced by 3” elbow in May 2009. This reduction in surface back pressure engendered increase in production as seen in Figure 13. Ultimately the well stopped to flow naturally, thus, attempts to restore production through scale removing were performed before installing gas lift system through a punch in tubing at 2350m. The water breakthrough occurred in august 2010. Production data show that the water production is consistent and increases with time. The gas production from EBR-1 is mainly solution gas that comes out of the produced oil. Gas production is not a problem as long as the reservoir pressure remains above the bubble point.
Many production tests were carried out for this well. Figure 13 shows production history and well test data. We observe that production test shows discrepancy as well as sudden change between the reported rates and the tests which underscore the inefficiency of rate allocation procedure in the field.

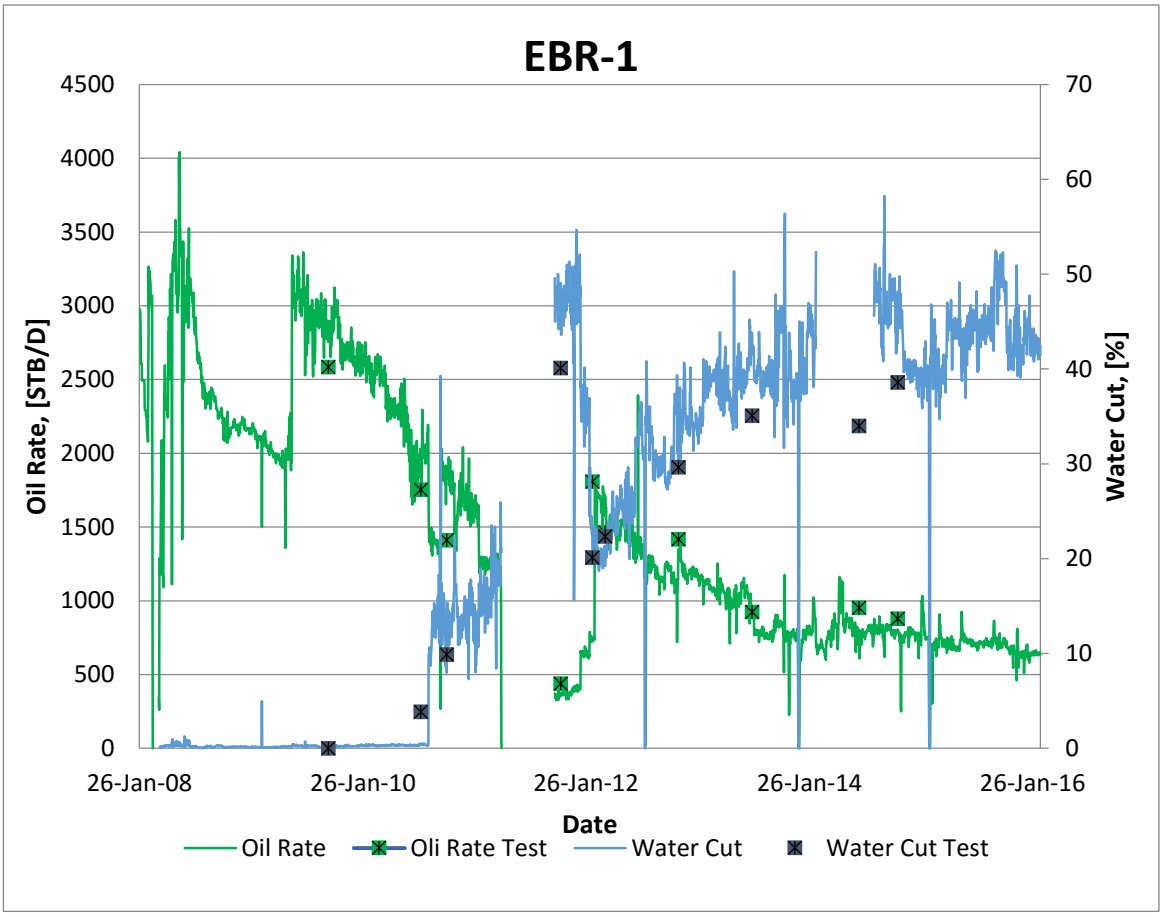

Figure 13. Production Rates versus Well Production Tests of EBR-1

EBR-1 has good reservoir characteristics. Average layers properties are summarized in Table 2. The pressure is averaged on pressure gradient estimated from MDT. The porosity, permeability and water saturation are averaged based on the values estimated from the open hole logs. Fluid properties are estimated from the PVT report conjunctly with the production tests. Table 3 presents the averaged properties for EBR-1 obtained from MDT and open hole logs interpretations and Figure 14 illustrates the pressure gradient estimated from MDT.

Table 2. Layers Rock Properties of EBR-1

		H(m)	Pr(Psi)	Phi(-)	K(md)	Sw(-)
SSD A	Bo	5	4779	0.11	12	0.35
SSD B	A1b	5	5048	0.09	0.7	0.35
	A1c	3.5	5028	0.16	13	0.22
SSD C	A2d	1	5104	0.11	7.48	1
	A2e	6	5124	0.14	14	0.37
SSD D	A5-1	5.5	5183	0.14	8.3	0.35
	A5-3	8	5236	0.17	62	0.35
SSD E	A8a	1	5310	0.05	1.2	0.5
	A9a	5	5317	0.12	1	0.35
SSD F	T2	5	5322	0.2	74	0.15

Table 3. Average Properties of EBR-1

Initial pressure	5165	psi
Reservoir temperature	212	°F
Net pay	45	m
Porosity	0.14	-
Permeability	16.6	md
Water Saturation	0.32	-
Oil gravity	40.5	°API
Gas gravity	0.98	
Water salinity	255000	ppm

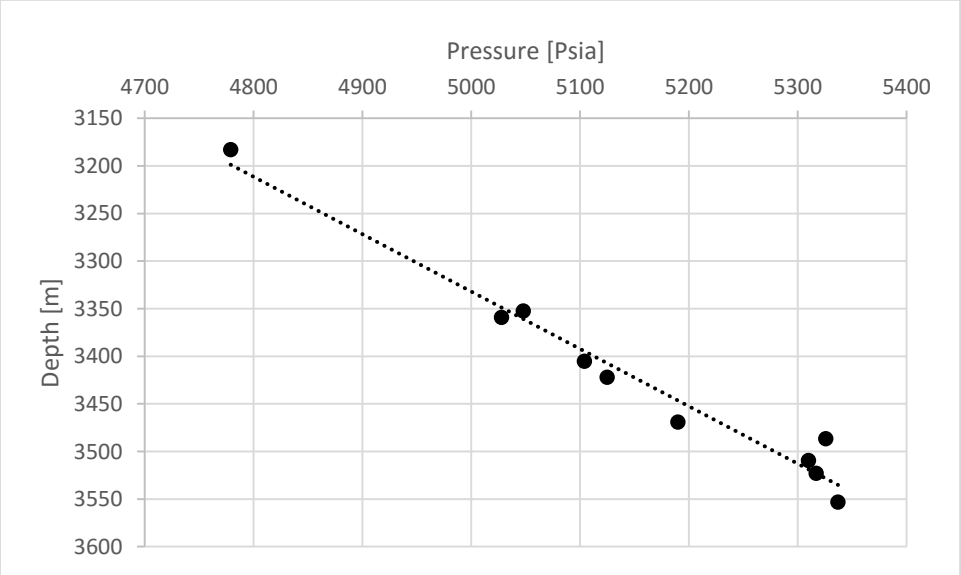

Figure 14. Pressure Gradient of EBR-1

Figure 15 and Figure 16 show the evolution of water cut and oil cut for each SSD obtained from PLTs. The water is mainly coming from SSD D which is about 90% of the total produced water. Similarly, SSD D contributes roughly to 60% of the oil production. Therefore the water production is considered as a good water in EBR-1, in other words, the water produced is below the economic limit and cannot be avoided without losing reserves.

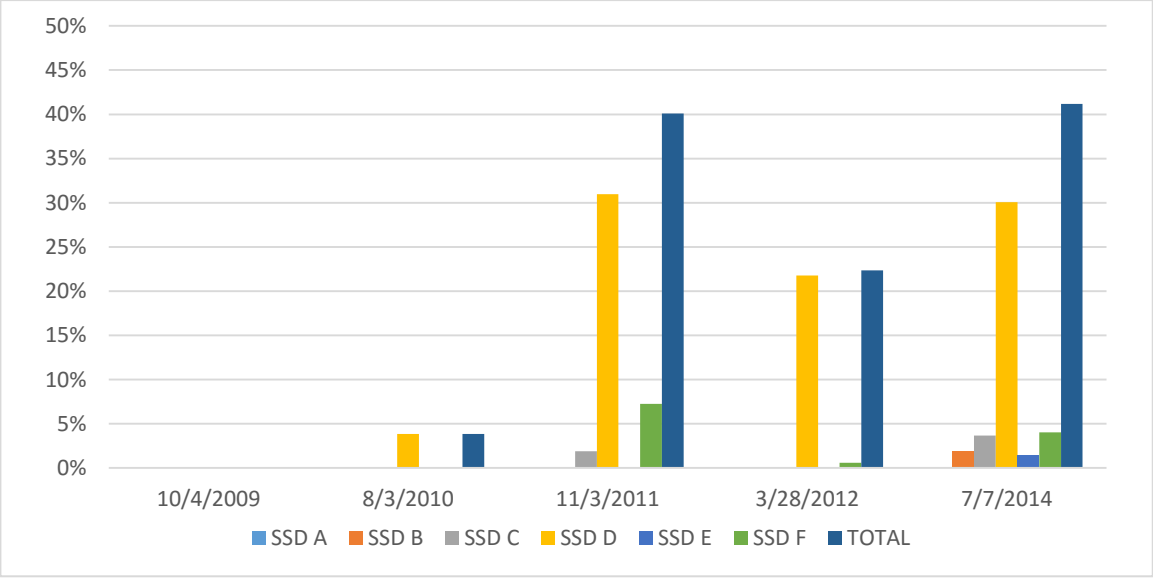

Figure 15. Water Cut Evolution for EBR-1

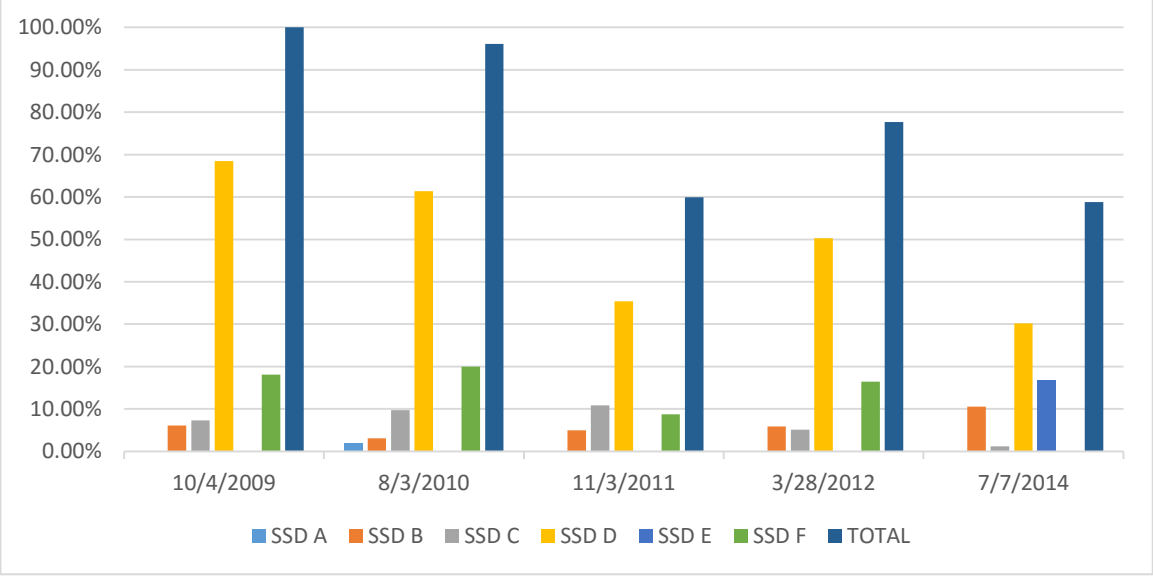

Figure 16. Oil Cut Evolution for EBR-1

2.6 EL BADR-3 WELL PRODUCTION PERFORMANCE

EBR-3 was drilled in 2010 and located approximately 1.1 km to the east of EBR-1. The well features a single tubing string with 2 7/8" diameter down to 3744m. The well is producing from Acacus/Tannezuft perforated intervals through three SSD (A, B and C). The tubing is fixed to the liner with a liner shoe at 3763m. The open hole section extends to 4162m in the Ordovician formation (Appendix A)

Similarly to the previous well, EBR-3 produced from 3" elbow starting from August 2010. In May 2011, the well started production with gas lift mandrels. Water production was seen since the early life of the well (Figure 17). Pressure gradient was found nonlinear due to partial depletion in some producing layers. These layers are mainly A2e, A5-1, A5-3 and T2 with pressure difference from EBR-1 of 160, 750, 1300, 170 and 431 psia respectively as shown in Figure 18.

In Table 4. Layers Rock Properties of EBR-3layers properties are the averaged well properties are summarized.

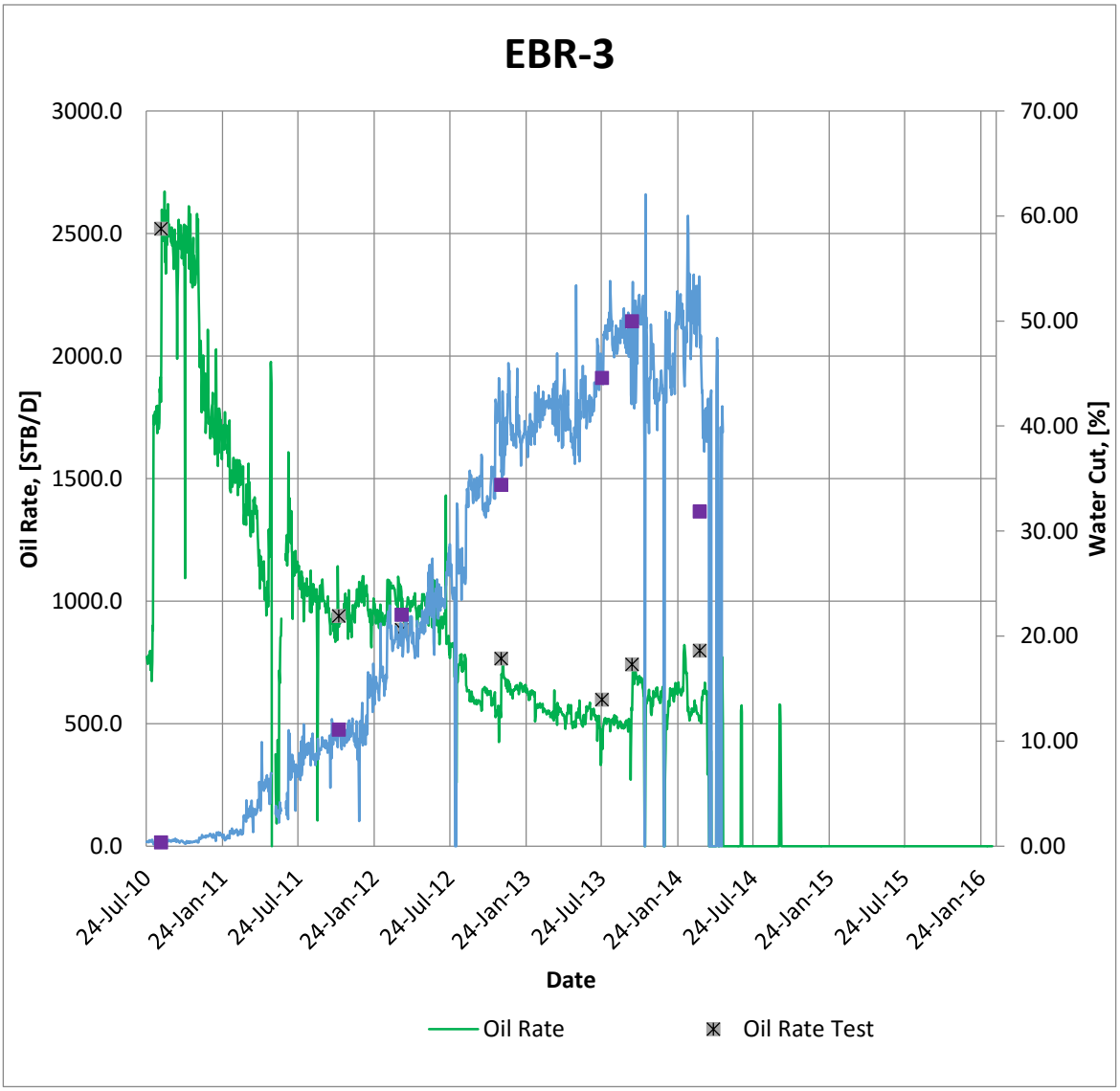

Figure 17. Production Rates versus Well Production Tests of EBR-3

Table 4. Layers Rock Properties of EBR-3

		H(m)	Pr(Psi)	Phi(-)	K(md)	Sw(-)
SSD A	A2d	2	5155	0.18	9	0.44
	A2e	7.5	5024	0.17	5	0.35
SSD B	A5-1A	2.5	4431	0.13	8	0.35
	A5-1B	2	4993	0.08	0.2	0.35
	A5-3	5	3900	0.14	4	0.35
	A7	4	5040	0.14	5	0.35
SSD C	A9a	8	5298	0.09	0.6	0.35
	T2	5	4906	0.24	18	0.15

Table 5. Average Properties of EBR-3

Initial pressure	4855	psi
Reservoir temperature	212	°F
Net pay	36	m
Porosity	0.14	-
Permeability	2.66	md
Water Saturation	0.36	-
Oil gravity	41	°API
Gas gravity	0.98	
Water salinity	255000	ppm

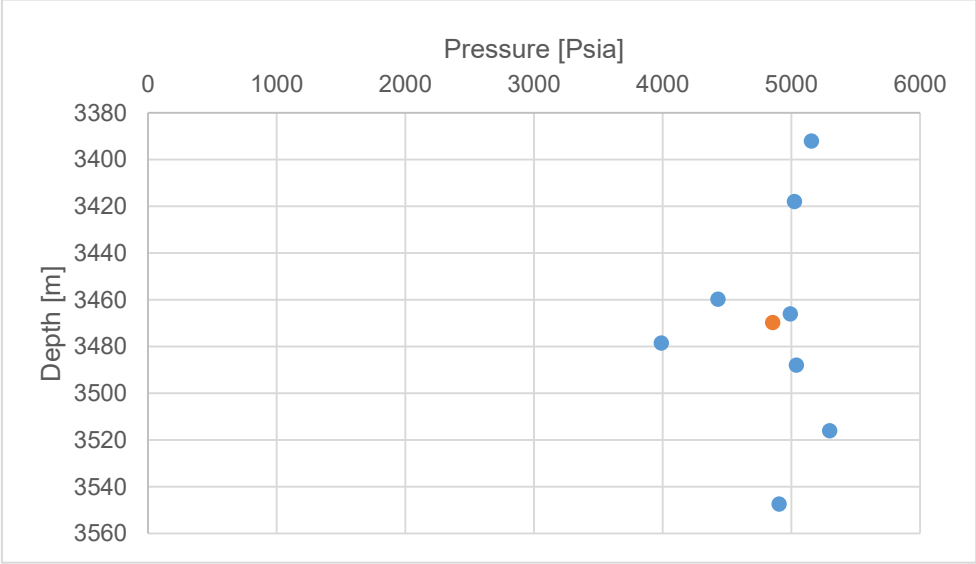

Figure 18. Pressure Gradient of EBR-3

PLT tests in Figure 19 and Figure 20 indicate that SSD B and SSD C are the most productive intervals while SSD A is found to be the cause of well loading up due to excessive increasing in water cut.

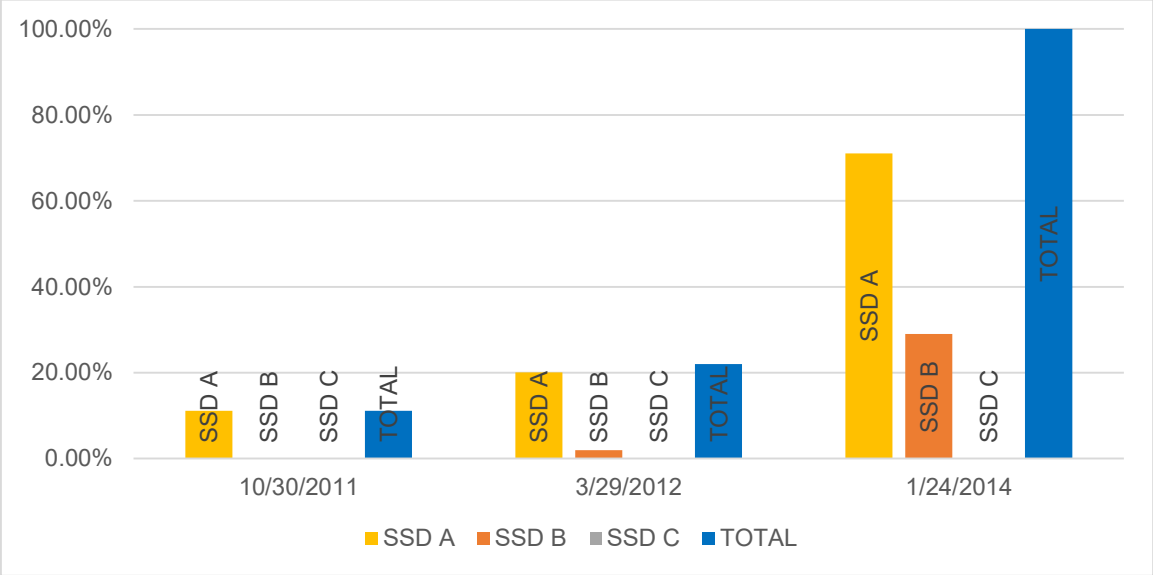

Figure 19. Water Cut Evolution for EBR-3

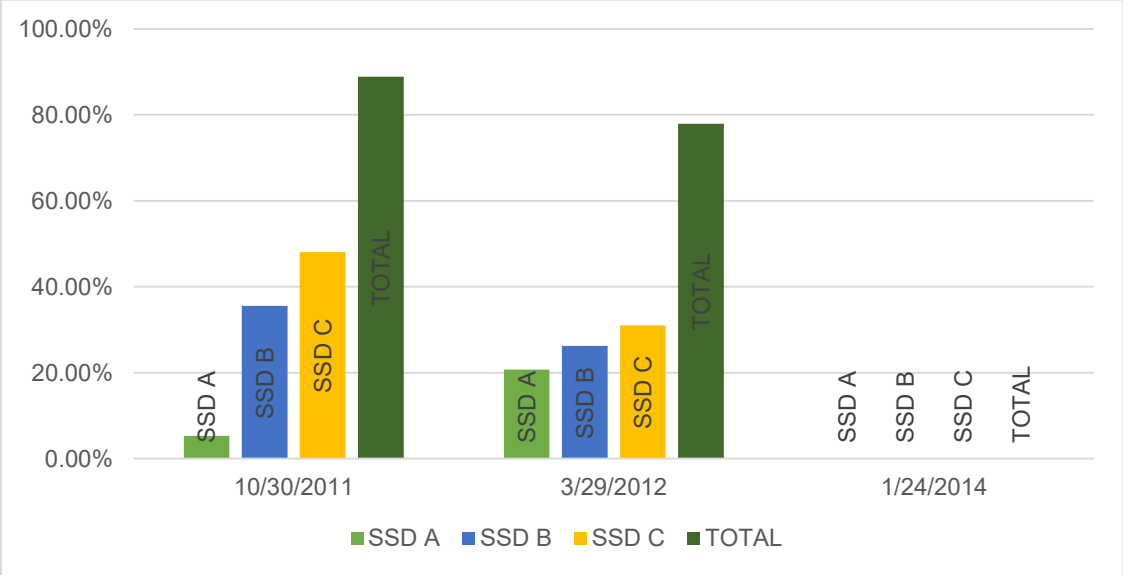

Figure 20. Oil cut Evolution for EBR-3

2.7 EL BADR-4 WELL PRODUCTION PERFORMANCE

EBR-4 was drilled in 2010 with a primary objective to extend the development of El Badr field by production of the Silurian Acacus reservoir. The closest well to EBR-4 is EBR-3.

EBR-4 produces from a single string with 3 ½ tubing down to 3665m, perforated in five intervals and set to production through three SSDs.
EBR-4 was produced first in February 2011 and quickly converted to gas lift in May 2011. Poor reservoir quality (i.e. low porosity and permeability and smaller net pay 22 m while for instance EBR-1 has 45m.) has led to small production contribution to the total field. Water production was observed since the first day of production. Cumulative oil reported is in the order of 0.7 MMSTB. However this well is good candidate for production rate allocation due to the erratic period of production that extend mainly from June 2011 to February 2012. Figure 21 shows the production history and the test points.
In Figure 22 depletion in pressure was also observed with an initial pressure of 4833 psia (while EBR-1 was 5165 psia). Layers A5-1a, A5-3 and T2 are found the most depleted while T3a is found to be abnormally pressured with respect to other layers due to the fact that it is encountered for the first time.

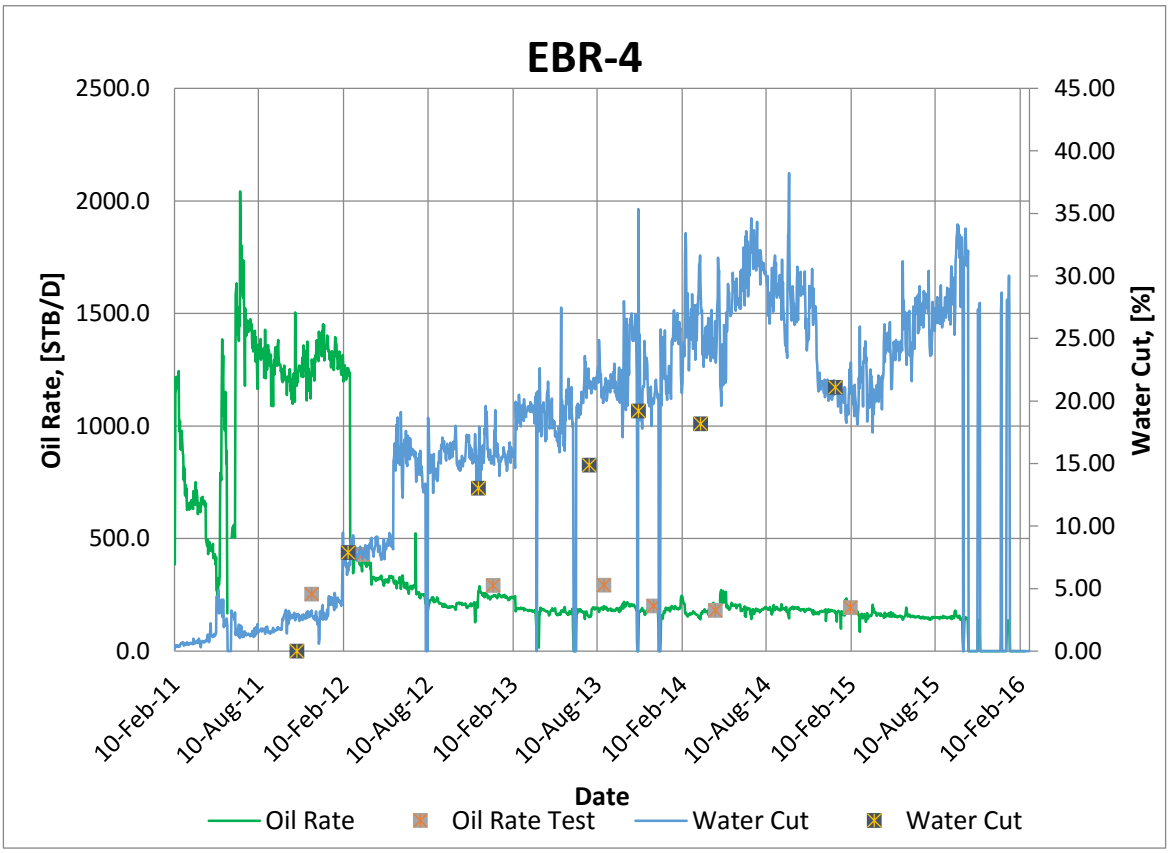

Figure 21. Production Rates versus Well Production Tests of EBR-4

The following tables list the layers properties and averaged well estimated values.

Table 6. Layer's properties of EBR-4

		H(m)	Pr(Psi)	Phi(-)	K(md)	Sw(-)
SSD A	A5-1A	2.5	3985	0.13	6	0.35
	A5-3	4	4058	0.08	8	0.35
SSD B	T2	6	4840	0.14	20	0.22
	T3a	3	5273	0.15	20	0.22
SSD C	T deep	6.5	5450	0.09	3	0.35

Table 7. Average Well properties of EBR-4

Initial Pressure	4833	psi
Reservoir Temperature	212	°F
Net Pay	22	m
Porosity	0.12	-
Permeability	11.2	md
Water Saturation	0.29	-
Oil Gravity	41	°API
Gas Gravity	0.98	
Water Salinity	255000	ppm

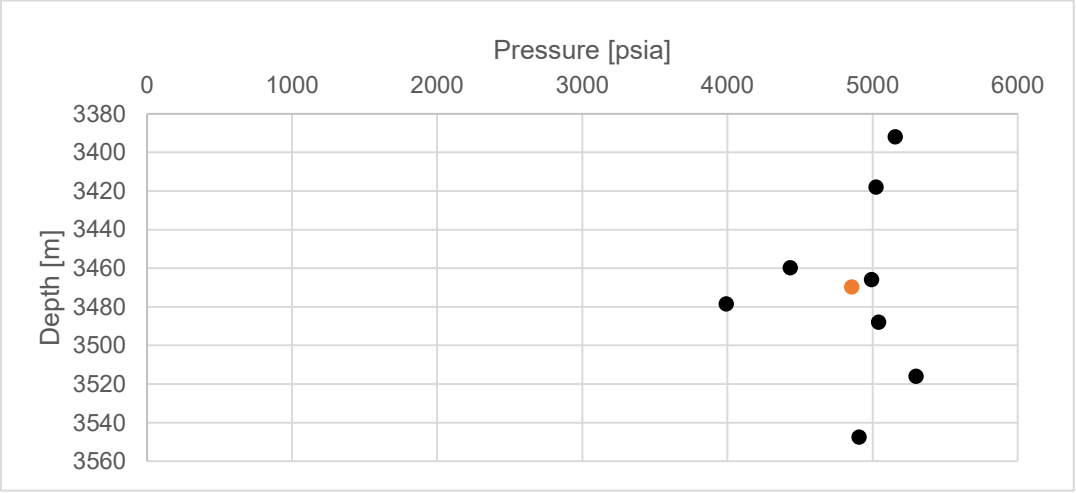

Figure 22. Pressure Gradient of EBR-4

EBR-4 has only one PLT measurement performed in October 2011, the results in Figure 23 and Figure 24 show that SSD B is the main producer for both oil and water.

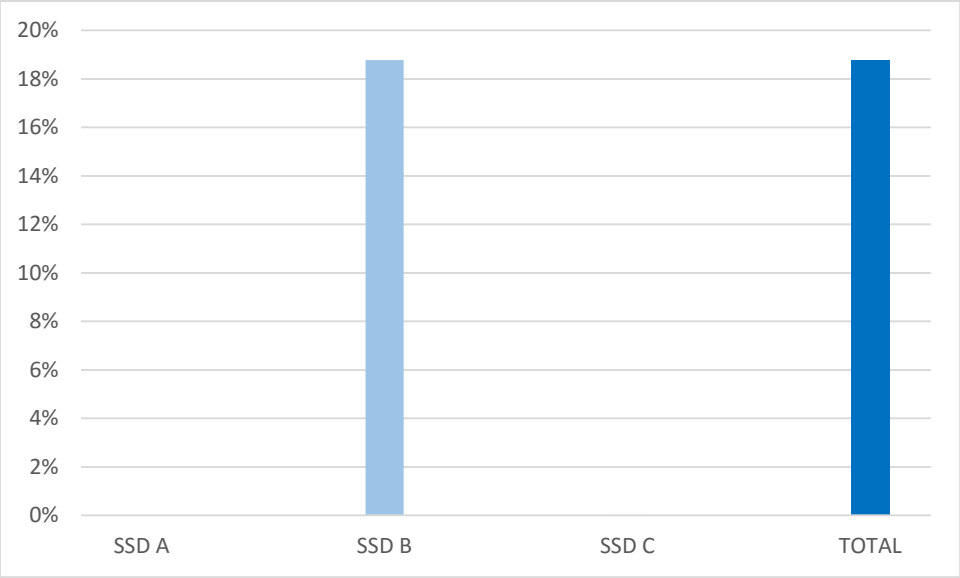

Figure 23. PLT's Water Cut of EBR-4

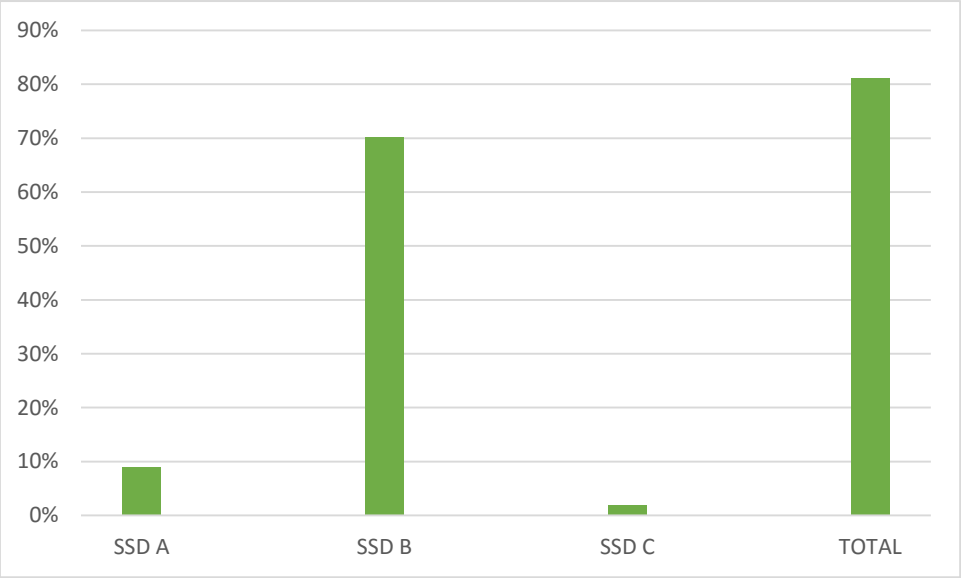

Figure 24. Oil Cut Evolution for EBR-4

2.8 EL BADR-5 WELL PRODUCTION PERFORMANCE

EBR-5 drilled in 2011, just 740m to the north-west of EBR-4. Despite the short distance to EBR-4, EBR-5 encountered good reservoir characteristics of Acacus sandstones (porosity exceeded 20% in some layers).
EBR-5 was completed with a single 3 ½“diameter tubing string that extends to 3458m. the tubing is set in 7” liner and the well was produced from 3 zones by the way of eight perforated intervals in 7” liner between the end of tubing and the plugged back total depth of the liner at 3734m (Appendix A).

One month after first production in EBR-4 production was carried out in EBR-5 and converted into gas lift in July 2011. The well has produced 0.63 MMSTB of oil and just 33.2 MSTB of Water which is about 5% in short time as illustrated in Figure 25.
Table 8 and

Table 9 summarize layers and well averaged properties found in this well.

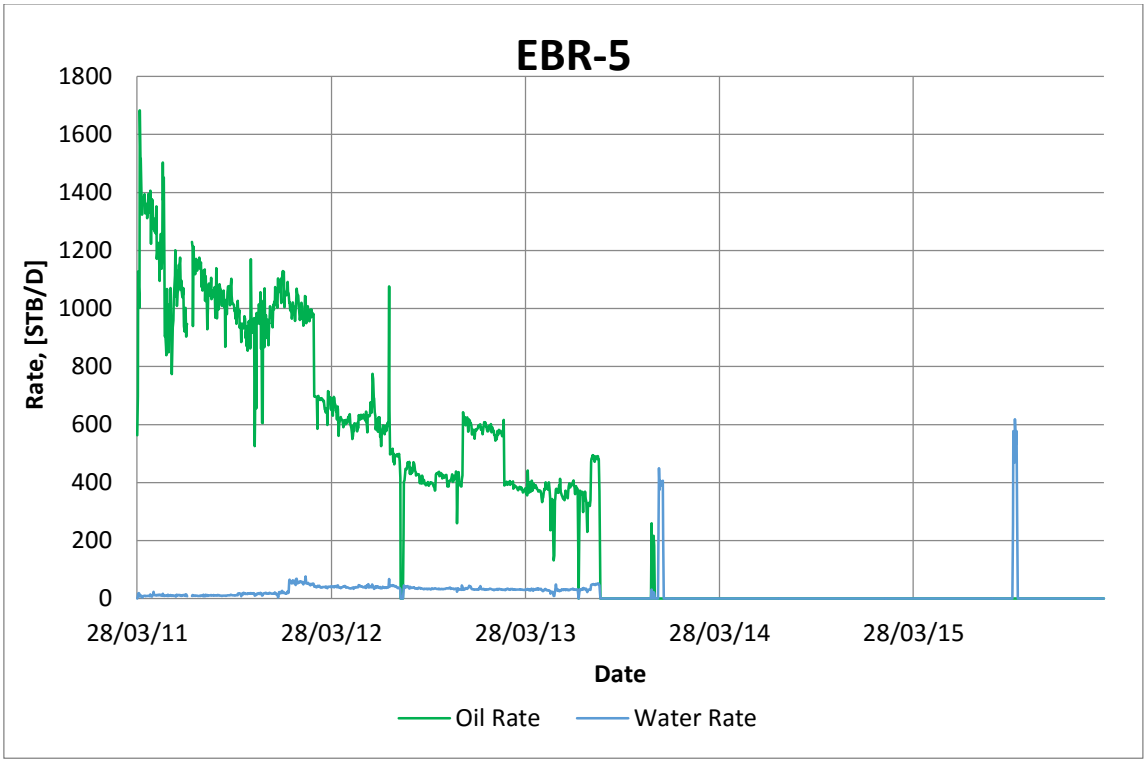

Figure 25. Production Rates of EBR-5

Table 8. Layer's properties of EBR-5

	H(m)	Pr(Psi)	Phi(-)	K(md)	Sw(-)
A2e	4	4767	0.17	7.5	0.15
A5-1A	2.5	3839	0.11	5.6	0.35
A5-3	4	3821	0.08	6.7	0.35

A7	6	3676	0.17	9.5	0.22
A9a	7	3586	0.17	9.5	0.22
T2	6	4060	0.22	24	0.15
T3a	3.5	4365			
T deep	6.5	5374			

Table 9. Average Well Properties for EBR-5

Initial Pressure	3793	psi
Reservoir Temperature	212	°F
Net Pay	39.5	m
Porosity	0.15	-
Permeability	8.56	md
Water Saturation	0.2	-
Oil Gravity	41	°API
Gas Gravity	0.98	
Water Salinity	255000	ppm

Pressure depletion was pronounced in the upper layers A5-1, A5-3, A7 and A9a as shown in Figure 26.

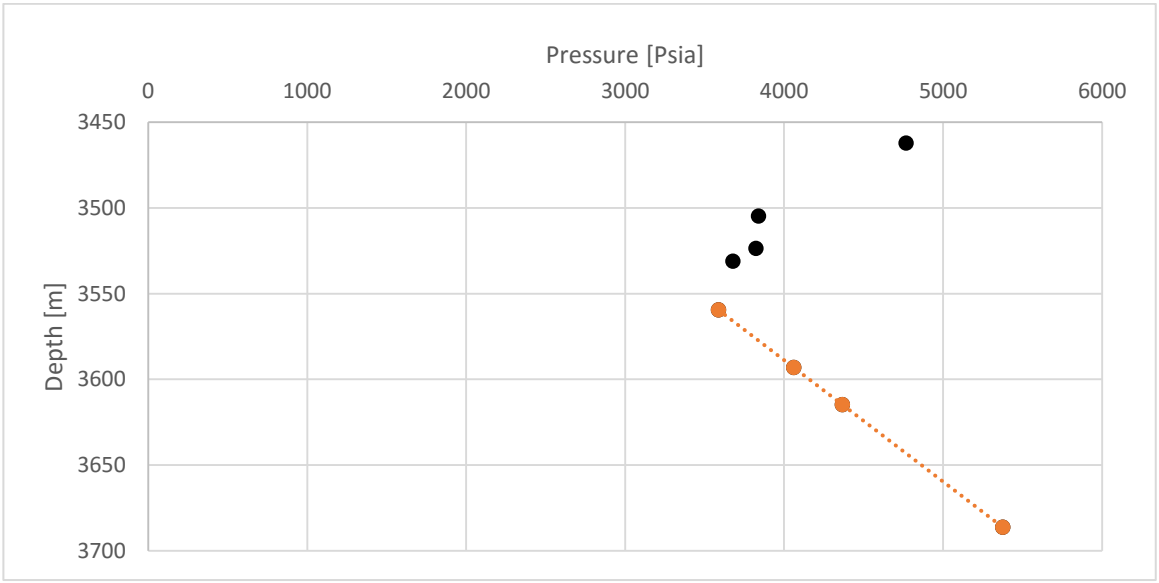

Figure 26. Pressure Gradient for EBR-5

Figure 27 and Figure 28 show the evolution of oil cut and water cut for EBR-5. The high initial water saturation caused the water production to increase inevitably. EBR-5 was shut in after only two years of production due to sudden increase in water cut where was reported to be 100% in

August 2013. EBR-5 has only one PLT measurement performed in March 2011 where it shows that the water comes basically from layer T3a.

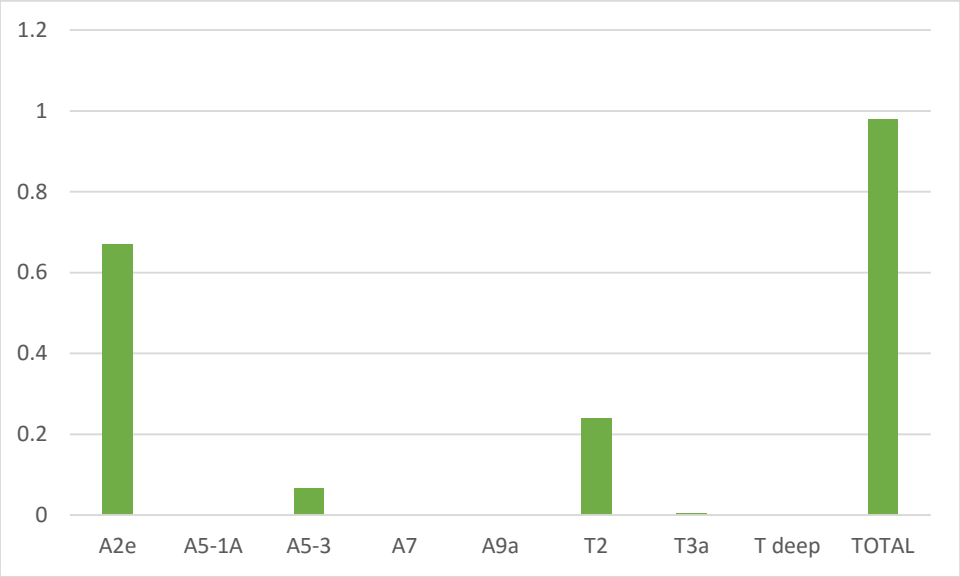

Figure 27. Oil cut Evolution for EBR-5

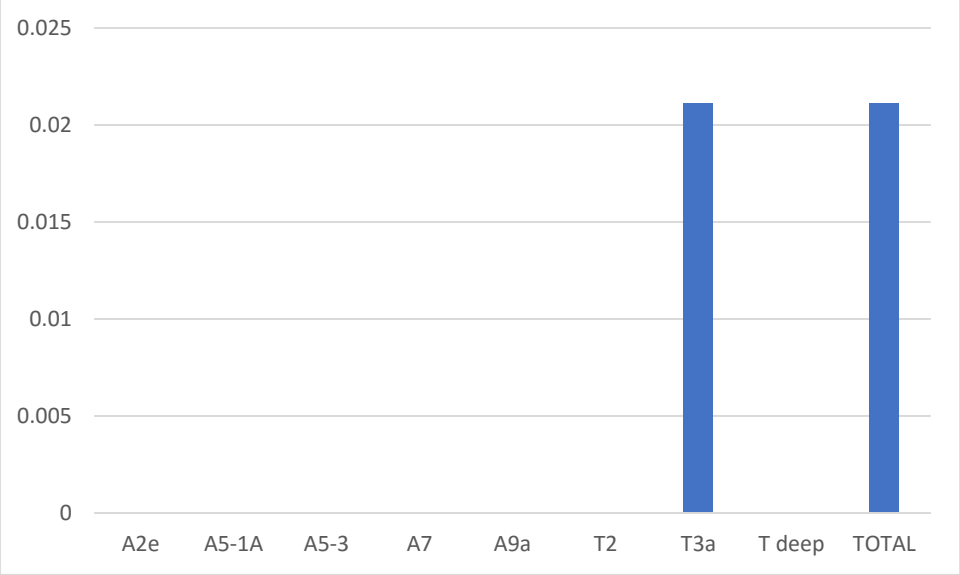

Figure 28. Water Cut Evolution for EBR-5

2.9 EL BADR-6 WELL PRODUCTION PERFORMANCE

EBR-6 is a development well drilled in May 2013 and located almost 0.6 km to the east of EBR-1 and 0.7 km to the west of EBR-3.
The well completed with a single 3 ½ “to 3234m and is producing through a tail pipe and perforated pup joint 3222m. Six perforation intervals in 7” liner established in phase I perforation program before adding perforation in the partially depleted layers as per phase II as shown in Figure 30 and

Figure 31. Because EBR-6 is too close to EBR-1 which is the main producer in the field, the contrast in the pressure gradient was notable. However, good reservoir characteristics allowed EBR-6 to gain a significant place in total field performance with cumulative oil production of 0.91 MMSTB (Figure 29). Water production was noted since the beginning in this well and it is progressively increasing after performing phase II perforations. The main water producing intervals are A5-3 and T2 as shown in Figure 32. Figure 33 shows that layers A1C, A5-3, A8a and T2 are the main oil producers.

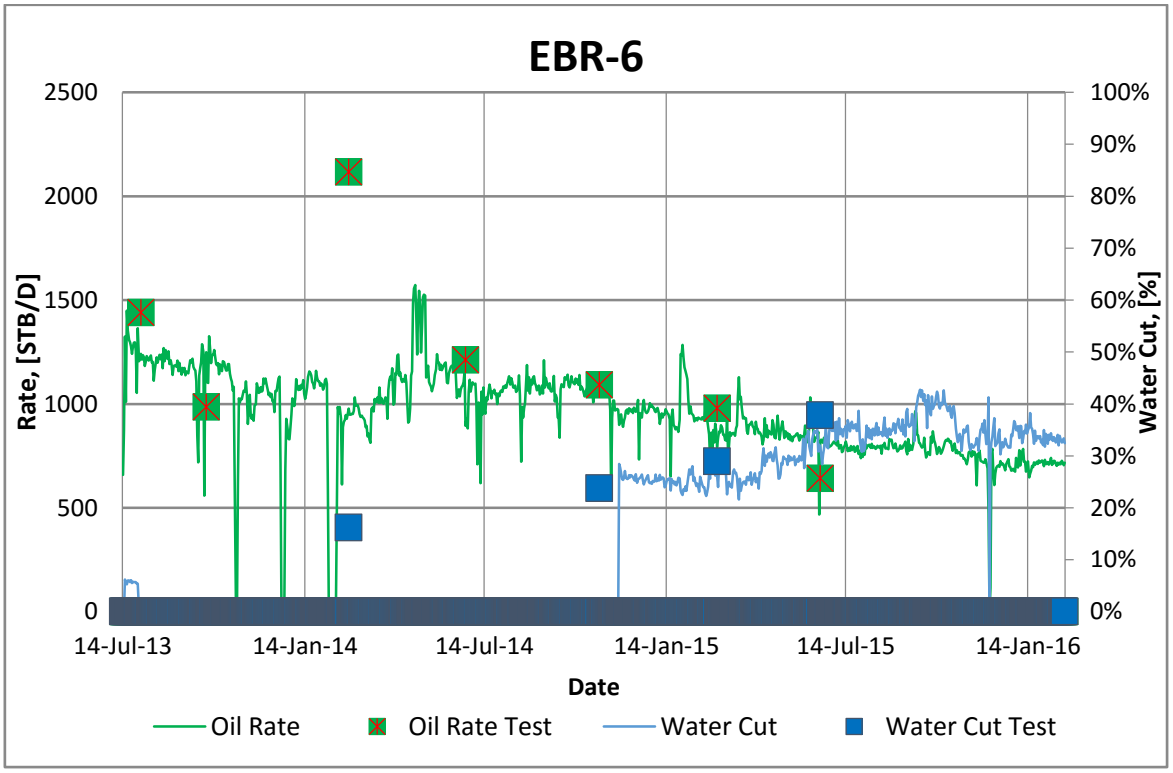

Figure 29. Production Rates versus Well Production Tests of EBR-6

The flowing tables list respectively layers properties and the averaged well properties.

Table 10. Layers Rock Properties of EBR-6

	H(m)	Pr(Psi)	Phi(-)	K(md)	Sw(-)
B2-1	0.8	4860	0.12	26	0.58
A1C	2.4	3673	0.18	30	0.58
A1C-2	0.8	3382	0.16	16	0.3
A2D	2	2712	0.14	14.6	0.3
A2D-1	1.5	5088	0.14	10	0.6
A5-1A	1.3	1990	0.15	50	0.15

A5-1B	2.2	4888	0.18	4	0.45
A5-3	5.9	2941	0.15	30	0.45
A8A	1.5	5248	0.12	33	0.2
A9A	3.3	5038	0.15	3.5	0.54
T2	3.8	2941	0.25	97.3	0.5

Table 11. Average Properties of EBR-6

Initial Pressure	4800*	psi
Reservoir Temperature	212	°F
Net Pay	10.5* 25.5**	m
Porosity	0.14	-
Permeability	-	md
Water Saturation	-	-
Oil Gravity	41	°API
Gas Gravity	0.98	
Water Salinity	255000	ppm
* Phase I ** Phase II		

The pressure depletion in this well is significant, especially in layers perforated in phase II. In Figure 31 orange points represent the layers pressure versus depth for Phase II and black points the pressure for Phase I.

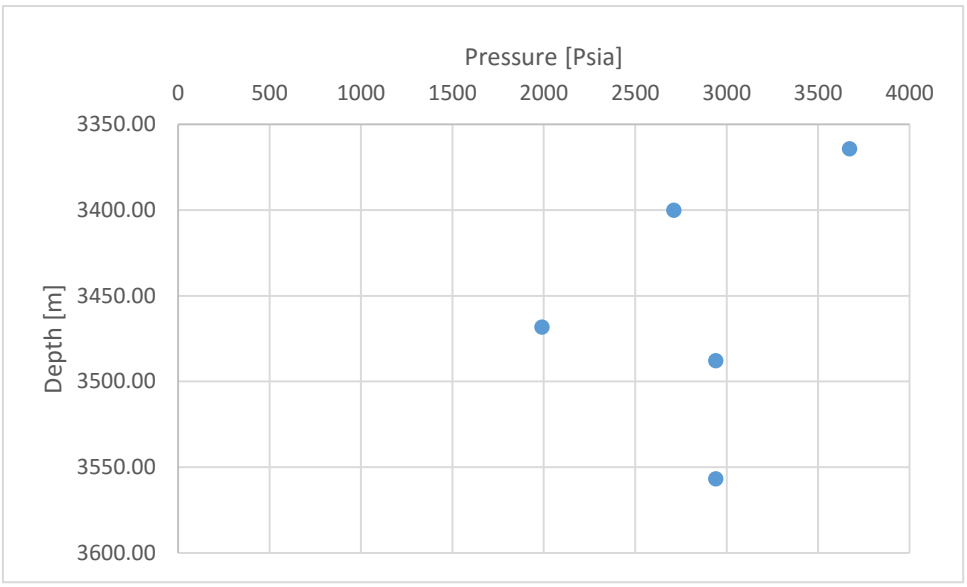

Figure 30. Pressure Gradient of EBR-6 Phase II

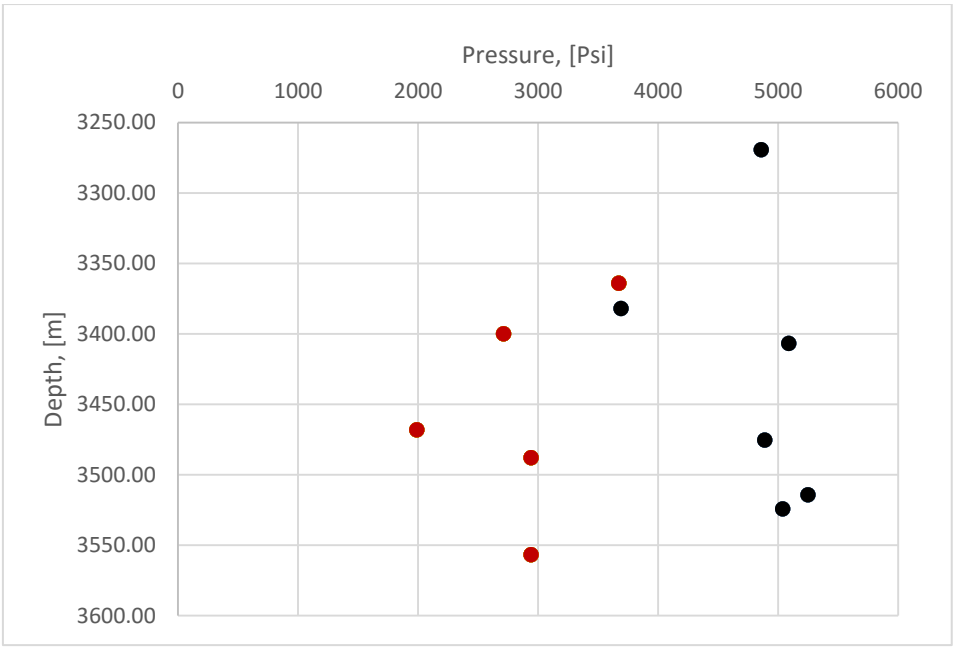

Figure 31. Pressure gradient of EBR-5 Phase I (Black) and II (Orange)

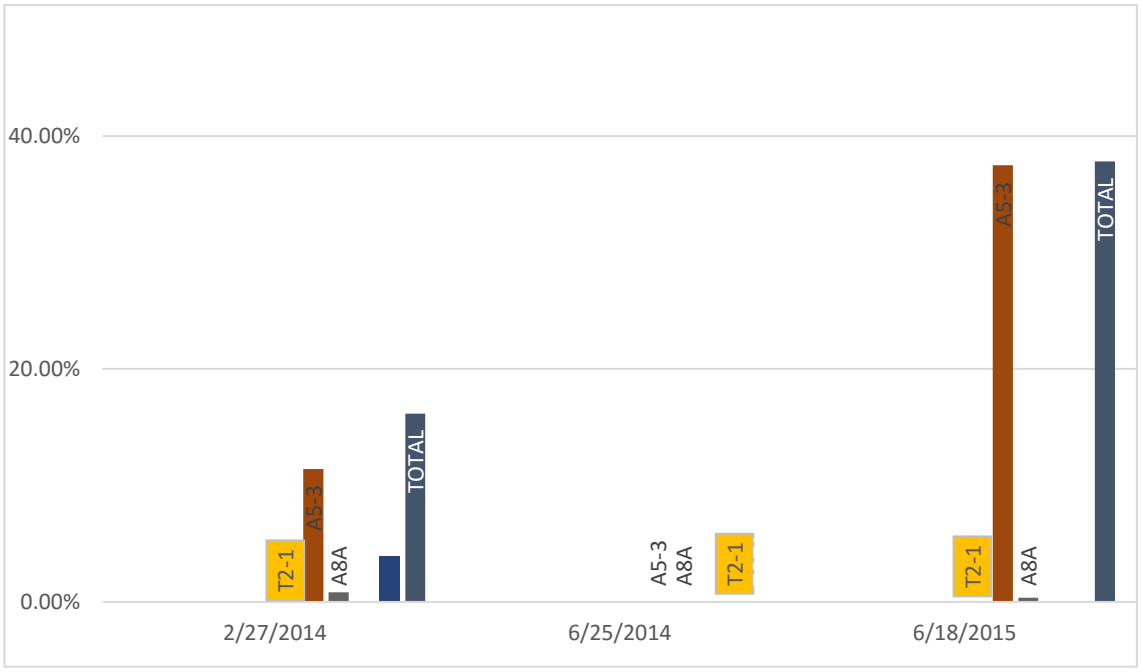

Figure 32. Water Cut Evolution of EBR-6

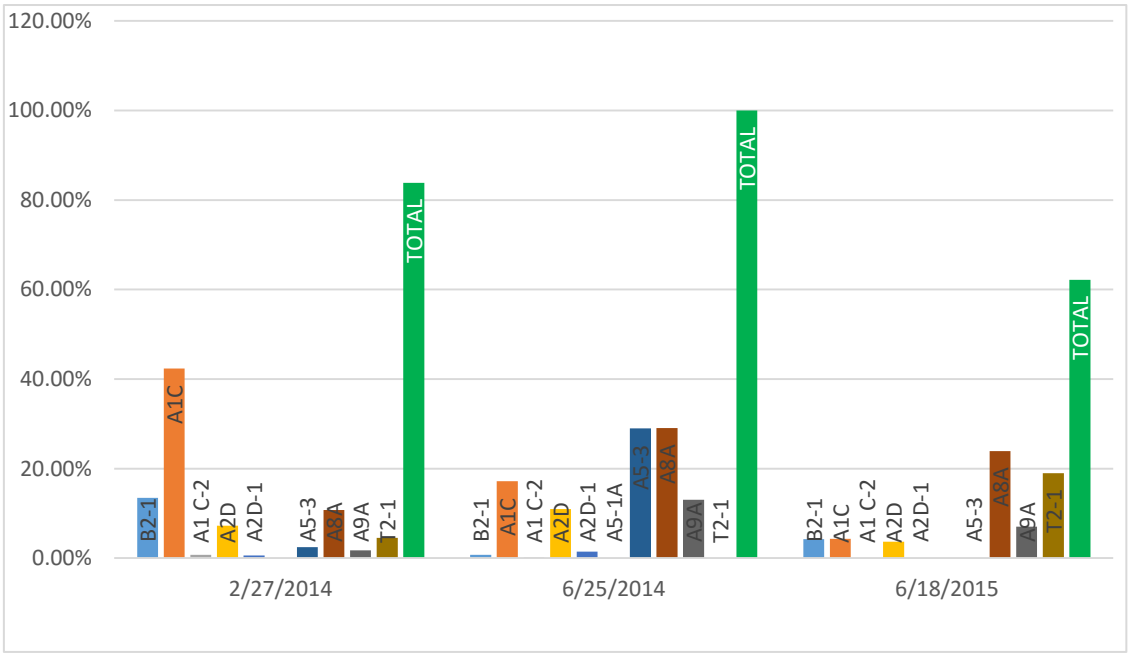

Figure 33.Oil Cut Evolution for EBR-6

3 El Badr Field Production Analysis

In this chapter we present the production analysis for each well. We estimate the well potentials and the oil in place. Moreover, we show consistency of the estimated well log properties with the results found by the production analysis. And finally we generate new rates consistent with the relative pressure drawdown. A systematic theoretical description of these plots is given in the next section:

3.1 Production Data Analysis and Diagnostic Overview

This section provides an overview of the existing production data analysis and diagnostics methods. These tools are important because they constitute a basis to assess reservoir condition, and estimate well/reservoir parameters. The production analysis methods can be subdivided into three groups [5].

- Empirical analysis of production data.
- Decline type curve analysis.
- Diagnostic methods for production data analysis

3.1.1 Empirical Analysis of Production Data

The use of rate-time data to estimate reserves was among the first industry practices to estimate reserves. Arp's formulation (1945) was the first systematic attempts to relate rate-time data in the petroleum literature when he presented his exponential, hyperbolic and harmonic decline relations. The objective of these relation is basically the estimation of reservoir performance and reserves under constant operation condition and for boundary dominated flow. The table below presents b exponent ranges and their significance on reservoir performance estimation.

Table 12. Drive mechanism versus b exponent value

b Value	Drive Mechanism
0	Single phase liquid
0.1-0.4	Solution gas drive oil reservoirs
0.4-0.5	Single phase gas
0.5	Effective water edge drive
0.5-1	Commingled layered reservoirs

These decline curves which are based on an empirical rate-time and associated cumulative-time equations, can be described in the general form as:

$$q(t) = \frac{q_i}{[1+bD_it]^{\frac{1}{b}}} \quad (2)$$

$$Q(t) = \frac{q_i^b}{D_i(1-b)}(q_i^{1-b} - q(t)^{1-b}) \quad (3)$$

Where: q_i is the initial rate, D_i is the decline factor, and b a parameter varying between 0 and 1 defining the decline type. Special forms of Arps decline curve when b=0 and b=1 are given as:

Exponential decline, b=0

$$q(t) = q_i e^{-D_i t} \quad (4)$$

$$Q(t) = \frac{q_i - q(t)}{D_i} \quad (5)$$

Harmonic decline, b=1

$$q(t) = \frac{q_i}{[1 + D_i t]} \quad (6)$$

$$Q(t) = \frac{q_i}{D_i}\ln(\frac{q_i}{q(t)}) \quad (7)$$

3.1.2 Decline Type Curves for Production Analysis

Fetkovich (1987) was the first reference for production decline curve analysis using type curves. In his work, Fetkovich assumed a constant flowing pressure which is the not the case in volumetric reservoirs for instance. In 1993, Blasingame and Palacio introduced a fundamental function plot accounting for variable-rate/variable pressure drop in production data. Their approach consists of plotting the normalized rate by pressure drawdown against material balance time and they used Bourdet approach to calculate the derivative. Although, their work was limited to gas wells, these types curve plots were extended to oil wells, horizontal wells, hydraulically fractured wells and multi-well reservoir systems [6].

3.1.3 Diagnostic Methods for Production Data Analysis

Few diagnostic plots exist in the literature for production data analysis when compared to transient pressure analysis due to the fact that production data are considered as low frequency and low resolution data [6].Yet, Mattar and Anderson have provided a systematic approach with examples for production data diagnostics [3] [7]. The approach can be summarized as:

1- Assess the quality and completeness of data using production history plots
2- Calculate the bottom hole flowing pressures (if necessary)
3- Estimate reservoir parameters (fluid and rock properties)
4- Identify expected reservoir type (volumetric, Water drive, Gas cap)
5- Range filter the data

In 2006, Kabir [8] presented diagnostic tool in terms of a Cartesian pressure-rate plot data with a highlight on identifying the reservoir production mechanism in a simple way to perform a diagnosis.

To sum up, Anderson et al [6] proposed in their work a set of diagnostic plots to consider in terms of production data correlation and reservoir diagnostics and the most challenges and pitfalls encountered as well as their influence/severity in production data interpretation (Table 13).

Table 13. Challenges and Pitfalls encountered in Production Data

Type	Issue	Influence/severity
Well Completion	Zone changes: new/old perforations	Very High
	Changes in the wellbore tubulars	High
	Changes in surface equipment	Moderate to High
	Stimulation: hydraulic fracturing	High
	Stimulation: acidizing, etc.	Moderate
General	Reservoir properties	Moderate
	Gas properties	Moderate
	Oil Properties	Moderate

	Poor time-pressure-rate synchronization	Moderate to high
	Poor time-pressure-rate correlation	Very high
Pressure	No pressure measurement	High
	Incorrect initial pressure estimate	High
	Poor wellhead to bottom hole pressure conversion (models	Moderate
	Incorrect location of pressure measurement	Very high
Rate	Rate allocations (potential for errors)	Moderate
	Liquid Loading	Moderate

3.1.4 Common Plots in Production Data Analysis

Production History Plot: This is a plot of rate versus time attached with a plot of bottom hole flowing pressure versus time. This plot aids to picture changes in time and uncorrelated behaviors. Such uncorrelated behavior is when the rate changes not accordingly to pressures. In other words, the rate may decrease but the pressure does not change or increases.
The diagnostic importance of this plot is the simultaneous visualization of time series changes in rate and pressure

Pressure-Rate Plot: This is simple plot to evaluate the direct correlation of the rate and pressure data. Basically three trend can identified from this plot (Figure 34) and the well production life can be divided into an infinite acting radial flow exhibiting a negative slope and a positive slope signifying the pseudo steady state flow periods.

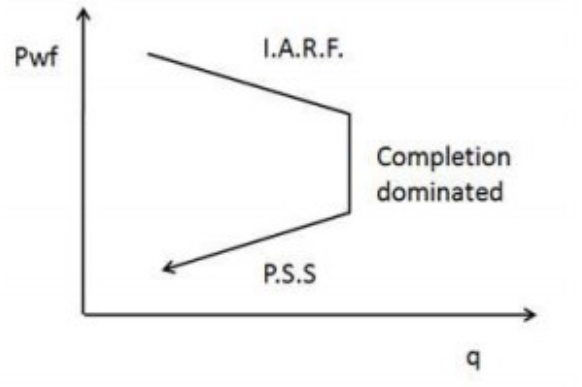

Figure 34. Typical Pressure Rate Plot [9]

Blasingame Plot: This is a re-plot of the traditional Fetkovich plot with consideration of the variable rate and pressure. This plot is created by plotting the logarithm of the pressure drop normalized rate functions versus the logarithm of appropriate material balance time function and its derivative and recently this plot incorporated the concept rate integrals to smooth the data. In this plot the material balance time and the normalized rate is defined by:

$$t_{mb} = \frac{Q(t)}{q(t)} \quad (8)$$

$$\frac{q_0}{\Delta p} = \frac{q(t)}{p_i - p_w(t)} \quad (9)$$

When the normalized rate is plotted versus the material balance time on log-log scale, the boundary dominated flow will exhibit a negative unit slope line. The pseudo steady state rate equation is defined as:

$$\frac{q_0}{\Delta p} = \frac{1}{b_{o,pss} + m_{o,pss}\overline{tmb}} \quad (10)$$

With:

$$m_{o,pss} = \frac{1}{Nc_t}\frac{B_o}{B_{oi}} \quad (11)$$

$$b_{0,pss} = 141.2\frac{\mu_o B_o}{kh}\left[\frac{1}{2}\ln\left[\frac{4}{e^{\gamma}}\frac{1}{C_A}\frac{A}{r_w^2}\right] + s\right] \qquad (12)$$

Log-Log Plot: This is a plot of the logarithm of rate normalized pressure drop function and its derivative versus the logarithm of appropriate material balance time function. This plot is used to diagnose specific flow regimes (infinite-acting radial flow, pseudo steady state, etc.) which offers alignment to which portion of the data set should be used to estimate a specific reservoir property. For example, the infinite acting flow regime leads to a constant derivative from which skin and permeability can be estimated. Shortly, this plot is an inverse version of Blasingame plot.

Normalized rate cumulative plot: Agarwal and Gardner proposes the use of rate-cumulative type curves for estimating fluid in place. In this plot Dimensionless rate is plotted against dimensionless cumulative production which is defined as follow for an oil case:

$$q_D = \frac{141.2qB\mu}{kh(p_i - pw)} \qquad (13)$$

$$Q_{DA} = \frac{0.8936QB}{\emptyset hAc_i(p_i - p_w)} \qquad (14)$$

The resulting type curves are straight lines with negative slopes on a Cartesian graph that converge to the same value on the x-axis and provides estimate of fluid-in-place in boundary dominated flow as shown in the Figure 35 below:

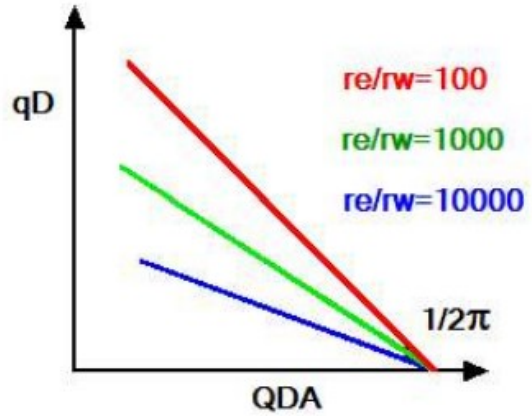

Figure 35. Typical Normalized rate Cumulative Plot [9]

Fetkovich Plot: this Plot is only valid for the case of constant bottomhole pressure. The logarithm of flowrate is plotted versus the logarithm of time

and the logarithm of cumulative production is plotted versus logarithm of time. This plot creates a fairly consistent diagnostic for assessing the quality of the rate data when the pressure is constant. But, the main application of the Fetkovich plot is estimating reserves and identifying drive mechanism owing to their empirical nature inherited from the incorporation of Arps decline theory.
In the following figure the left region of the curves (green to blue) correspond to the transient part of the response. On the right hand side, are the Arps decline curves (red to yellow) [9].

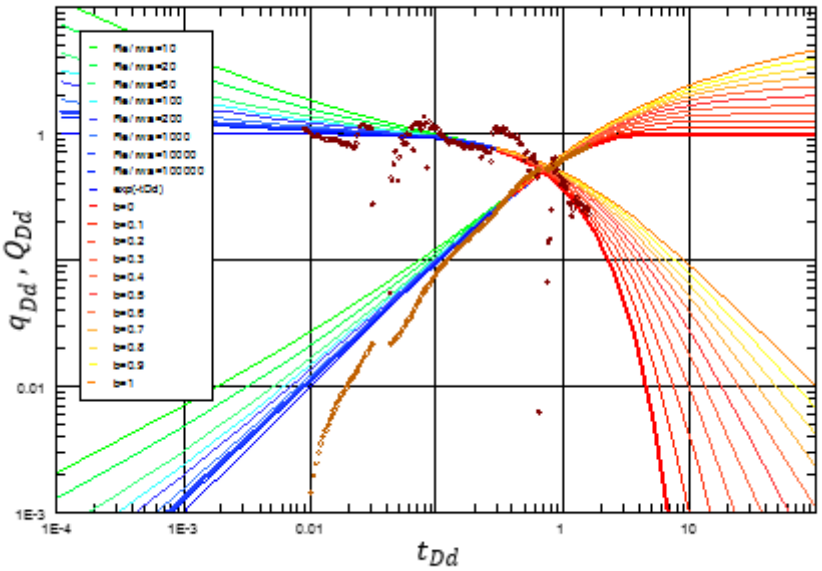

Figure 36. Fetkovich Type Curve Plot

And the variables are defined as:

Time
Decline curve dimensionless time

$$t_{Dd} = D_i\, t \qquad (15)$$

Dimensionless time

$$t_D = 0.0002637 \frac{k}{\emptyset \mu c_i r_w^2} \Delta t \qquad (16)$$

Related by:

$$t_{Dd} = \frac{t_D}{\frac{1}{2}\left[\left(\frac{r_e}{r_w}\right)^2 - 1\right]\left[\ln\left(\frac{r_e}{r_w}\right) - \frac{1}{2}\right]} \quad (17)$$

Rate

Decline curve dimensionless rate:

$$q_{Dd} = \frac{q(t)}{q_t} \quad (18)$$

Dimensionless flow rate, oil:

$$q_D\ oil = \frac{141.2q(t)\mu B}{kh(p_i - p_{w)}} \quad (19)$$

q_{Dd} And q_D are related by:

$$q_{Dd} = \left[\ln\left(\frac{r_e}{r_w}\right) - \frac{1}{2}\right] \quad (20)$$

Cumulative production

Decline curve dimensionless cumulative:

$$Q_{Dd} = \frac{Q(t)}{Npi} \quad (21)$$

Where N_{pi} defines the ultimate recovery.

3.2 PRODUCTION ANALYSIS OF EBR-1

In this well, we consider the case of homogeneous circular reservoir producing from a vertical well. The main objective of this analysis is to come up with a model capable of reproducing the production/Pressure history. EBR-1 serves as good candidate for production analysis as it exhibits a good correlation between rates and pressures which leads to reliable analysis expectations.

As complete demonstration of our analysis procedure, we used the following specific stepwise sequence described by Ilk et al [5].

First, we reviewed the data using “Production History Plot” in Figure 37. In this case, it is observed that the correlation is acceptable for regularly basis taken data. Besides, a shut in portion of this data is available. We note that performing a pressure transient analysis can confirm the results obtained from production analysis. However, as mentioned earlier, regularly taken data (i.e. daily and averaged) is insufficiently accurate to give the transient response of the reservoir.

The second review of the data is performed using a pressure rate plot (Figure 38). We note that 3 drainage volumes can be easily identified from the slopes 0.28, 0.33 and 0.35 psi/STB/d. Well draining from different compartments of different pore volumes will exhibit different slopes. In other words, production performance of a well in a large drainage volume will exhibit a shallower slope than those in small drainage volumes [8]. Another advantage of this plot is that erroneous / spurious data are easy to identify. In this case, we found that the data are mostly free of such issue. Additionally, we note that the transient regime is nearly missing due to the dominated signature of Pseudo Steady state flow regime.

To estimate reservoir properties, fluid in place and reserves from EBR-1, we use log-log plot, Blasingame type curve plot, and normalized rate-Cumulative plot.

We used Blasingame “Decline type curves” in Figure 40 to compare/match the data with reservoir model. For this well we have identified a pressure support by the skewed off-trend at late times. Similarly, using log-log plot (Figure 39), we found that the data exhibit different flow regimes. At early times, with multilayer system we believe that this signature could be caused by the dominance of such abnormally pressured layer over the others. Hence, this response cannot be considered representative for the whole system. At mid times, we found another response controlled by transient and pseudo steady state flow regime. The third period, which reflects the late time period, is considered to be more optimistic in determining the fluid in place. We note that this period showed an off-trend signature in Blasingame type curve. Therefore, relying on this period to estimate the fluid in place will yield inevitably to an overestimation.

Figure 41 shows the normalized rate curve, the trend of normalized rate is extended to estimate the oil in place which is around 54.2 MMSTB. The analysis shows similar results as found in in Figure 40 where the oil in place is about 51.4 MMSTB.

Figure 42 presents the productivity index versus time plot. We can identify the increasing trend of the productivity index at late time rather than converging to constant value in pseudo steady state flow regime. This could be simply due to downhole gauge drifting and/or the pressure support identified earlier. And yet, we highly recommend running a gradient survey and production logging test for EBR-1.

Having identified the best suitable reservoir parameters, the last step is to generate pressures and rates model response. This final history match indicates whether our model does agree with the measured data or not. Figure 37 shows that the trend of the model (i.e. dashed green line) is in agreement with measured data, more importantly, it honors better the test data points which confidently validate our model. We state that time dependent skin is used as tuning factor for the history match. The reason

is that test point data are better honored with the simulation model and would better account for productivity index and/or permeability reduction (i.e. due to compaction) near the wellbore [7].

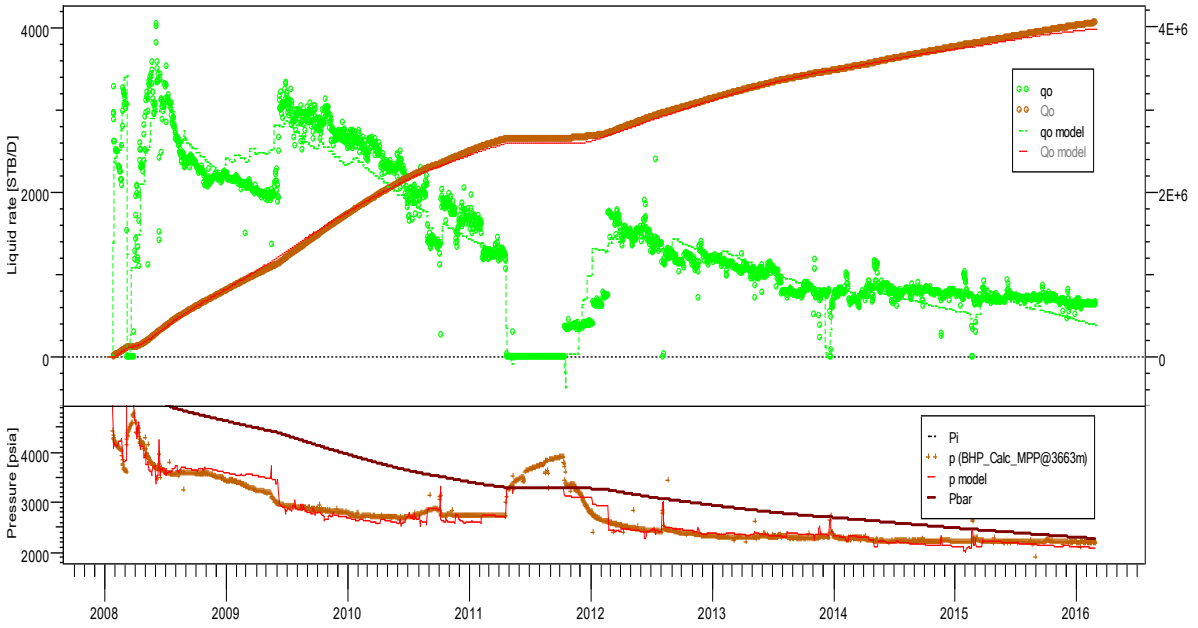

Figure 37. Production History Plot for EBR-1

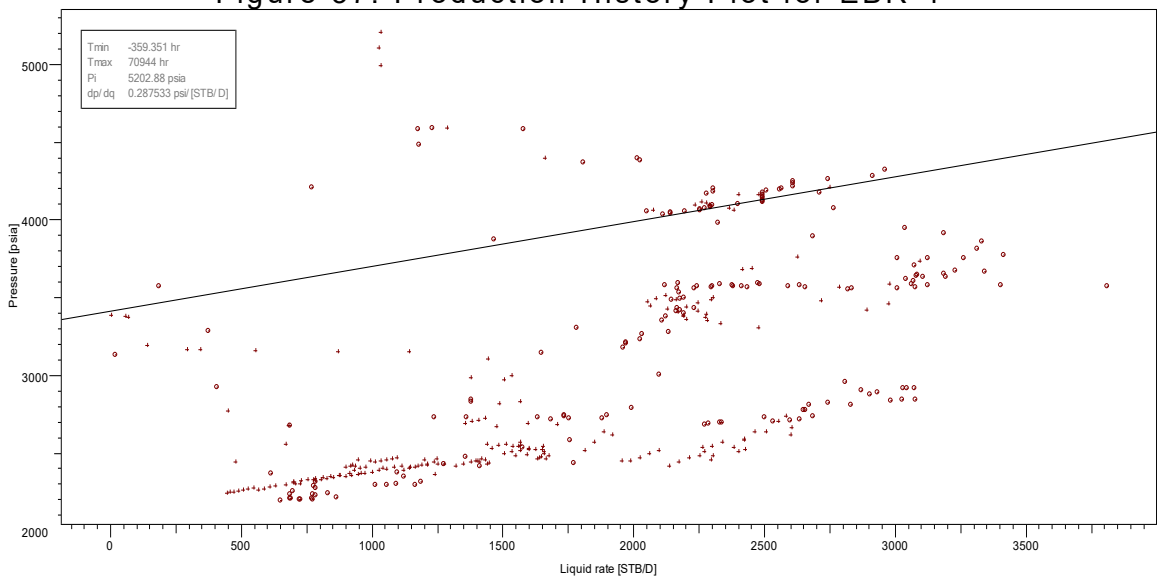

Figure 38. Pressure-Rate Correlation Plot for EBR-1

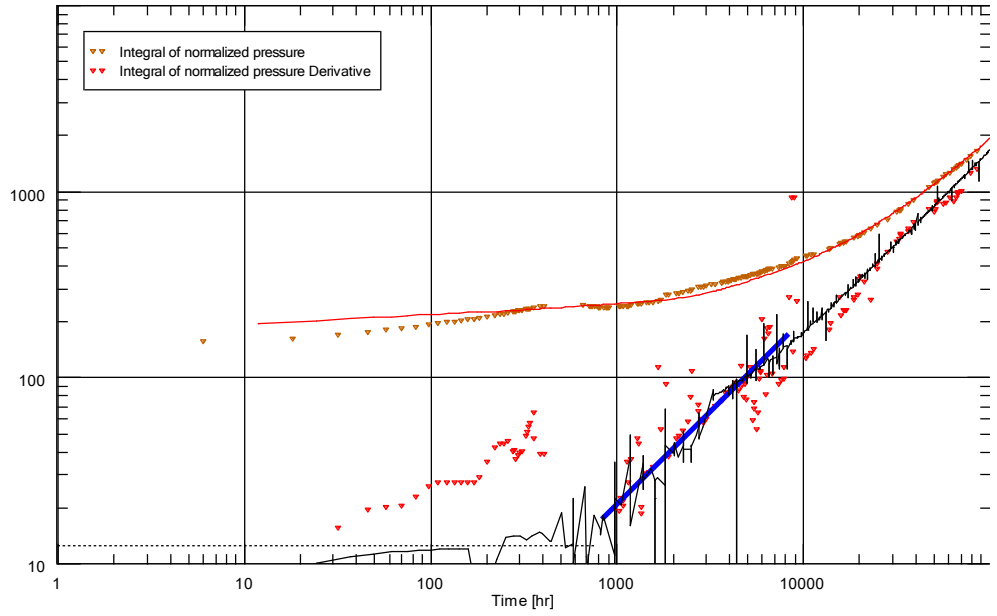

Figure 39. Log-Log Plot for EBR-1

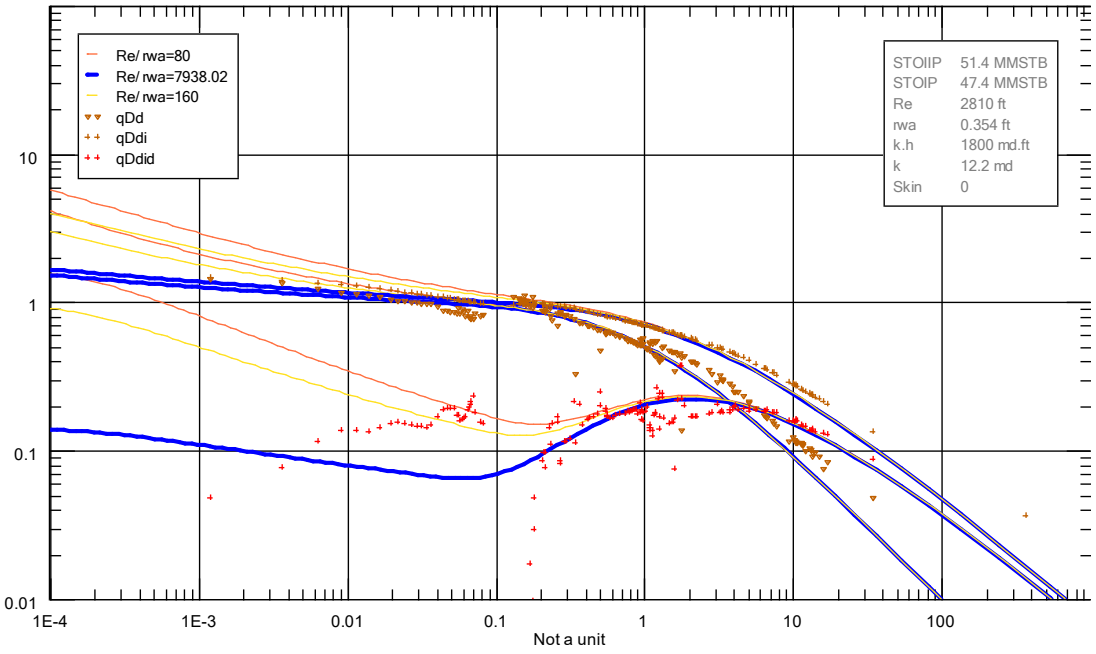

Figure 40. Blasingame Type Curve Plot for EBR-1

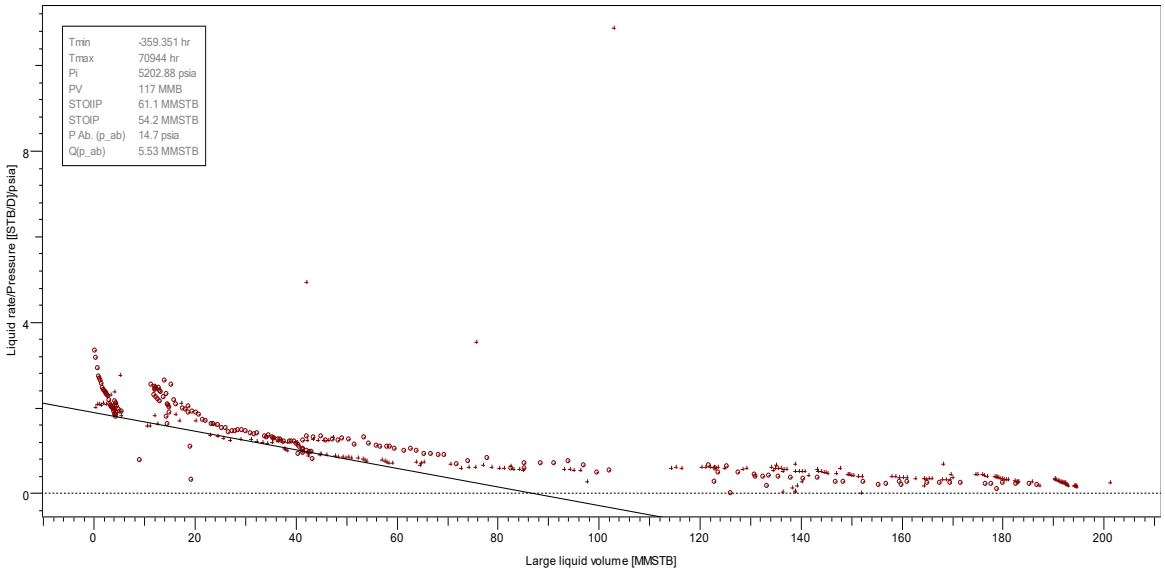

Figure 41. Normalized Rate-Cumulative Plot for EBR-1

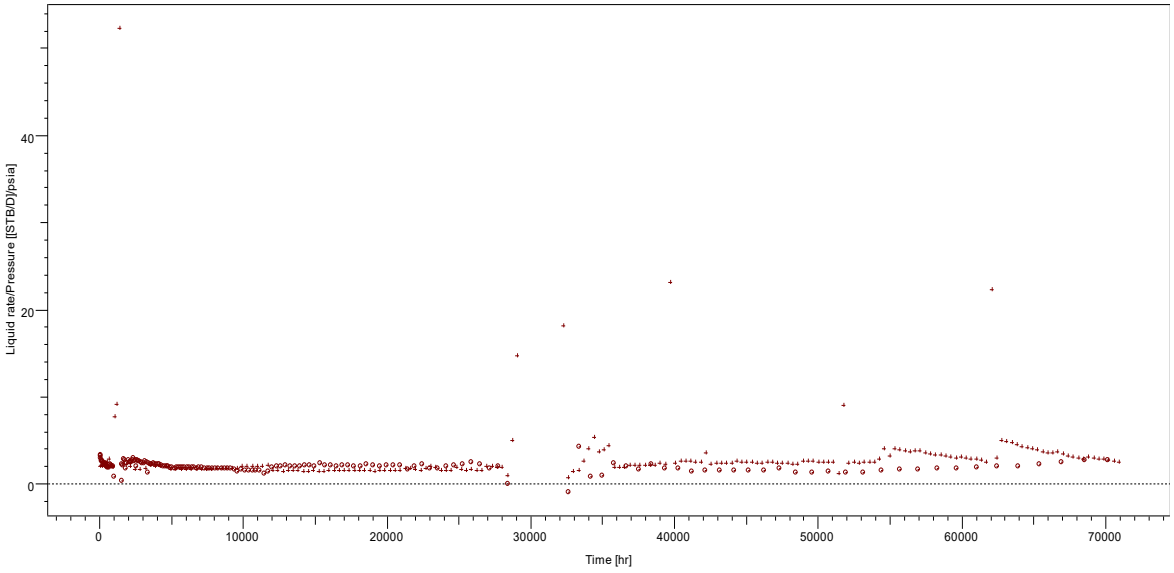

Figure 42. Productivity Index Plot for EBR-1

To investigate the current performance of the well, we used the Arps decline curve analysis. Figure 43 shows the decline profile of the well on late time period. The estimated ultimate recovery is about 1.68 MMSTB and therefore the well would achieve 4.65 MMSTB of oil for an abandonment rate of 100 STB/Day and maximum water cut of 95%. Figure 44 shows the linear extrapolation of the logarithm of water cut versus cumulative oil shows reserves of 4.97 MMSTB. Figure 45 shows the decline performed on the inverse of oil rate versus the material balance time. Figure 46 shows a decline performed on inverse of water cut versus cumulative oil plot. Both analysis show similar results and the ultimate recovery is estimated from this well is about 3.3 MMSTB. The results are summarized in the following table:

Table 14. Decline Curve Analysis results of EBR-1

Method	Period	Reserves (MMSTB)
Log(qo) vs Qo	Late time	4.65
Log(fw) vs Qo	Late time (fw=95%)	4.97
1/qo vs Qo	Average production	3.33
1/fw vs Qo	Average productionws	3.33

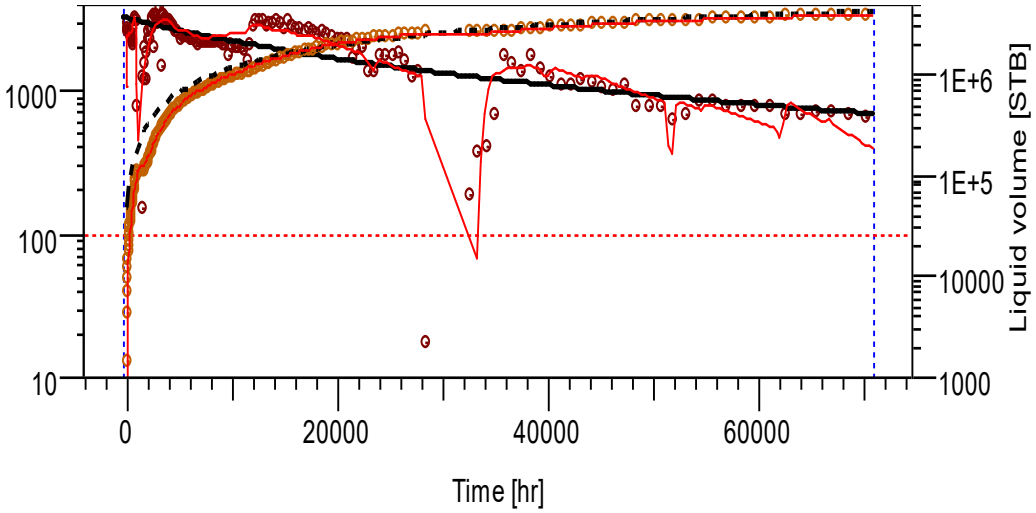

Figure 43. Log (qo) and Cumulative Volume versus time Plot for EBR-1

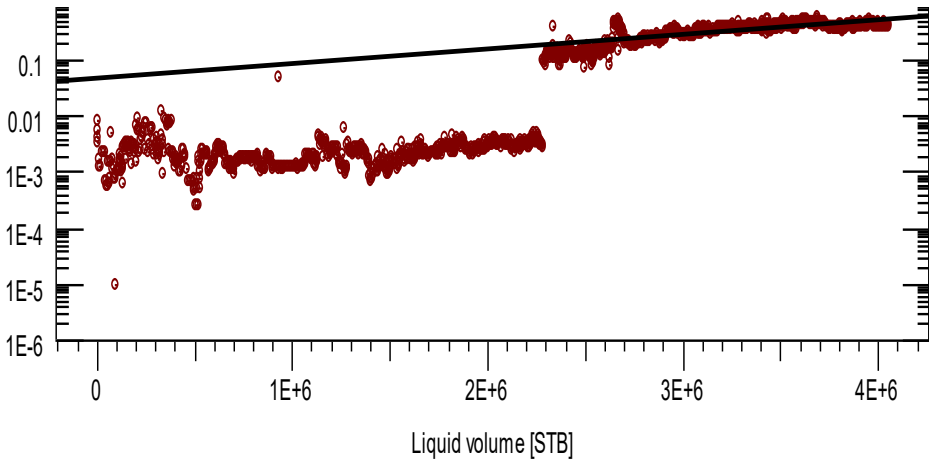

Figure 44. Log (fw) versus Qo Plot for EBR-1

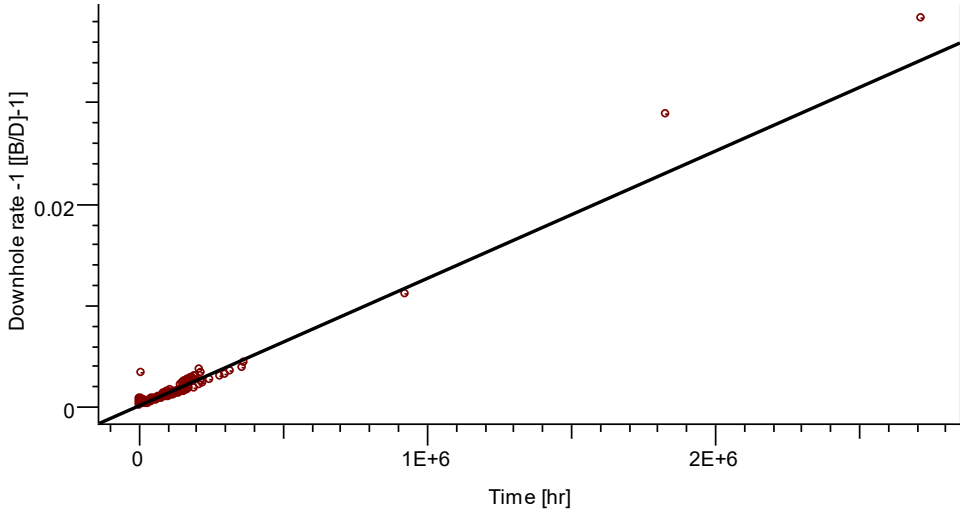

Figure 45. 1/qo versus Material Balance Time for EBR-1

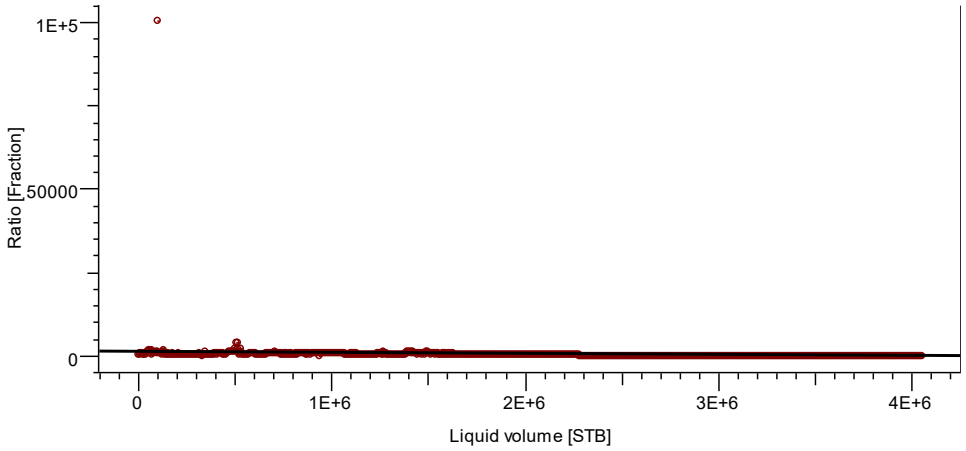

Figure 46. 1/fw versus Qo Plot for EBR-1

To inspect the origin of produced water, we plotted the WOR and the WOR derivative versus time on log-log scale, Figure 47. The results shows noisy data points incapable of identifying trends. Therefore, in Figure 48 we plotted WOR integral and WOR integral derivative on log-log scale. A dominant zero slope and negative slope trends are clearly identified. Thus the water comes basically from water oil contact rising and coning in this well [10].

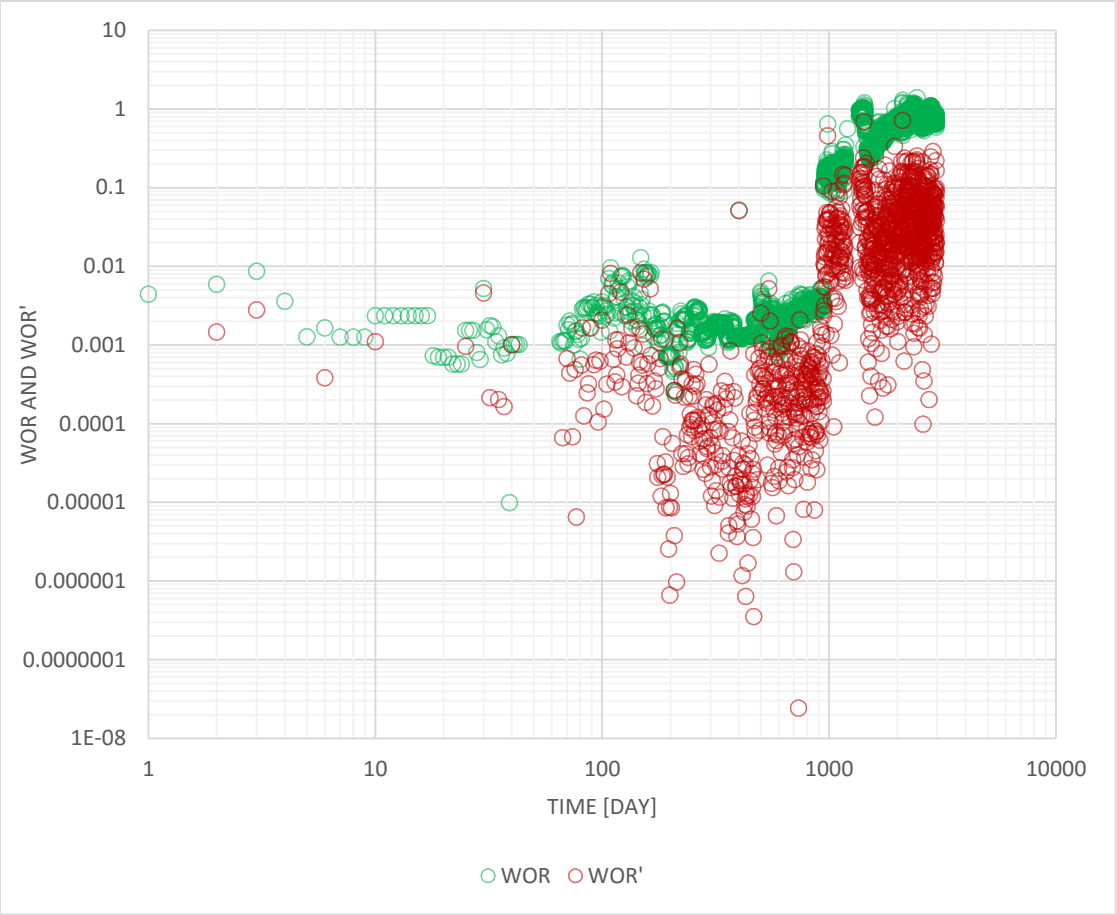

Figure 47. WOR and WOR' diagnostic plots

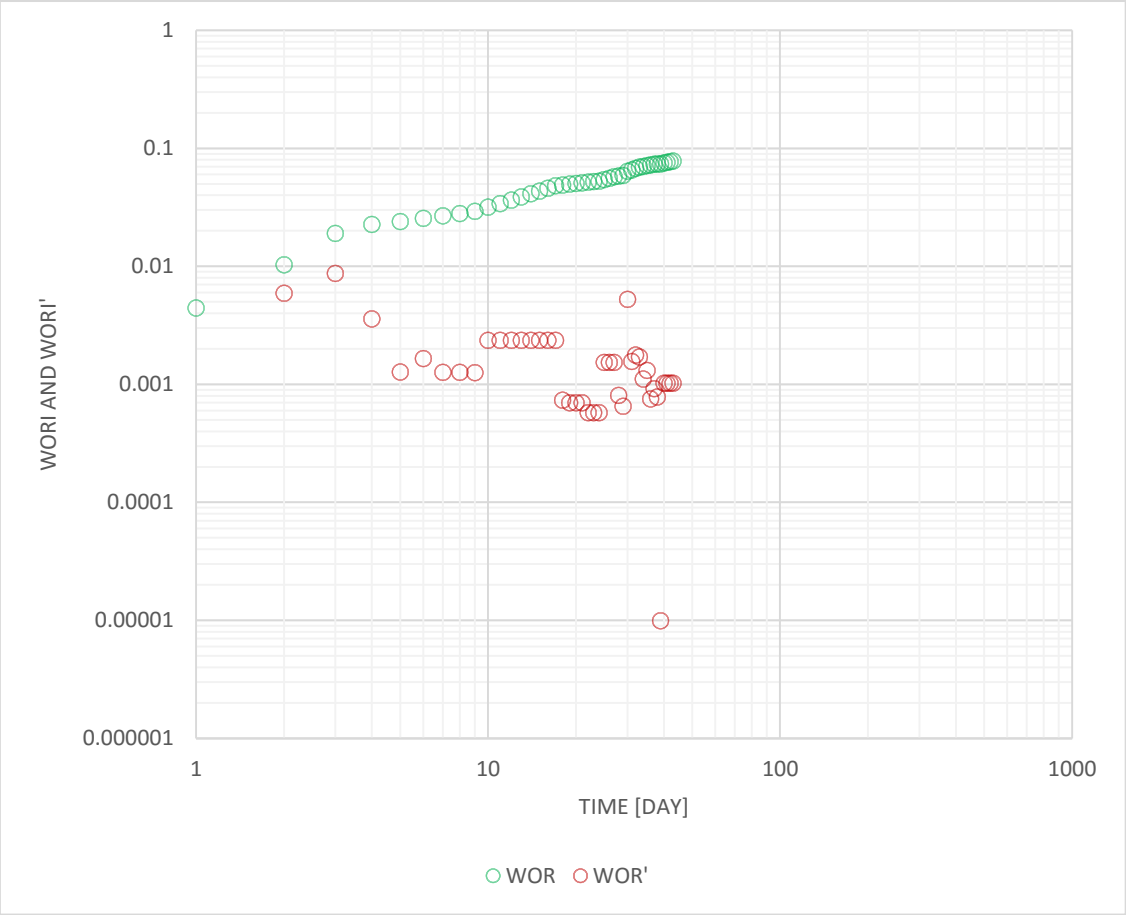

Figure 48. WORi and WORid Diagnostic Plot

3.3 Production Analysis of EBR-3

EBR-3 is currently shut in due to the excessive water production from the well. We note that only wellhead pressures are available. Hence, we focused only on the “Old Stuffs” to analyze EBR-3 performance.

Figure 49 shows the poor correlation between rates and pressures. We point out that the well has undergone different production changes from choke size adjustment to implementation of gas lift system. The one-to-one correlation between well head pressure and flowing bottom hole pressure has allowed us to plot the well head pressure against the rates on a Cartesian scale in Figure 51 [11]. As validation to Figure 50, the pressure-rate plot depicts clearly the poor the correlation between pressure and rates. And yet, we tried to convert the wellhead pressure to bottom hole pressure from generated VLP using the well intake option in Topaze. Figure 49 shows the new calculated pressures. Several reservoir models were tried including circular, rectangular and multilayers with different boundaries. We found that none of them can validate the pressure/rate history due to the fact of poor correlation. This latter was noticeably identified in the Log- Log plot and Blasingame plot with an off-trend in the transient period. To remove ambiguities, we plotted the calculated bottom hole pressure against rates. Indeed, this plot asserted

the inconsistent trends obtained from other methods. However, a weak transient signature can be extracted out of the plot with a slope of -0.039 Psi/STB/D. Blasingame plot and Normalized rate-Cumulative plots in Figure 52 Figure 53 give an estimation of oil place around 22.5 MMSTB and 21.3 MMSTB respectively. We conclude that these estimates are far from reality due to the suspected accuracy in bottom hole pressures calculations.

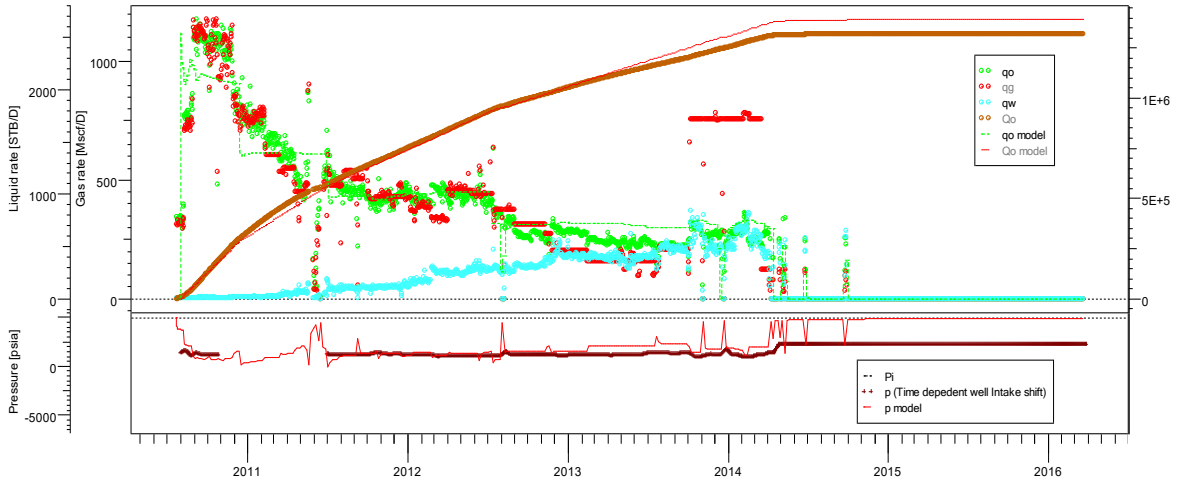

Figure 49. Production History Plot for EBR-3 using Bottomhole Pressure.

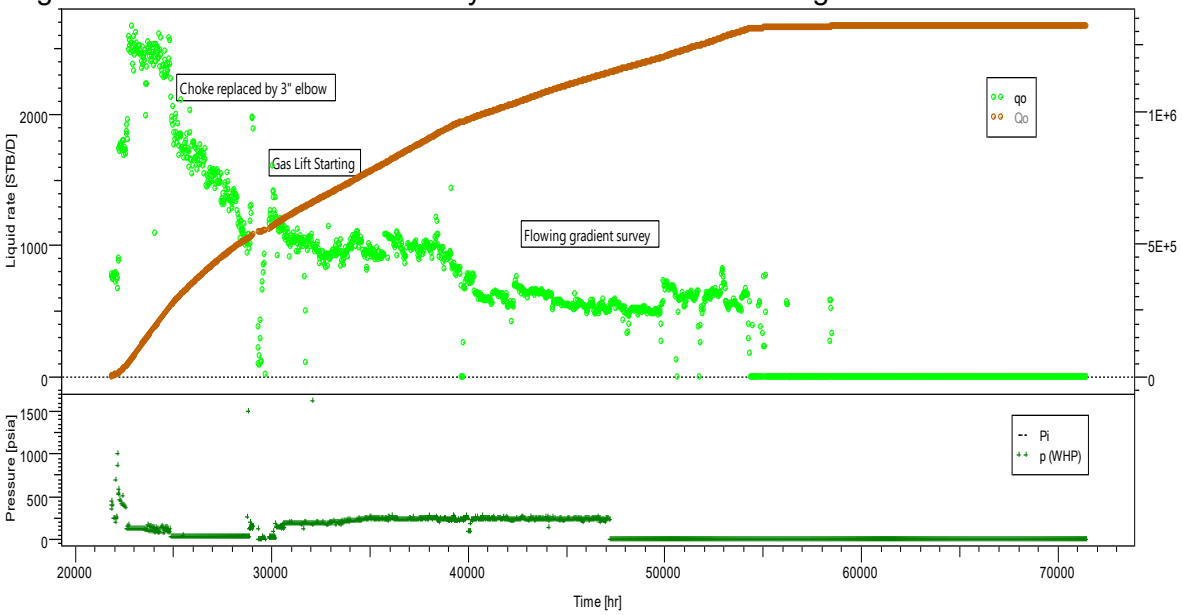

Figure 50. Production History Plot for EBR-3 using Wellhead Pressures

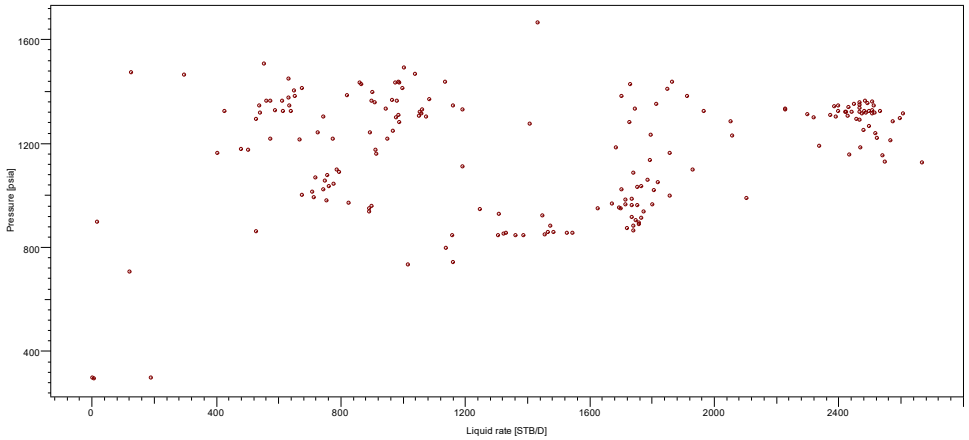

p-q plot: p [psia] vs q [STB/D]

Figure 51. Pressure- Rate Plot for EBR-3 using Bottom Hole Pressure

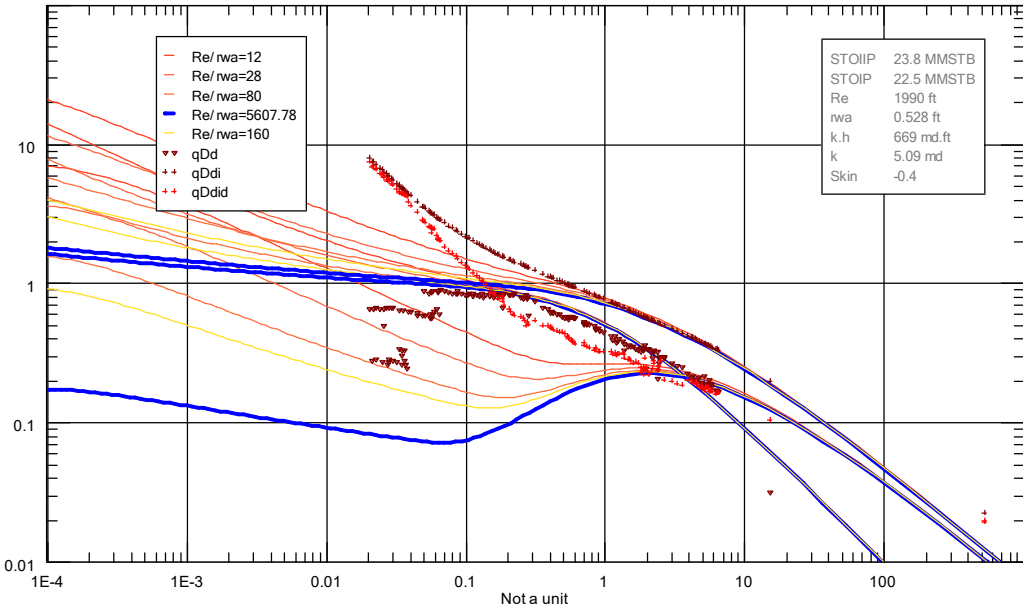

Figure 52. Blasingame Type Curve Plot for EBR-3

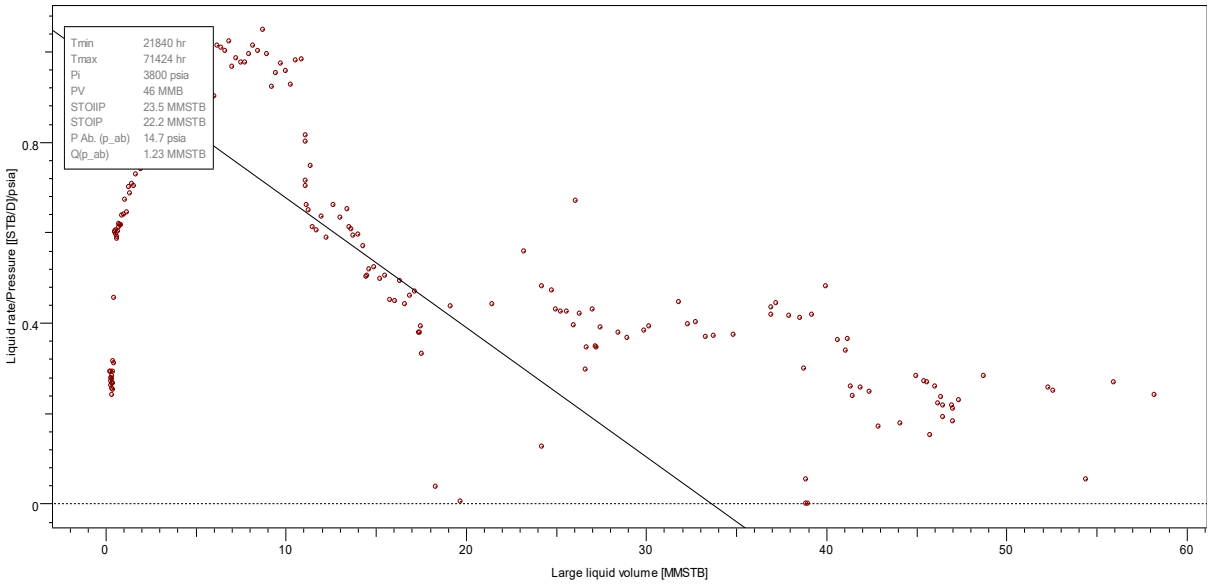

Figure 53. Normalized Rate-Cumulative Plot for EBR-3

Furthermore, in Figure 49, we present the simulated model as a final step to assess the validity between pressure/rate histories. We found that the raw data are better simulated using infinite reservoir model. These results lent credence to our judgment about the oil in place which cannot be reliably estimated from such model as boundaries are not reached.

Figure 54 to Figure 57 represent the “old stuff” (i.e. Arp’s plots) decline curve analysis. In Figure 54, we plotted oil versus cumulative oil produced and the reserves were estimated as 0.95 MMSTB. The decline curve analysis is based on the average decline observed on production data for an abandonment rate of 100 STB/D. In Figure 55 we used the inverse of oil rate against the material balance time and we estimated the reserves from 99% water cut. The analysis shows that total recoverable reserves from EBR-3 are around 1.33 MMSTB. Figure 56 presents the water cut versus the cumulative oil rate on a semi-log plot and Figure 57 illustrates the inverse of water cut versus the cumulative oil rate. The extrapolation of the line on average production yields to estimated reserves of 1.35 MMSTB in Figure 56while the extension based on late time in Figure 57 yields to recoverable reserves of 1.08 MMSTB.
Table below summarizes the reserves found from different methods and corresponding extraction period accordingly.

Table 15. Decline curve analysis results

Method	Period	Reserves (MMSTB)
Log(qo) vs Qo	Average production	0.95
1/qo vs Qo	Late time (fw=99%)	1.33
Log(fw) vs Qo	Average production	1.35
1/fw vs Qo	Late time	1.08

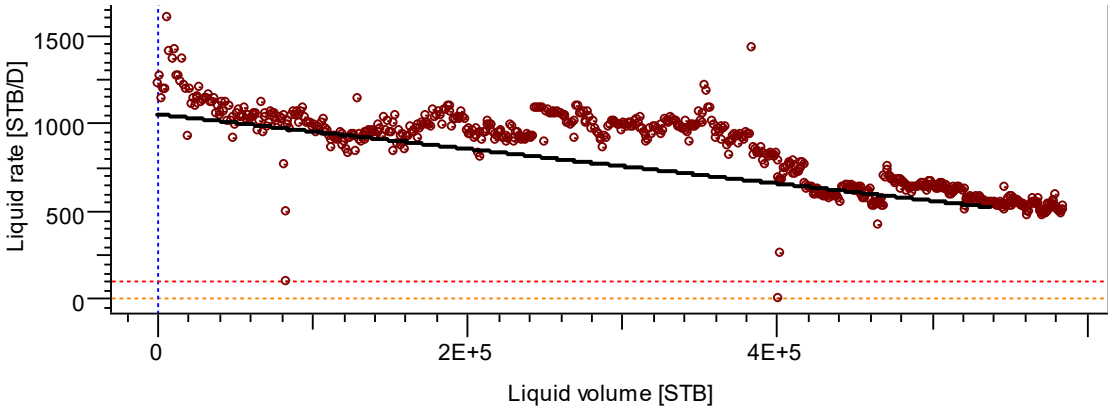

Figure 54. Oil rate versus cumulative oil plot

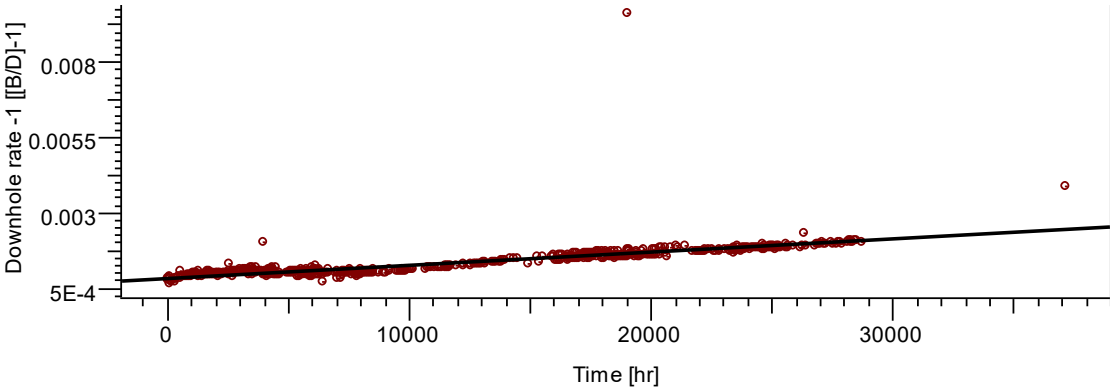

Figure 55. 1/qo versus material balance time plot

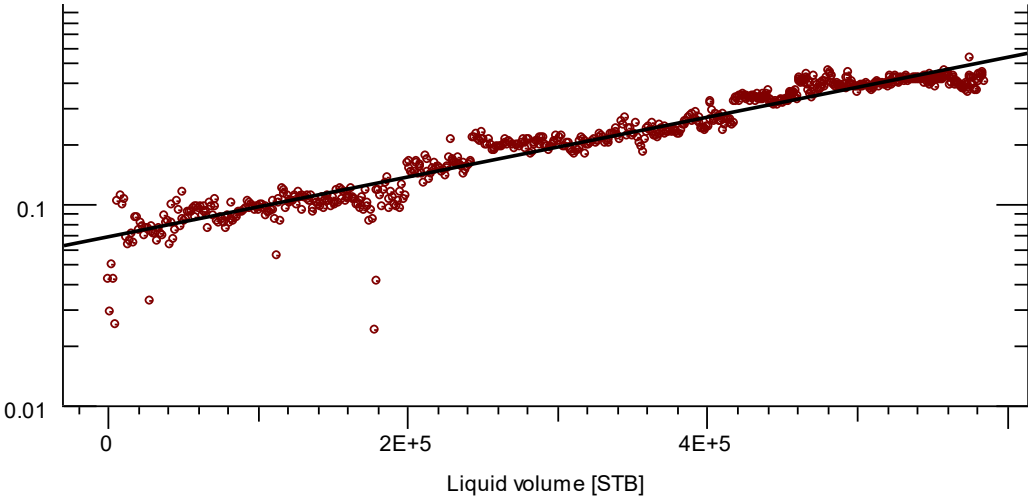

Figure 56. Log (fw) versus Cumulative oil plot

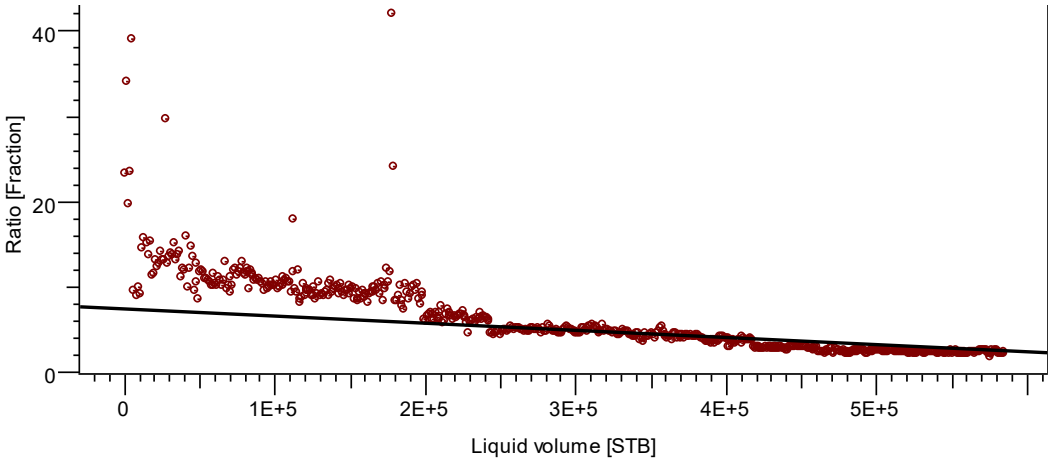

Figure 57.1/fw versus cumulative oil rate plot

At late time, water production increased inevitably due to the higher rates produced in this period. Eventually, the well was loaded up in March, 2014. To investigate the origin of water we used diagnostic plots suggested by Chan and lately by Bondar and Blasingame [10] [12]. In Figure 58, we plotted the WOR and its derivative versus time on a log-log plot. We clearly identified a positive slope of WOR a positive slope in the WOR curve in the late time while derivative curve shows noisy signature. To eliminate the noise illustrated in Figure 59, we plotted the WOR integral and its derivative on a logarithmic scale. Figure 59 shows clearly the positive slopes on both curves. The analysis, therefore, proves that the water origin is from multilayer channeling which could be the high permeability streaks. Further analysis, this Figure, indicates that the occurring of negative slope on derivative accompanied by two consecutive positive slopes characterize the combination of two water production mechanisms, Chan explained this as water coning with late time multilayer channeling. Moreover, the presence of two different positive slopes in the late indicates the

channeling from layers [10]. As discussed earlier in the well performance section, the water was mainly producing through SSD A. this part of the completion obviously has relatively high initial water saturation and permeability with respect to other SSD's. Therefore, we recommend the shut-in of SSD A to curtail the water production. Additionally, SSD B shows depleted pressure with respect to SSD A, we believe that crossflow occurred within the well and slowed down oil production. If successful, this simple operation can allow the well to recover approximately 1 MMSTB as demonstrated from Decile curve analysis.

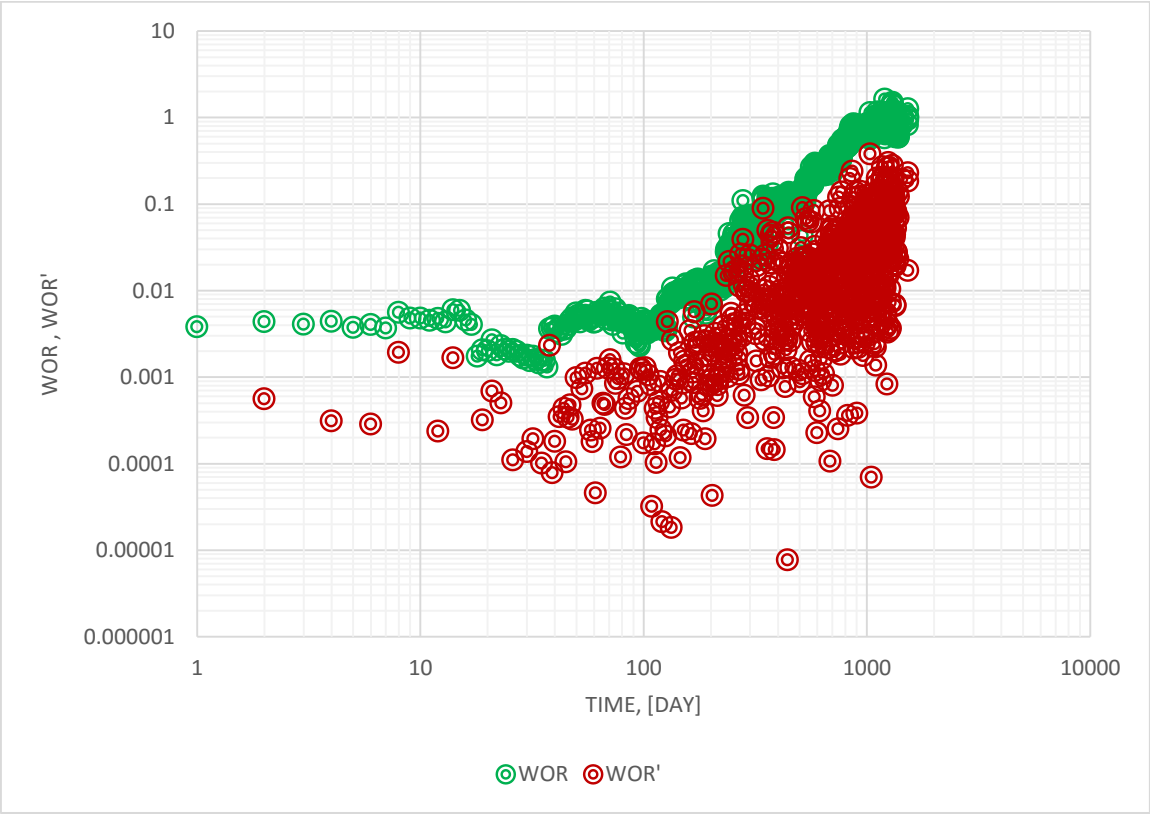

Figure 58. WOR and WOR' diagnostic plot of EBR.3

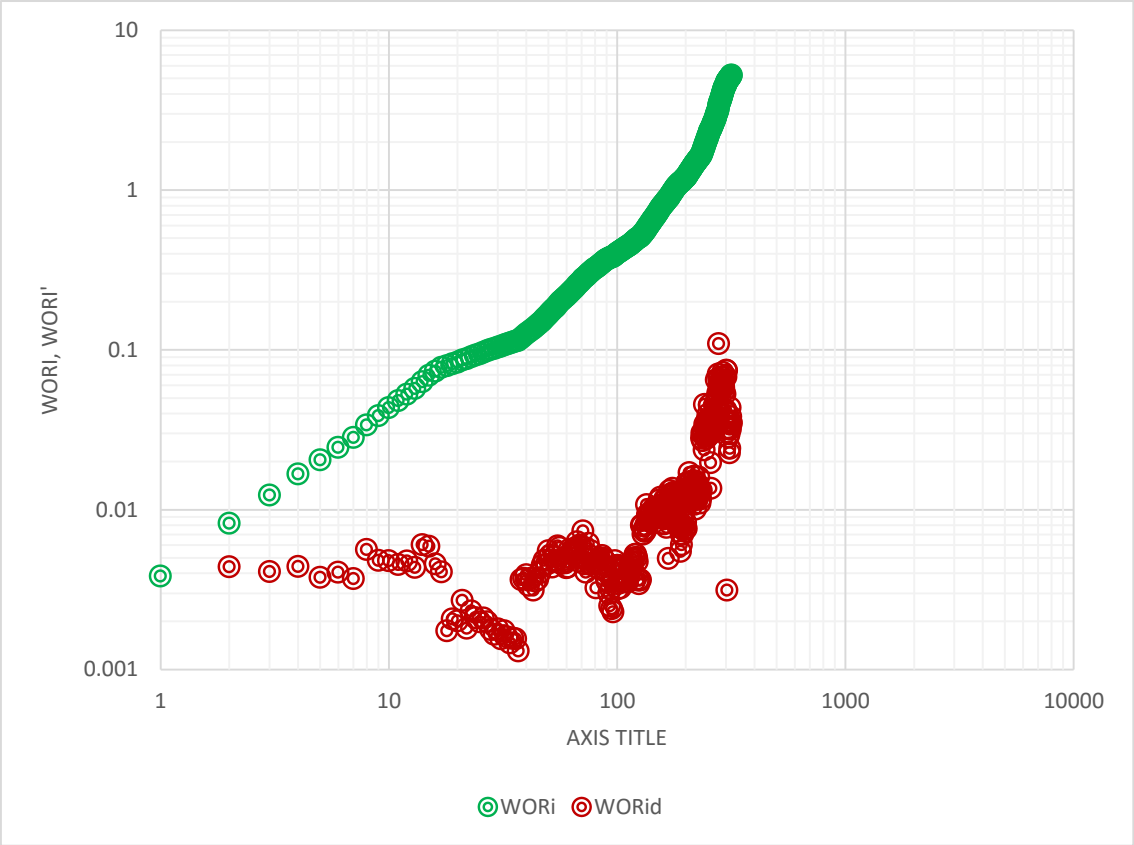

Figure 59. WORi and WORid diagnostic plot of EBR-3

3.4 Production Analysis of EBR-4

EBR-4 has been produced quite erratically. Figure 60 shows the production/pressure history of the well. We mark that the downhole gauge has given wrong response in the late time. However, we note that part of this increase in pressure is due mainly to water production which leads to increase in mixture density and decrease in Gas-Liquid ratio. We observed also that between June, 2011 and February, 2012 the production rates were over allocated. This unrealistic behavior was confirmed by the production test performed in November, 2011.

Further diagnostic is provided by pressure-rate plot in Figure 61. We found that the early time (i.e. before the erratic behavior) has exhibited a pseudo steady state flow regime whereas the late time indicated a weak correlation between pressure and rates, though, a negative slope indicating transient flow regime was identified as well.

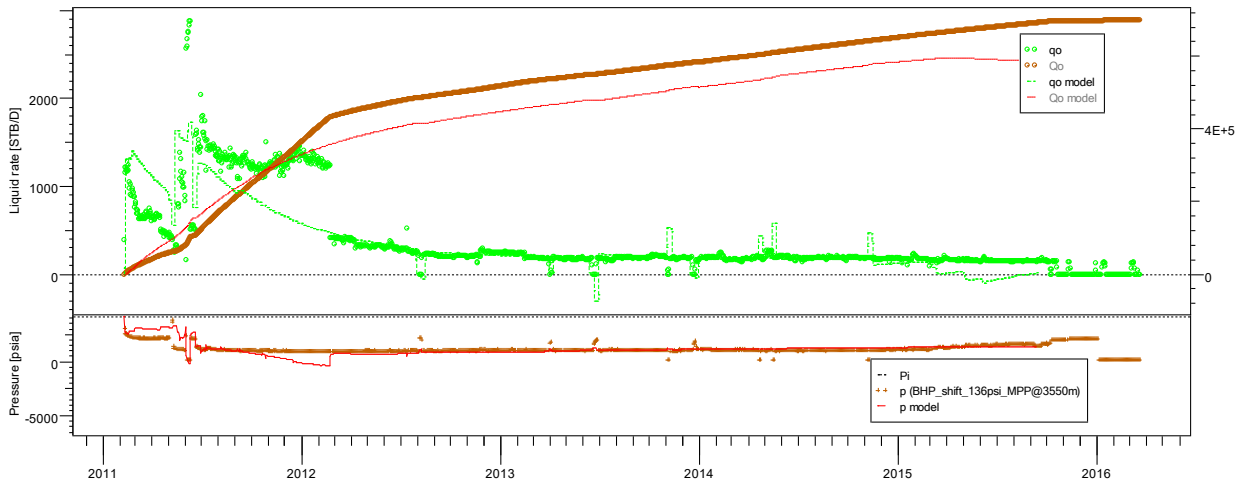

Figure 60. Production History and Simulated model response of EBR-4

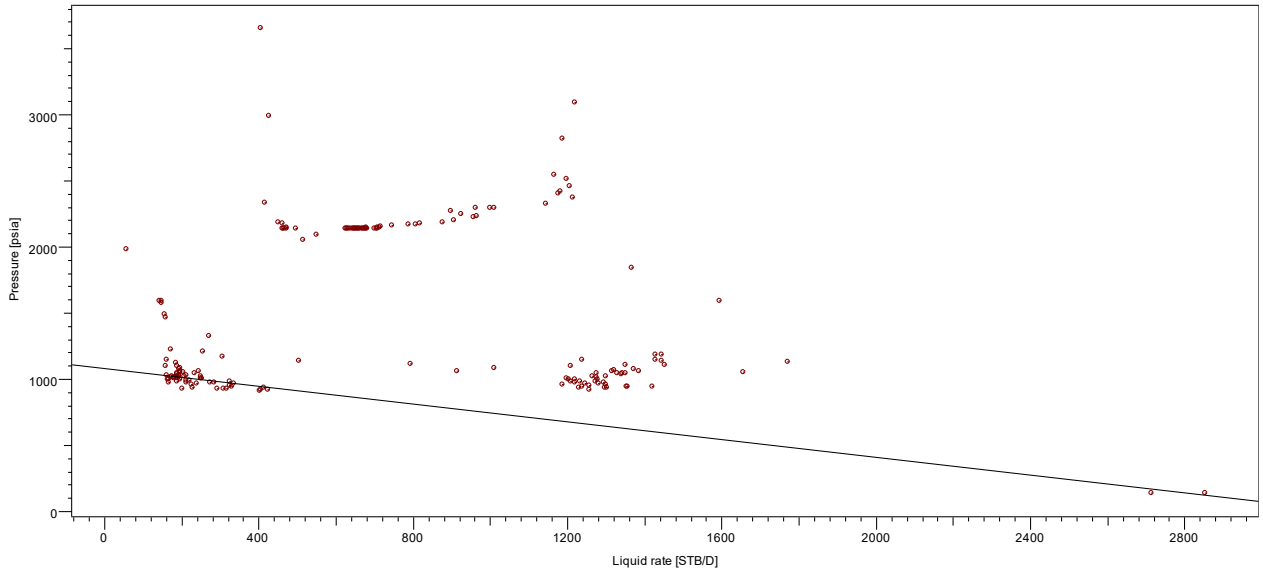

p-q plot: p [psia] vs q [STB/D]

Figure 61. Pressure- Rate Plot for EBR-4

Blasingame plot and rate cumulative plots are shown in Figure 62 Figure 63. The extrapolation of the identified pseudo steady state period in figure 60 indicated that the oil in place are around 11.3 MMSTB. The trend matching in Blasingame type curves estimated the oil in place as 11.4 MMSTB. On the other hand, Fetkovich type curve in Figure 64 Figure 60shows a decline exponent of 0.7 which is typical for multilayer reservoirs.

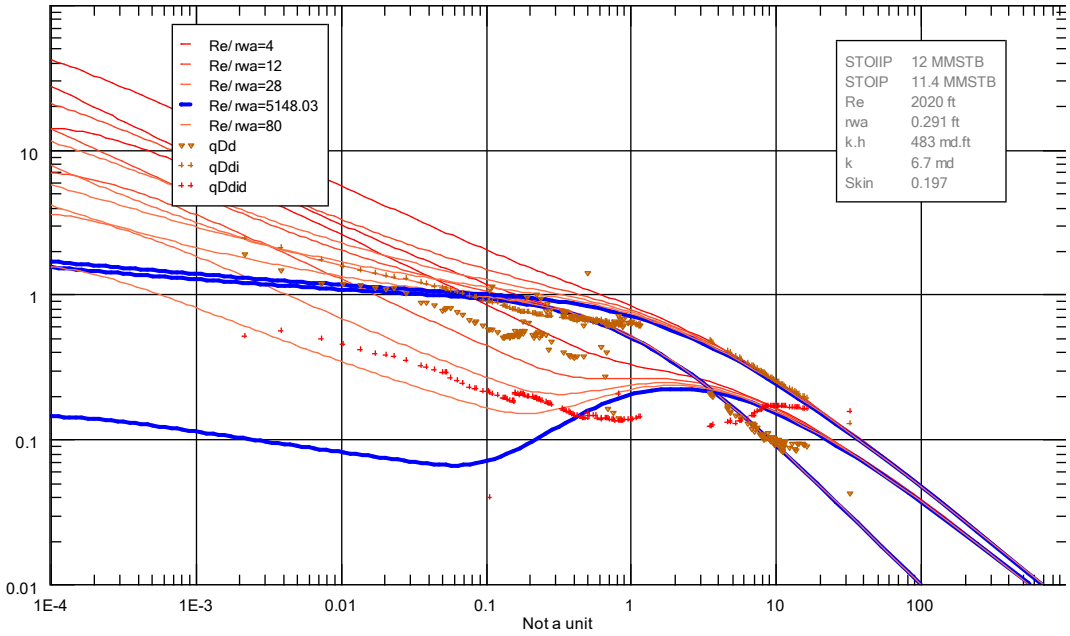

Figure 62. Blasingame Type Curve Plot for EBR-4

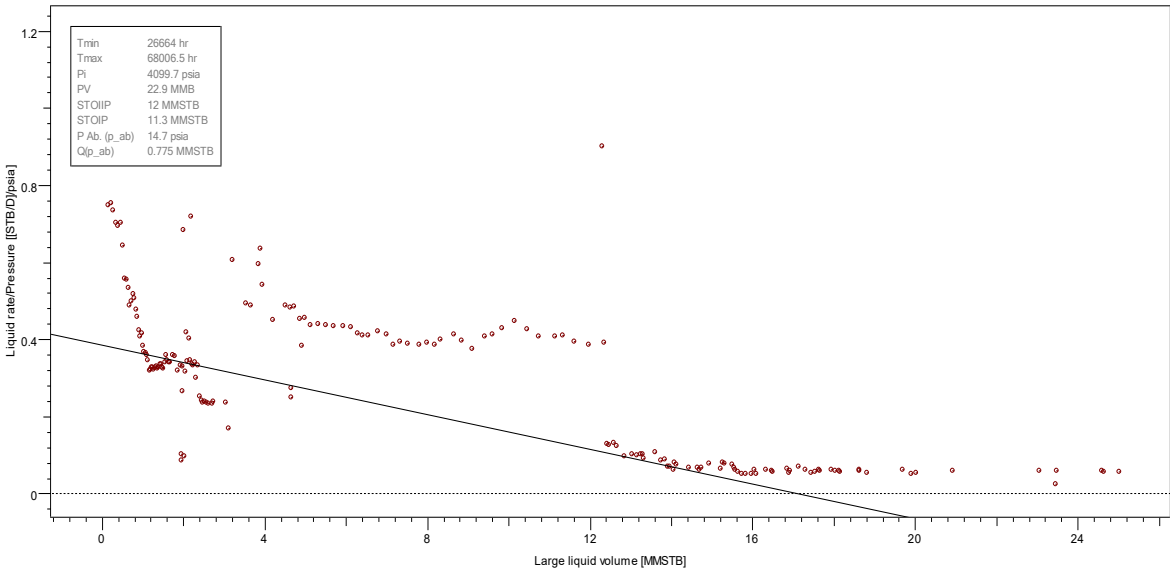

Normalized Rate-Cumulative: q/(Pi-Pwf) [[STB/D]/psia] vs Q/Ct/(Pi-Pwf) [MMSTB]

Figure 63. Normalized Rate-Cumulative plot for EBR-4

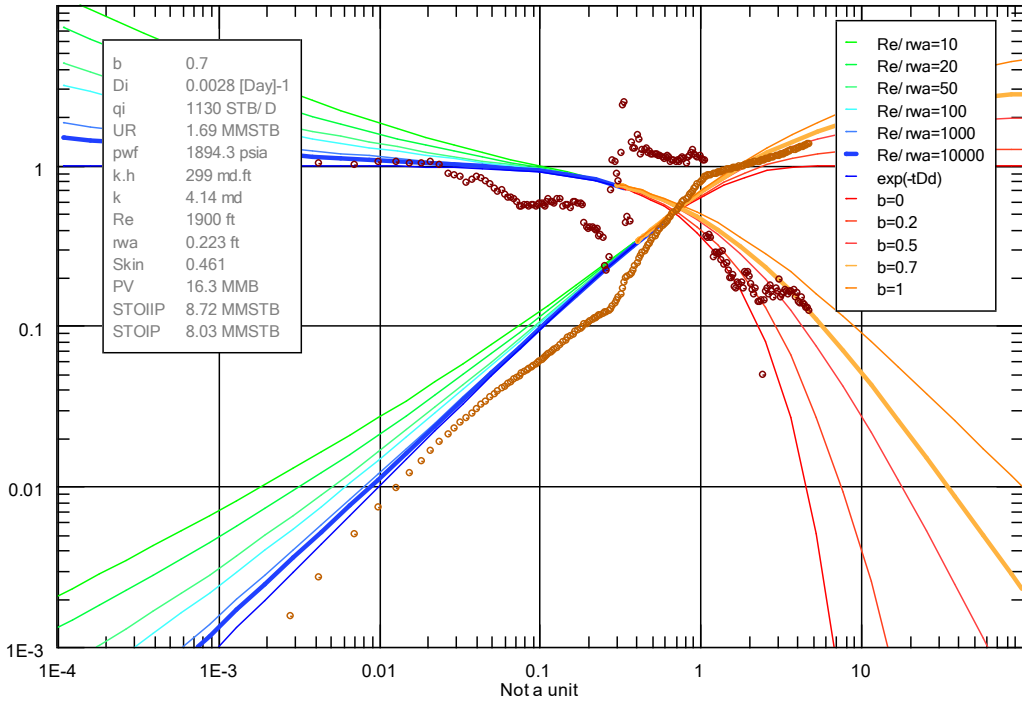

Figure 64. Fetkovich Type Curve Plot for EBR-4

The final validation of production analysis is shown in Figure 60 where the simulated rates depict clearly the erratic production between June 2011 and February 2012. Production allocation of the wells will be discussed in details in the next chapter.

The analysis of decline curves using different methods are shown in Figure 65 to Figure 68. In Figure 65, the linear extrapolation of the late time period yields to 0.632 MMSTB as recoverable oil for an abandonment rate of 20 STB/D. Figure 66 shows the decline analysis of logarithm of water cut against cumulative oil. The estimated reserves are around 0.865 MMSTB from average production. The analysis of the inverse of water cut vs the cumulative oil for late time period shows that the reserves are about 0.74 MMSTB in Figure 67. Figure 68 shows the inverse of rate versus the material balance time. The linear extension of the line for late time period shows that the well reserves are around 0.677MMSTB. These low estimates from decline curve analyses reflects the poor reservoir rock characteristics of the well.

Table 16. Decline Curve Analysis results of EBR-4

Method	Period	Reserves (MMSTB)
Log(qo) vs t	Late time	0.632
1/qo vs Qo	Late time (fw=99%)	1.33
Log(fw) vs Qo	Average production	1.35
1/fw vs Qo	Late time	1.08

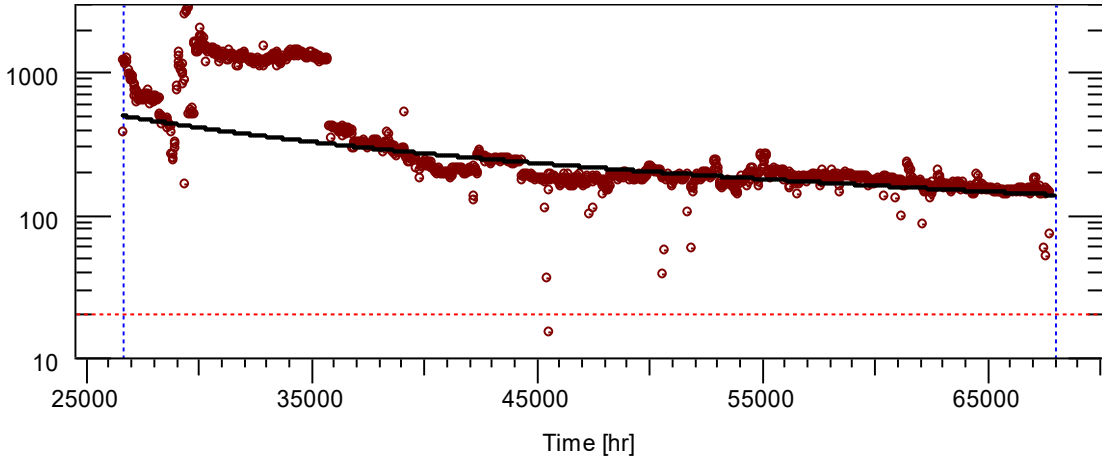

Figure 65. Log (qo) versus time plot

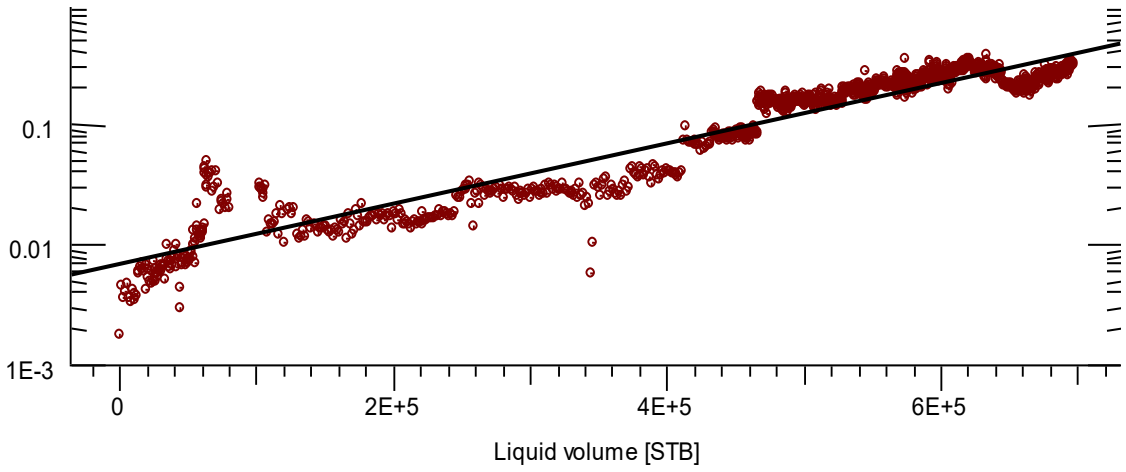

Figure 66. Log (fw) versus Cumulative oil plot of EBR-4

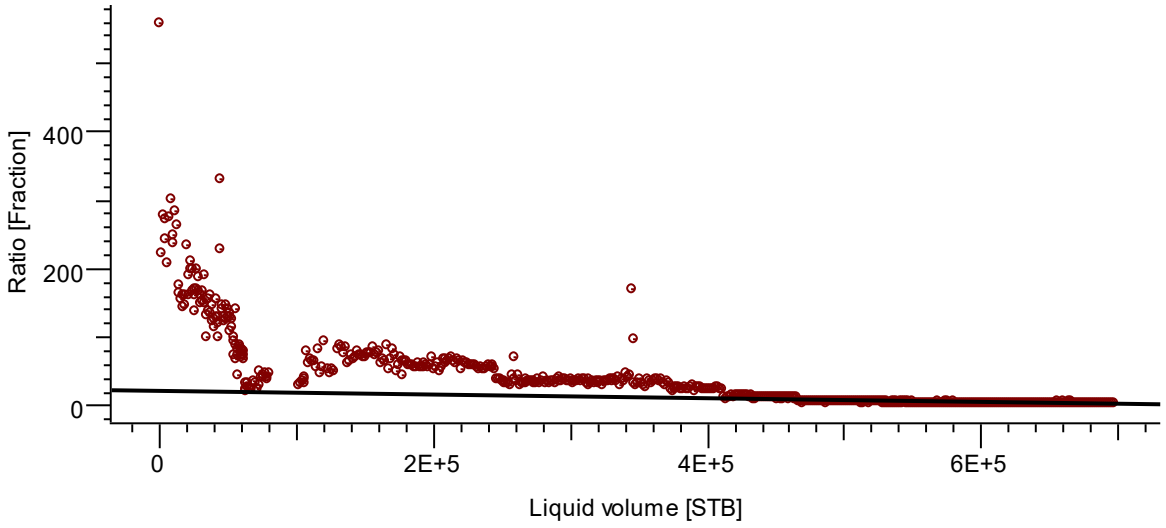

Figure 67. 1/fw versus Cumulative oil plot of EBR-4

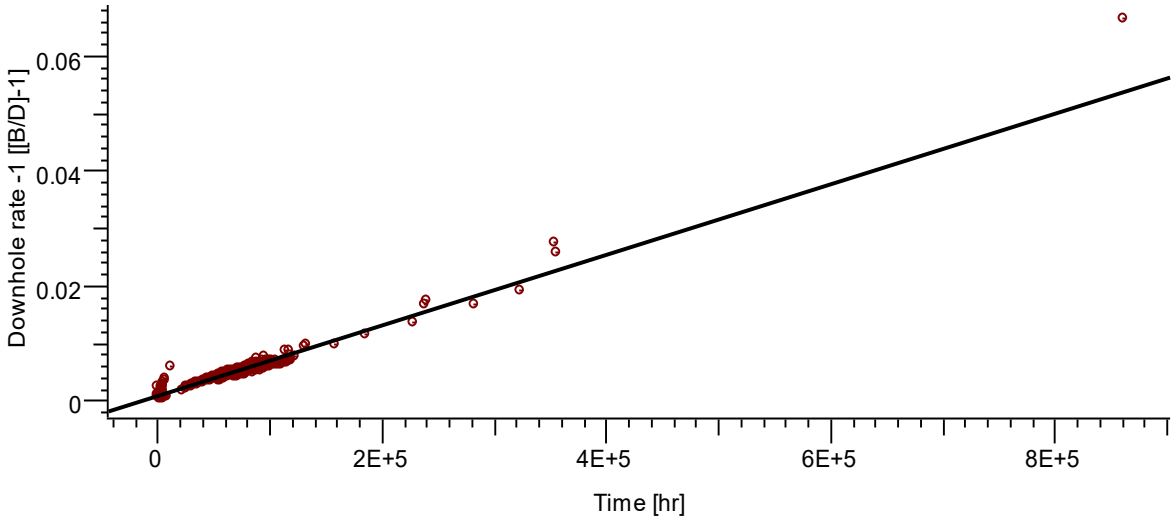

Figure 68. 1/qo versus material balance time of EBR-4

Figure 69 and Figure 70 show the WOR diagnostic plots for EBR-4. We observe a slightly positive slope and a negative slope on WOR integral derivative curve in Figure 70. This is probably due to water channeling followed by water coning in more than one layer. Although, EBR-4 has produced low amount of water, this phenomena should be resolved as early as possible to avoid water problems like those seen in EBR-3 and EBR-5.

Figure 69. WOR and WOR' diagnostic plot of EBR-4

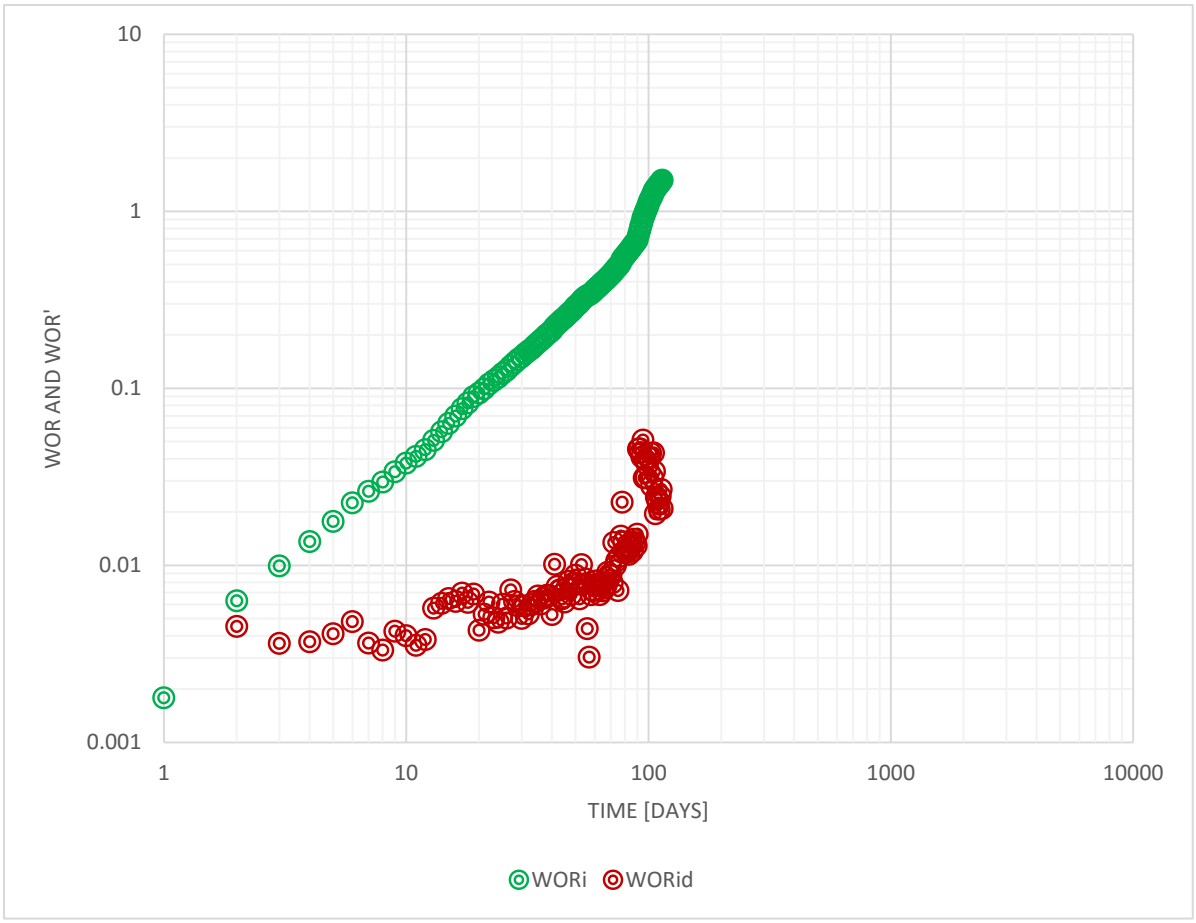

Figure 70. WORi and WORid diagnostic plot of EBR-4

3.5 Production Analysis of EBR-5

EBR-5 was loaded up in July 2013 due to the excessive water production. In Figure 72 the pressure- rate plot shows two positive slopes indicating the pseudo steady flow regime. In Figure 73 and Figure 74, the Blasingame type curve plot and Normalized rate-Cumulative plot indicate a good match. The oil in place is around 10.3 and 9.26 MMSTB respectively. Fetkovich plot prove that well is depleting from multilayer system with decline exponent of 0.9 (Figure 75).

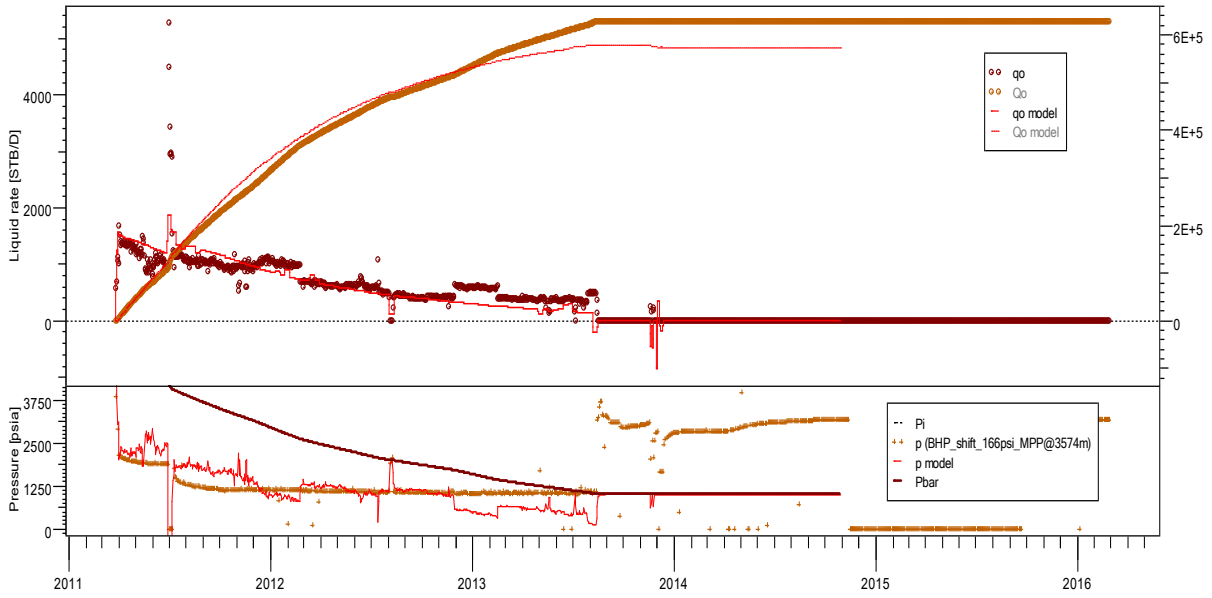

Figure 71. Production History and Simulated Model Response for EBR-5

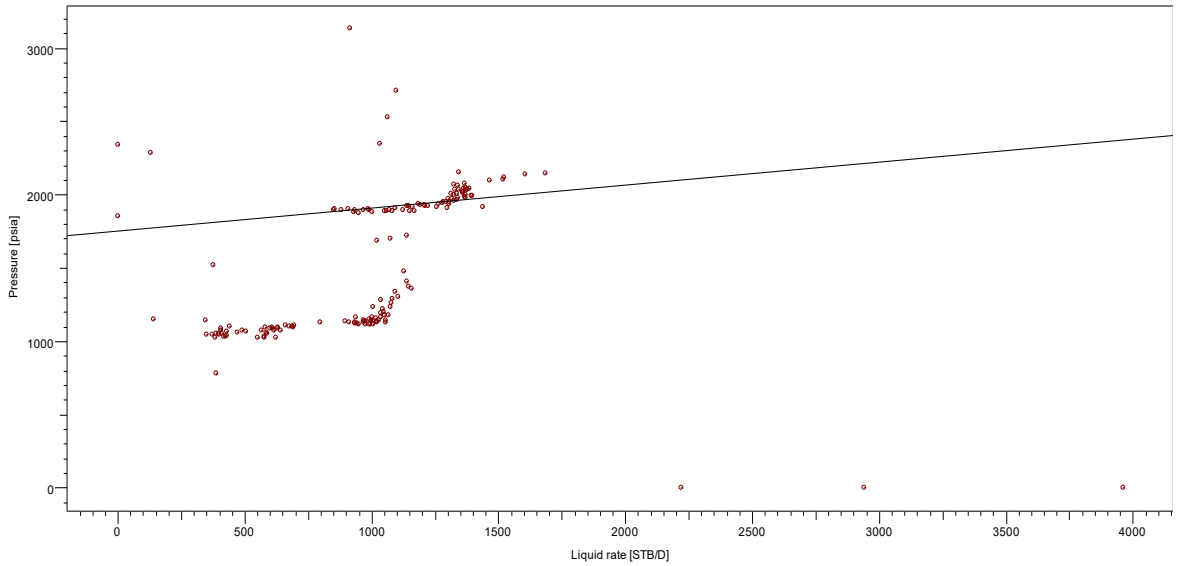

Figure 72. Pressure-Rate Plot for EBR-5.

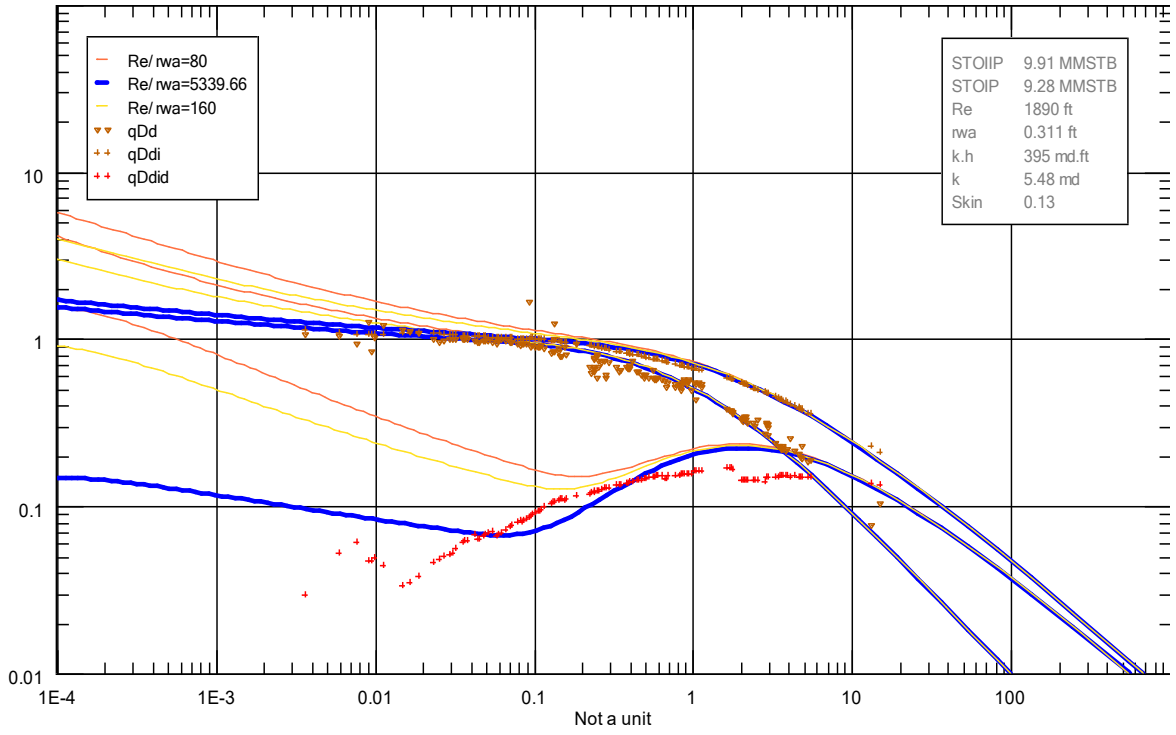

Figure 73. Blasingame Type Curve Plot for EBR-5

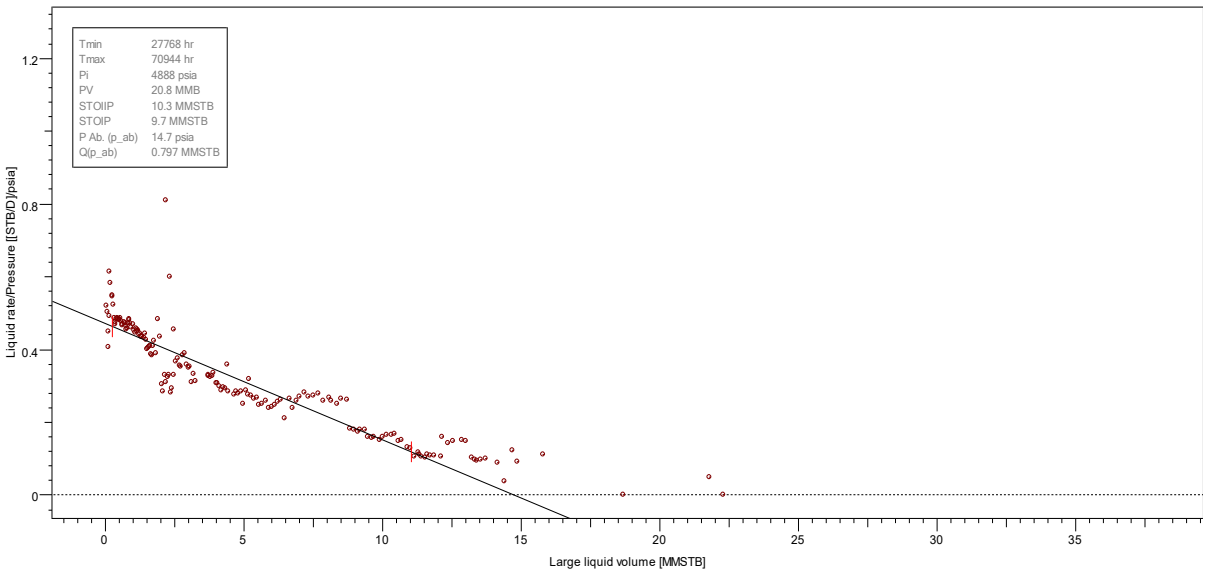

Figure 74. Normalized Rate-Cumulative Plot for EBR-5

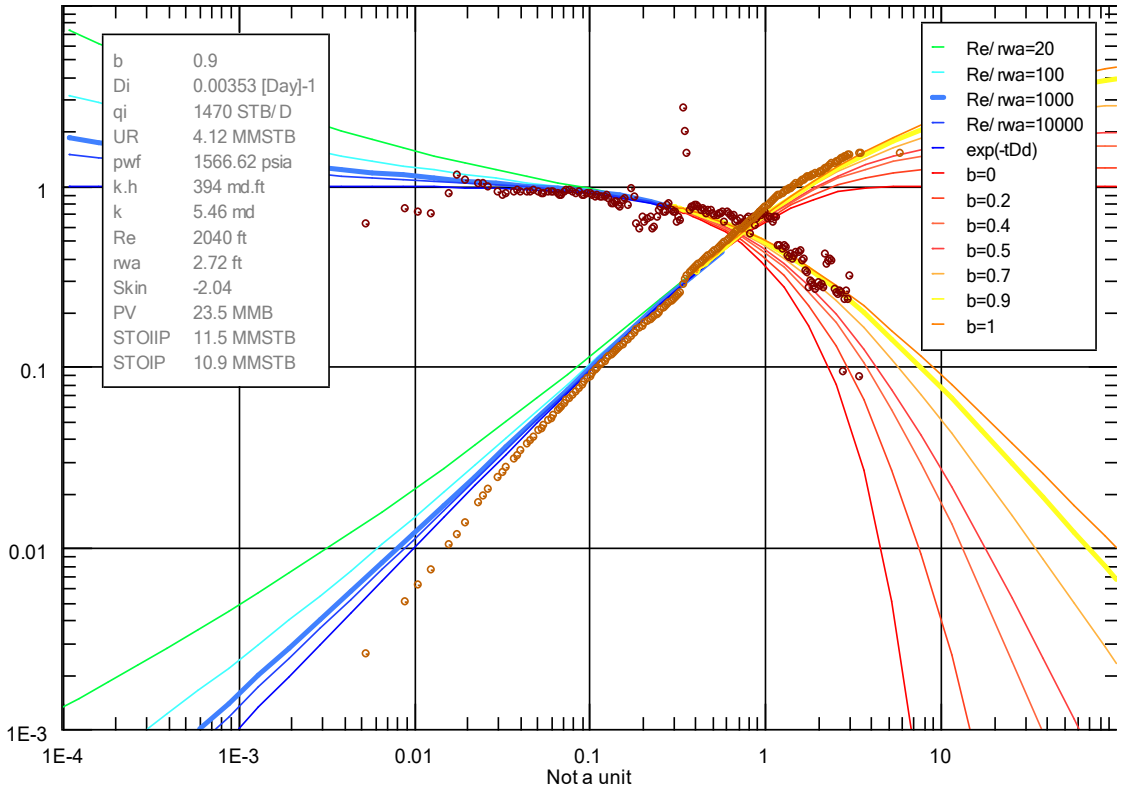

Figure 75.Fetkovich Type Curve for EBR-5

The decline curve analysis in Figure 76 and Figure 77 of oil rate versus cumulative oil rate and the logarithm of water cut against cumulative oil rate show that the current estimated reserves are about 0.132 MMSTB and 1.31 MMSTB for 99% water cut respectively, while linear extrapolation of the inverse of water cut versus cumulative oil rate and the oil rate versus material balance time show respectively reserves of 0.901 MMSTB and 0.629 MMSTB in Figure 78 and Figure 79.
The table below represent the reserves estimated from different methods and the corresponding extrapolation period accordingly.

Table 17. Summary of Decline Curve Analysis for EBR-5

Method	Period	Reserves (MMSTB)
qo vs Qo	Average production	0.132
Log(fw) vs Qo	Average production	1.31
1/fw vs Qo	Late time	0.901
Qo vs Tmb	Late time	0.629

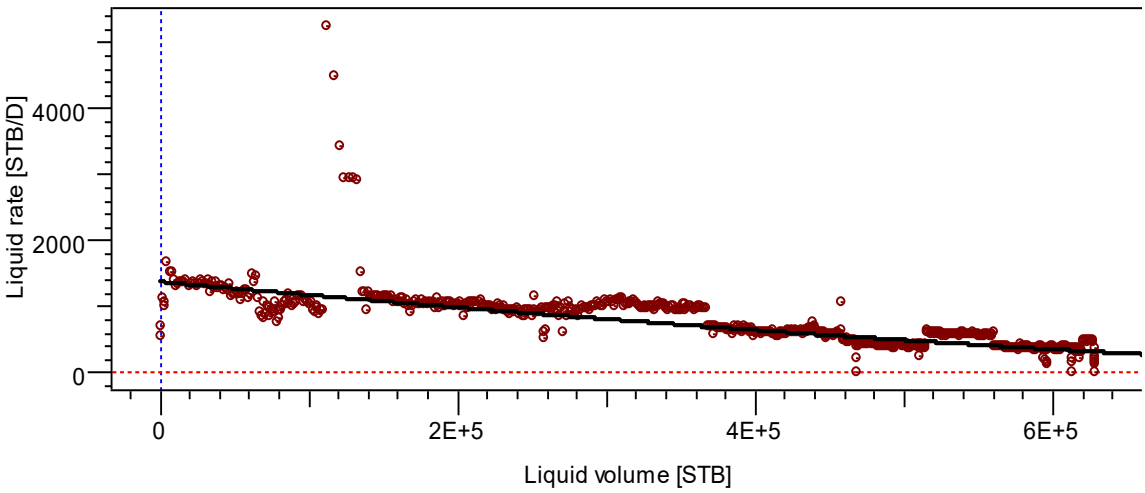

Figure 76. qo versus Qo plot for EBR-5

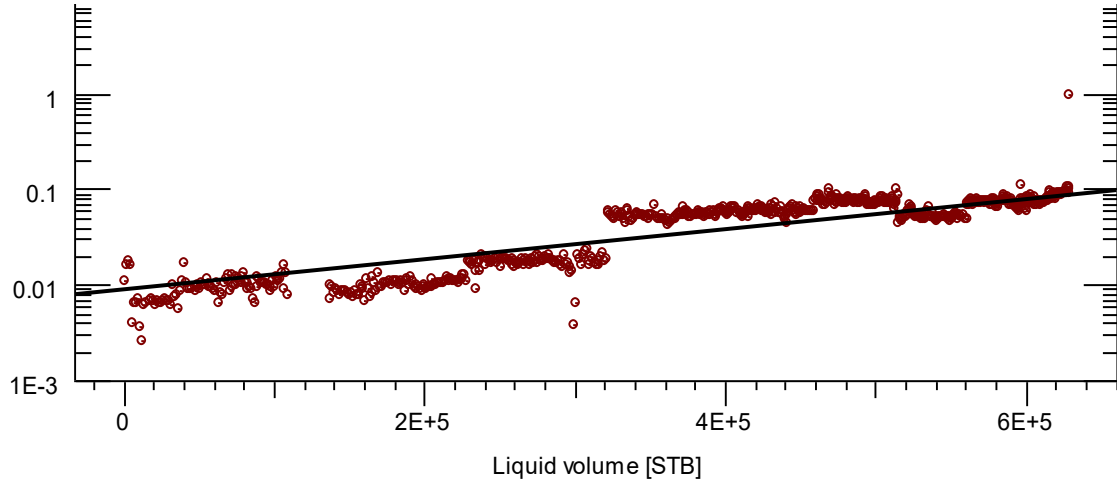

Figure 77. Log (fw) versus Qo plot for EBR-5

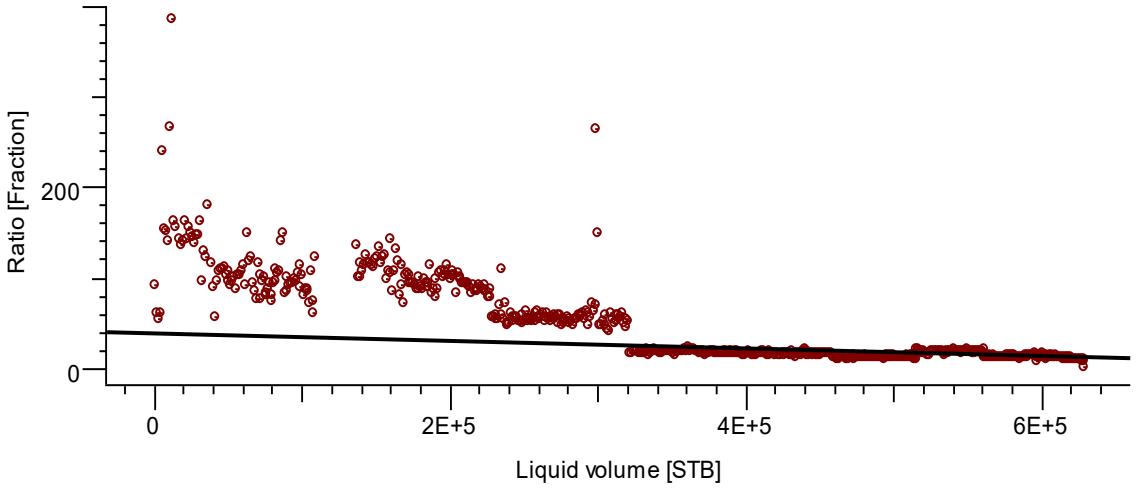

Figure 78. 1/fw versus Qo Plot for EBR-5

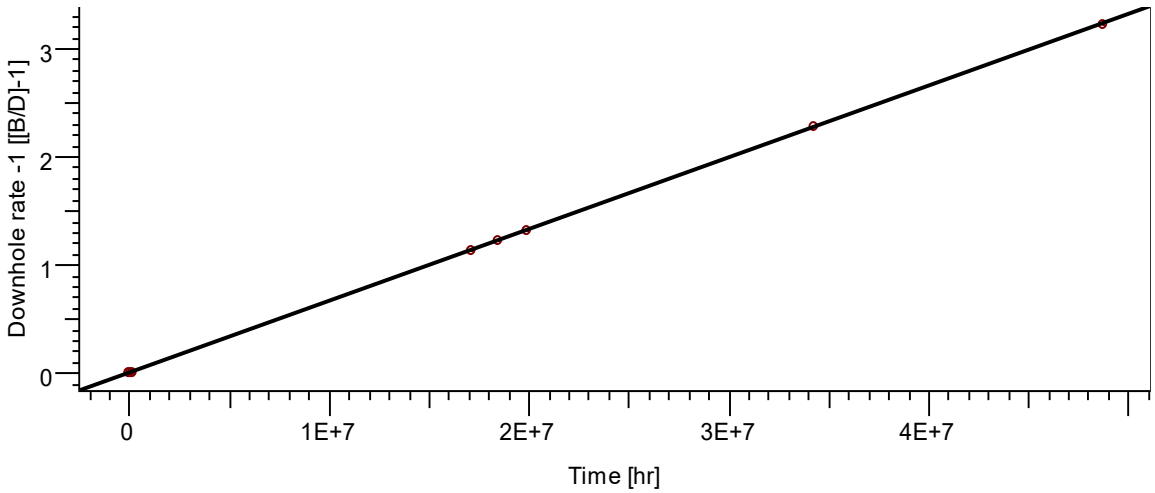

Figure 79. 1/qo versus material Balance time plot for EBR-5

The water oil ratio diagnostic plots in Figure 80 and Figure 81 show that the main water origin is the raise of the water oil contact in more than one layer. However the late time period in Figure 81 indicate that layer channeling is probably the cause for the loading up of the well. EBR-5 showed high performance during his producing life, thus the shut in of the water producing layer can lead to additional recovery from this well (at least 0.629 MMSTB in a conservative way as shown by decline curve analysis).

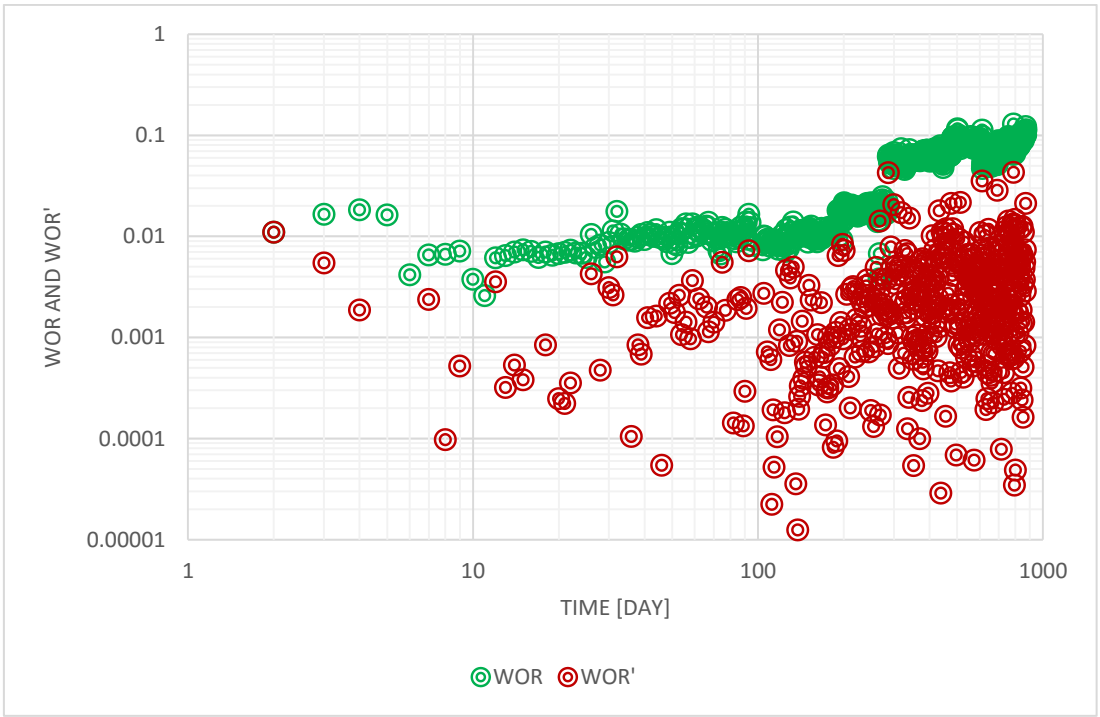

Figure 80.WOR and WOR' diagnostic plot of EBR-5

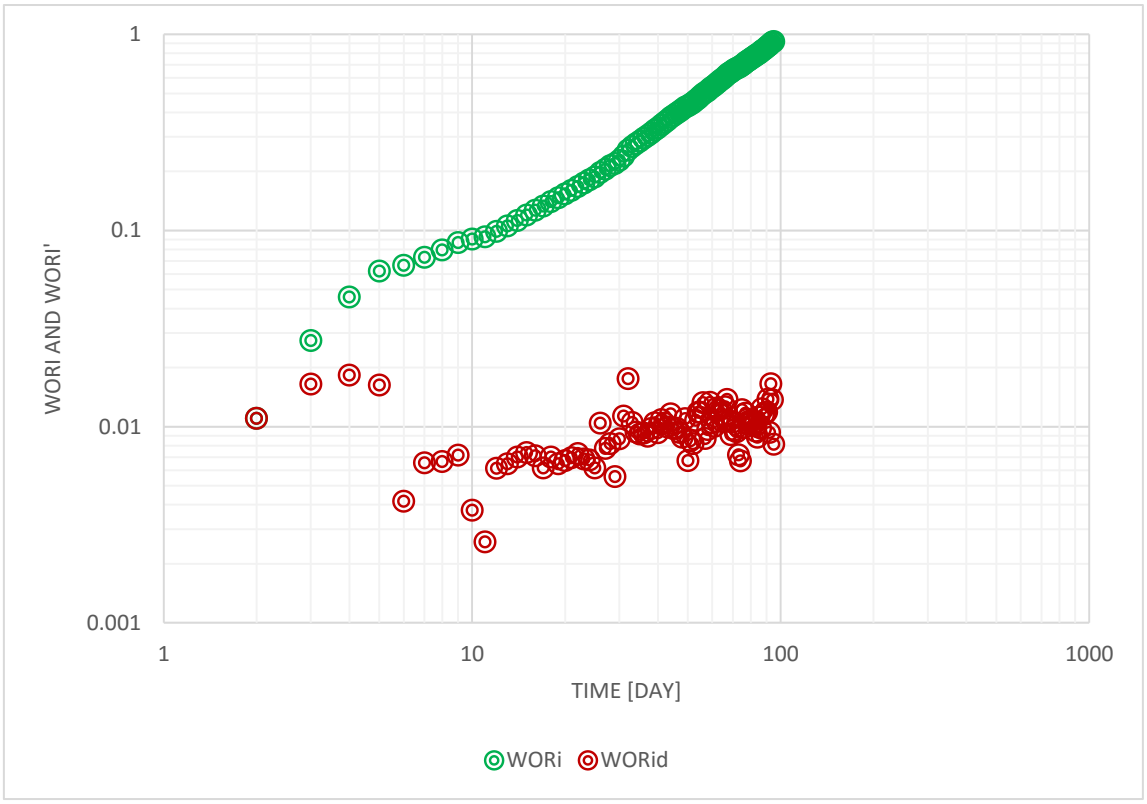

Figure 81. WORi and WORid diagnostic plot of EBR-5

3.6 Production Analysis Of EBR-6

3.6.1 Phase I

EBR-6 represents a challenge in modeling and properties estimation. The will has been produced in different phases. Phase I consists of 10.5m interval perforated initially in the undepleted layers while the total interval after February, 2014 corresponds to 25.5m. Therefore we treated the well as two wells with different performance. The first phase in which the rate pressure plot is illustrated in Figure 83 indicates a poor correlation between pressure and rates. However we modeled the rate response model in order to estimate the rate of first which will be used later in rate allocation. During this phase Blasingame plot and normalized rate cumulative plot showed an estimation of oil in place 9.6 and 9.06 MMSTB respectively in Figure 84 and Figure 85

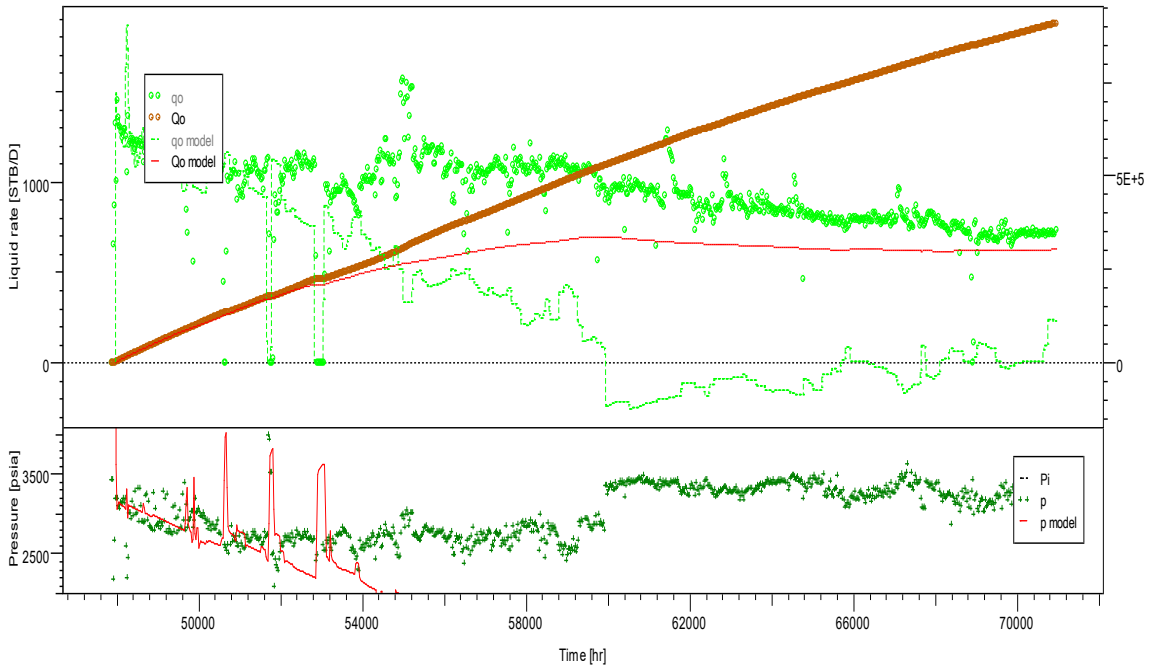

Figure 82. Production History and Phase I simulated model response of EBR-6

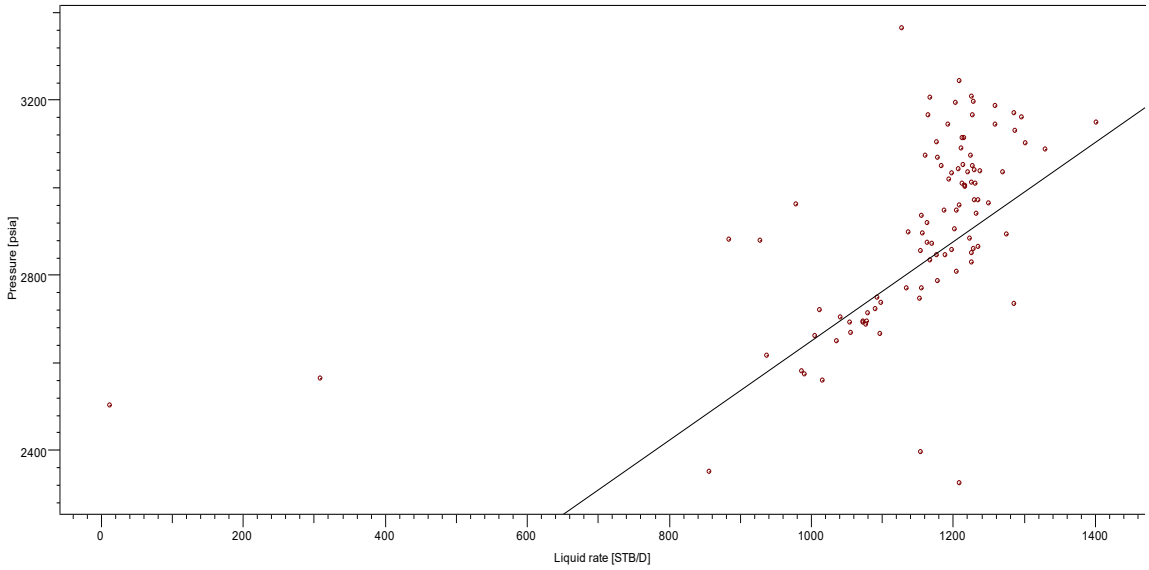

Figure 83. Pressure-rate plot of Phase I EBR-6

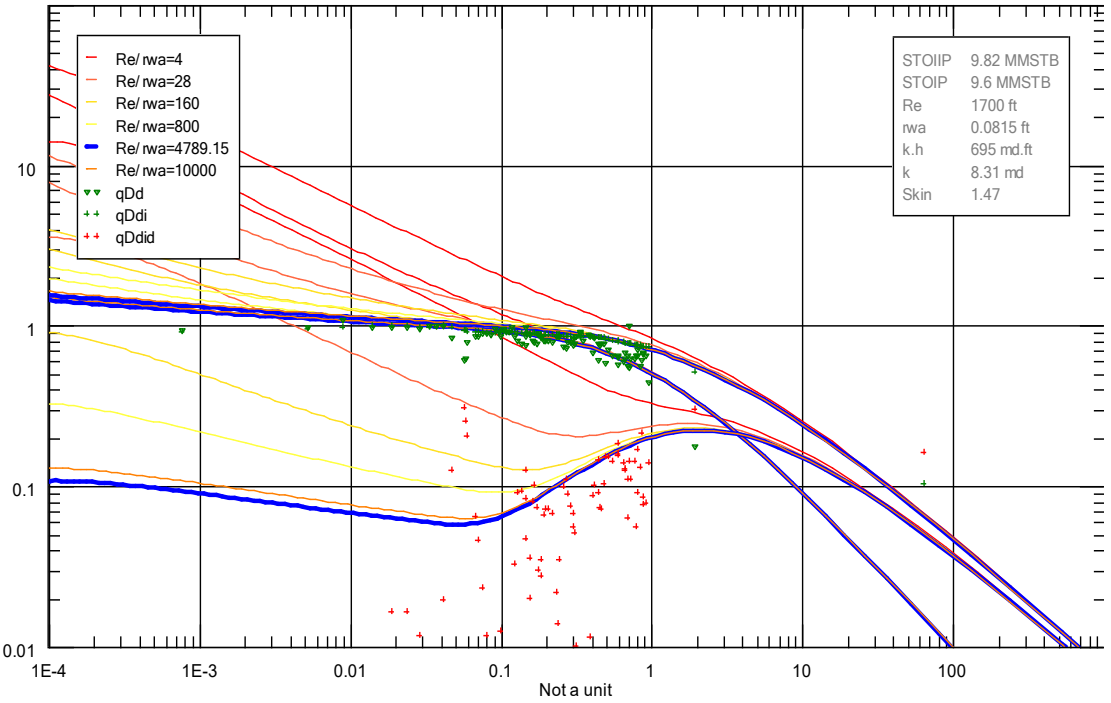

Figure 84. Blasingame Type Curve plot of Phase I EBR-6

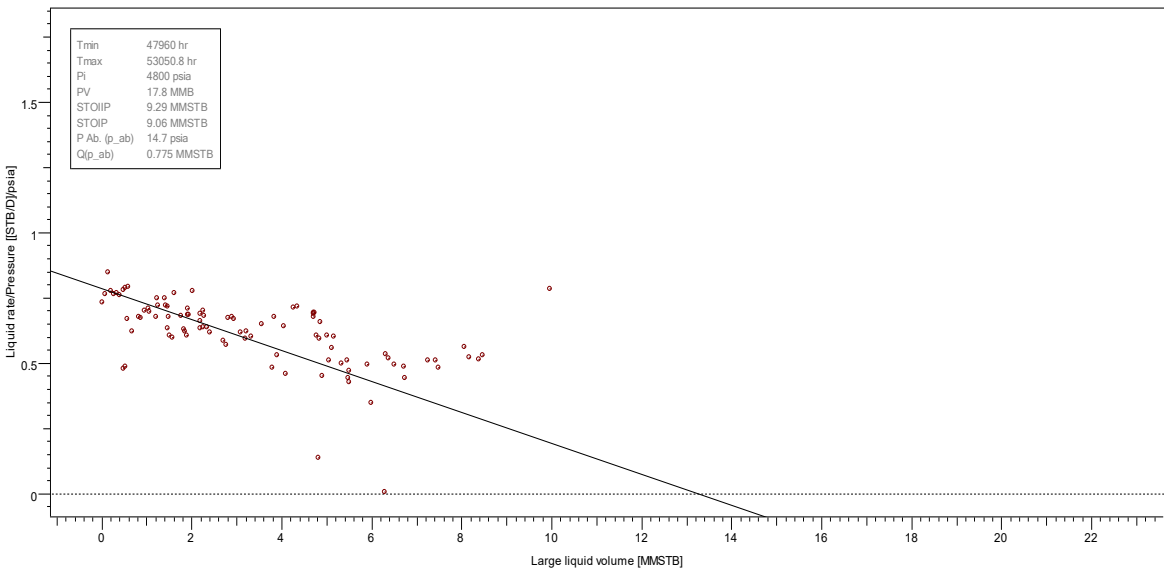

Figure 85. Normalized-Rate Cumulative plot of Phase I EBR-6

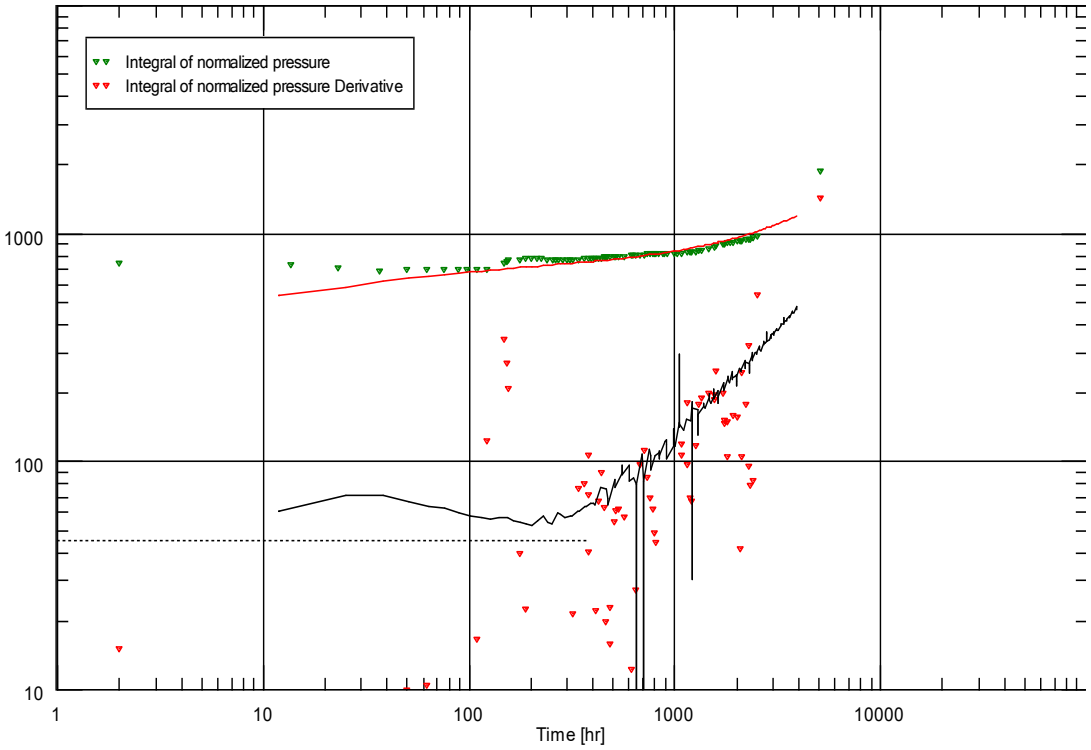

Figure 86. Log-Log Plot of Phase I EBR-6

3.6.2 Phase II

Phase II performance is subdivided also to the water cut evolution accordingly. This subdivision hided trend identification in Blasingame plot and Normalized rate Cumulative plot which is asserted by the poor correlation between the pressures and the rates in Figure 87.

The decline curve analysis based on the late time performance show an ultimate recovery of 0.994 MMSTB and 1.09 MMSTB on oil rate versus cumulative oil on a semi-log plot and the inverse of oil rate versus material balance time accordingly (Figure 88-Figure 89).We note that other method for decline analysis are not represented due to the inconsistent results estimated. Similarly, Blasingame plot and Normalized cumulative rate showed poor match for this well. This is due mainly to the changing behavior of the well (two phases of perforation) and the poor pressure rate correlation.

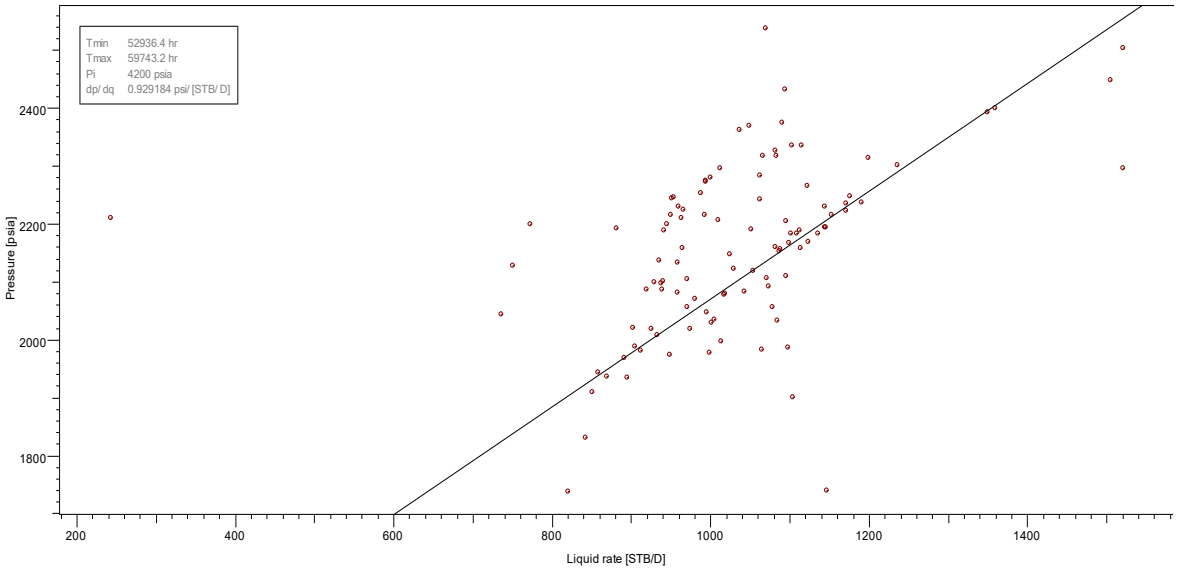

Figure 87. Pressure Rate plot of EBR-6

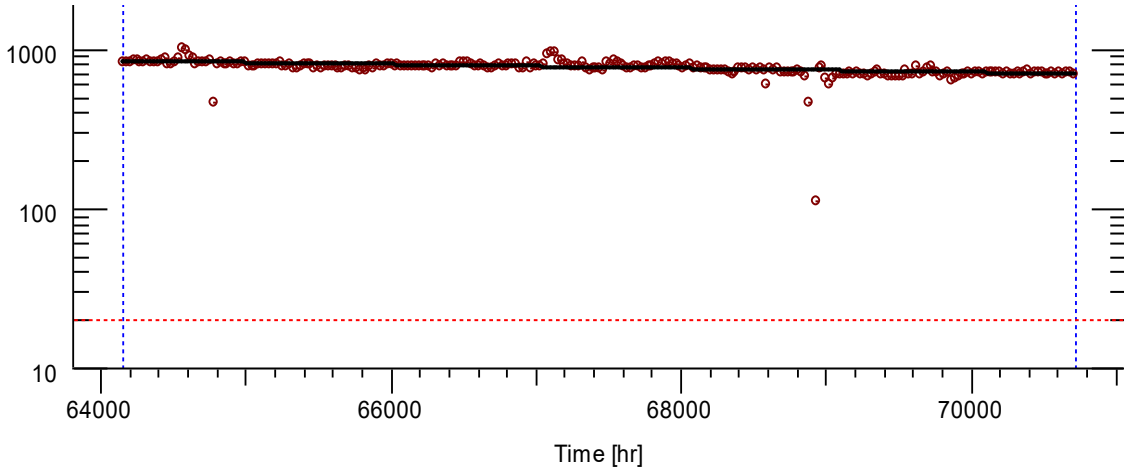

Figure 88.log (qo) versus time plot of EBR-6

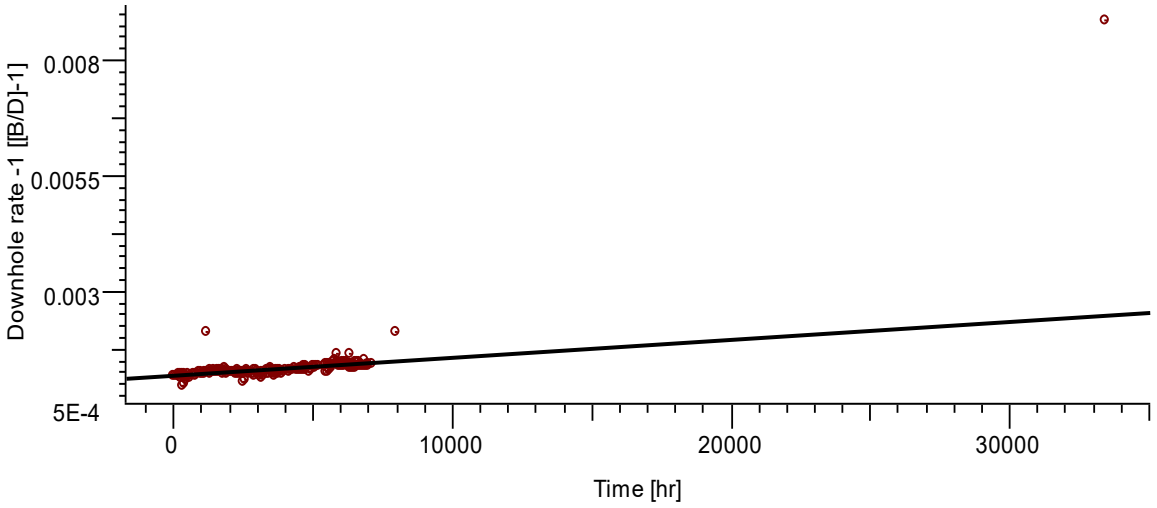

Figure 89. 1/qo versus material balance time plot of EBR-6

Figure 90Figure 91show the water oil ratio diagnostic plots. We observe that the water evolution in this well is due to the raise of the water oil contact in more than one layer which can be solved by water shut-off intervention.

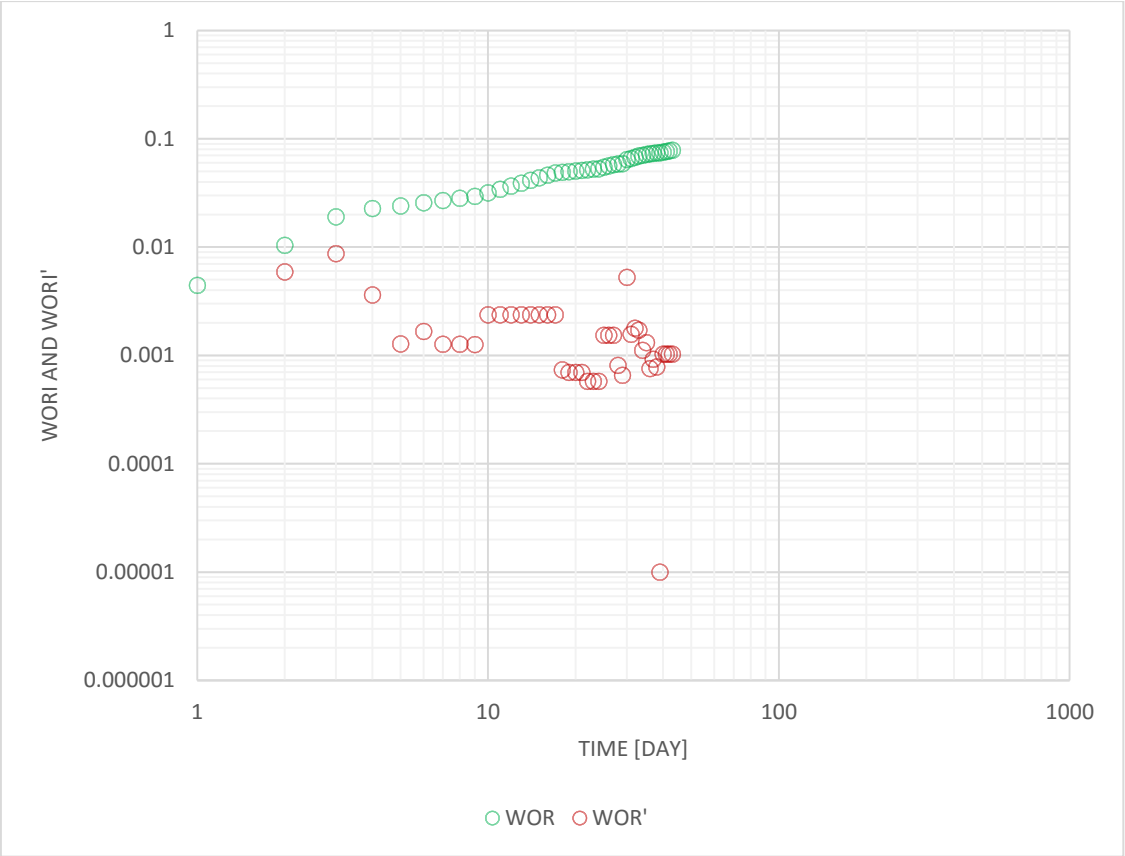

Figure 90.WOR and WOR' Diagnostic Plot of EBR-6

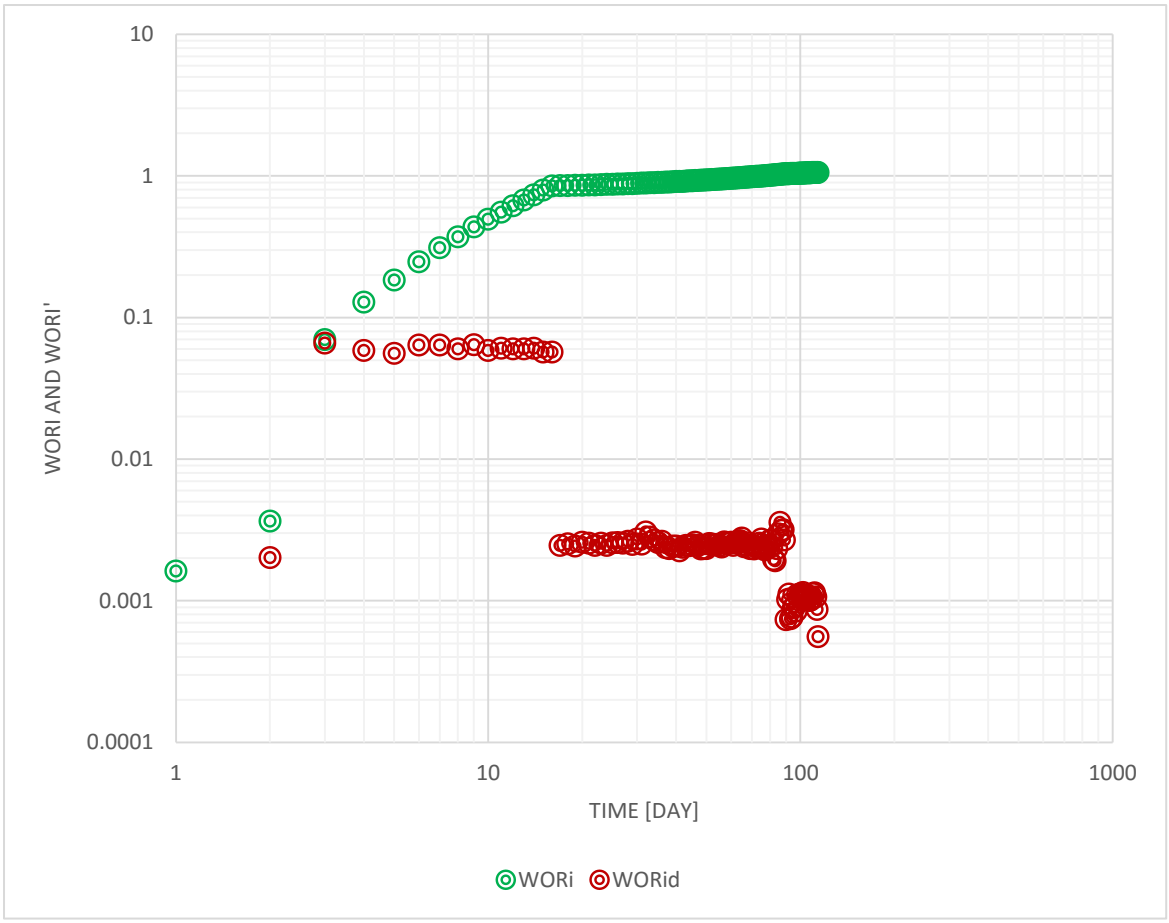

Figure 91. WORi and WORid Diagnostic Plot of EBR-6

4 Production Allocation of El Badr Field

4.1 Theory Background

Individual well rate measurement can be achieved using different approach. Most direct one is to use multiphase meter for each. This allocation system consists of set of producing wells where each well is equipped with a multiphase meter as shown by Figure 92. The flow from these wells is commingled and sent to a processing facility where oil, water and gas rates out of the process facility are measured with fiscal meters.

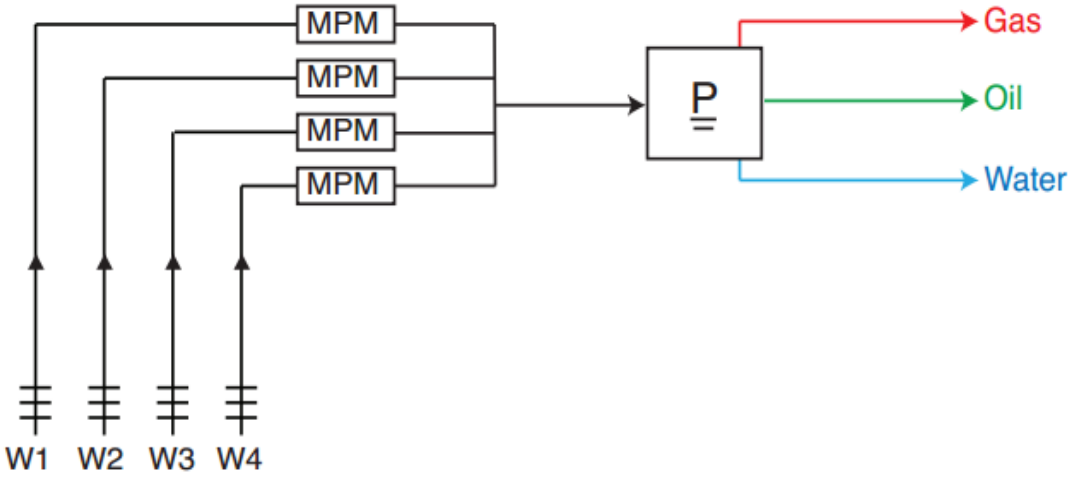

Figure 92. Illustration of measured rates with multiphase meters

The multiphase meters measure the in-situ gas and oil rates at the line conditions, on a continuous basis. These measured rates need to be converted to surface conditions in a consistent way and then compared to fiscal meters rates. If the fluid model used to convert the rates from line condition to surface condition and the meters are accurate, the rates obtained from multiphase meters should be equal to those measured from fiscal meters. Otherwise, there will be an imbalance which can be defined as:

$$I = Q\ export - \sum_{i=1}^{n} Q\ upstream \qquad (22)$$

Where I is the system imbalance, Q export is the rate measure out of facility, and Q upstream represents the measured rates from the individual sources (after being converted to surface conditions).

Most fields do not have multiphase meters installed on every well because of cost constraints. Another allocation system usually used is shown in

Figure 93, where the producing wells are monitored with downhole gauges. The field also has a test separator which is shared amongst all the wells, and can be used to get periodic tests for the individual wells.

The accuracy of a test separator will usually be higher than that for multiphase meters. This is because the test separator will physically separate the well stream into an oil, water and gas phases and measures these rates separately. However, because a test separator only allows for periodic tests, it will have problems capturing the dynamic behavior of the well. The rate of a well may change considerably from test to test, for example due to change in back-pressure at flowline, change in choke position, or unexpected shut-downs.

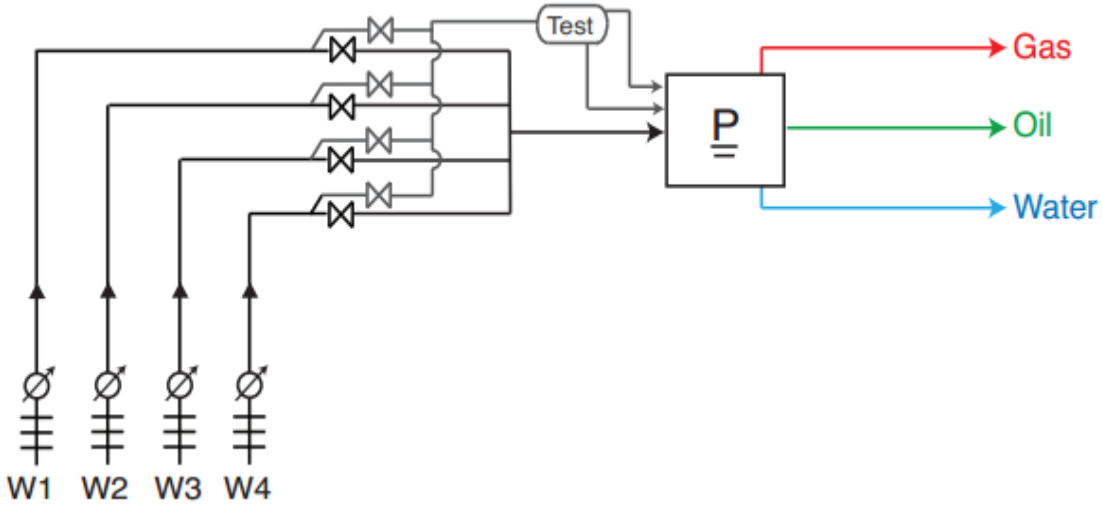

Figure 93.Illustration of measured rates with a test separator

The number of tests and the frequency of the measurements will depend on the number of wells and the availability of mobile test separator. Installation of permanent pressure gauges is increasingly common in the industry, and they can be used to get high frequency pressure measurements. These measurements can be used together with theoretical models to calculate the flow-rates. Theoretical models may use nodal analysis (IPR versus VLP match) or may use the analytical solution of the diffusivity equation to get the rates out the pressures when there is no reservoir pressure measurements available which the case for El Badr field is. Nevertheless, these models need to be updated and corrected on a regular basis. This correction is typically done based on the periodic measurements from the test separator.

The measured rate at test separator or those obtained from multiphase flow meters usually differ from the rates measured by fiscal meters (Imbalance). There are different methods that can be used to distribute the system imbalance between the individual well rates. The most common method is to use proportional-based allocation factors, and this is the method that is currently used for the El Badr field. Another method is called uncertainty-based allocation factors, which can be applied if the uncertainties of the different measurement equipment are known. An Example of uncertainty based allocation factor is given in Appendix B.

4.2 Literature Review

Rate allocation has been described in the literature as a problematic task as infrequent test are conducted and/or as it needs to be extended to individual zones [13]. Using even split factors or split factor that are based on the ratio of the permeability-thickness products usually returned erroneous results. Many attempts have been presented in the literature. These methods include satisfying the mass balance and honoring the Permanent Downhole Gauges measurements.

Economides et al. utilized the measured data without input well test coupled with a generic IPR that does not require information such permeability and skin. Then optimization using pipe flow simulator to determine the split factor for each well [13].

McCracken and Chorneyko used the PDG to tune the reservoir model that honor the total commingled production data [14]. PTA was employed to estimate reservoir properties and flow rates were adjusted until the simulated bottom hole flowing pressures match the recorded ones. For the sake of accuracy, in each iteration, the estimated rates need to be fed back to the PTA to re-interpret the test. Their approach appears comprehensive all reservoir parameters. However, they stated that their model may be no longer valid at some point during the forecast phase as some Productivity parameters may change like permeability and skin.

Hamad et al. established an empirical formula that associates the recorded wellhead pressures to the oil production [15].

Prabowo and Rinadi conducted a study of a layered gas reservoir where the transmissibility of each layer was changed to derive the layer contribution to the commingled production and basic assumption that no crossflow exists between layers [16].

Ibrahim constructed empirical IPR curves for the gas and condensate wells of their case using the well test data and the downhole data [17].

4.3 Method Applied

In this thesis, pressure based rate allocation is developed. The bottom hole flowing pressures are used to generate the oil rates in a single phase

analytical simulator. In his work, McCracken and Chorneyko estimated reservoir parameters using pressure transient analysis. Conversely, we used production analysis to estimate these properties using restricted ranges obtained from petrophysical analysis. The response was tuned based on the most uncertain values (i.e. drainage radius, skin and permeability).

A stepwise workflow for rate can be defined as:

The cumulative production is obtained by integrating the measured commingled rate q_T over a specified time period.

$$Q_{Export} = \int_{t0+\Delta t.(i-1)}^{t0+\Delta t.i} q_T\,(t)\,dt \qquad (23)$$

Similarly, from the simulated rates, the cumulative production for each well is calculated by integrating the well rate over the specified time period.

$$Q_{upstram} = \int_{t0+\Delta t.(i-1)}^{t0+\Delta t.i} q_j\,(t)\,dt \qquad (24)$$

The difference between the measured and the calculated cumulative production is calculated for each specified period as:

$$I = Q\,\text{export} - \sum_{i=1}^{n} Q\ upstream \qquad (25)$$

Then, the fraction of each well that will account for the excess or shortage in cumulative production is given by:

$$\alpha_i = \frac{Q_{i\ upstream}}{\sum_i^n Q\ upstream} \qquad (26)$$

If the meters show uncertainty in measurement then the uncertainty allocation will be (Appendix B):

$$\alpha_i = \frac{\sigma_i^2}{\sigma_z^2 + \sum_i^n \sigma_i^2} + \frac{Q\,\text{export}}{\sum_i^n Q\,\text{upstream}} * \frac{\sigma_z^2}{\sigma_z^2 + \sum_i^n \sigma_i^2} \qquad (27)$$

The adjusted cumulative production is calculated using:

$$Q_{i\,allocated} = Q_{i\,Upstream} + \alpha_i I \qquad (28)$$

4.4 RESULTS

El Badr field production is allocated based on periodic well tests and constant split factor for each well. The modified approach used in this thesis showed good results whenever there is downhole gauge installed in the well. In other words, the wells where only wellhead pressure is measured showed inconsistent results because of the poor quality of converting the wellhead pressure to bottom hole flowing pressure. Moreover, Well rates can vary unpredictably between well tests due to following reasons:

- Natural decline, especially during later stages of the life cycle.
- Well stream composition can suddenly change, for example from increasing water cut or increasing GOR.
- Production rates of artificially lifted wells can vary between well tests due to the effects of variables such as backpressure (gas lift) and pump speed and efficiency (electric submersible pumps, progressing cavity pumps, beam pumps, and hydraulic lift).
- Produced scale or sand that foul production lines, which need to be cleaned often.

All these factors will affect the proposed methods in terms of long periods. This means that the model will not be valid after a certain time and needs to be reviewed and updated.

EBR-1 has the longest production life amongst the others. Figure 94 shows good results of the predicted rates because this well has a downhole gauge and relatively higher production than others. Therefore, the effects of production line back pressure are limited. We have given this well 7% uncertainty in measurement. The table below represents the uncertainty given for each well and the total production uncertainty used for allocation based on uncertainty factors.

Table 18. Uncertainty in measurement for meters

Flow Location	Uncertainty Factor
Total Production (Stock tank)	5 %
EBR-1	7 %
ÊBR-3	10 %
EBR-4	10 %
EBR-5	10%
EBR-6	7 %

EBR-3 has only recorded wellhead pressures. We converted these pressures to flowing bottom hole pressures using generated VLP from PROSPER[2] according to the well history and matched to the available production tests. The resulted rates shown in Figure 95represent better results for matching well tests however the decline was not accurately represented because of the time dependent well intake used.

EBR-4 has been corrected from the erratic behavior during 2011, a spike was noted even in the simulated rates due to gas lift effect but rapidly declined. The late time period for this well looks challenging to simulate using the analytical solution of the diffusivity equation as it effects the flowing bottom hole pressure. As water cut increases the mixture density increases leading to higher flowing bottom hole pressure. The multiphase diffusivity equation formulation assumes constant mobility of phases with respect to time. Hence, it does not consider the evolution of water over time for instance.

EBR-5 has the shortest life and lowest production tests. The predicted rates are lower than the reported rates during the initial life of the well and higher during the late time. We note that the predicted rates are consistent with downhole pressure measurements which would lead to consider the new rates confidentially.

EBR-6 has been produced from undepleted zones, then when pressure equalized a second phase of perforation was performed. Therefore, the predicted rates as explained earlier in chapter 3 were divided accordingly to the changed thickness and permeability. The predicted rates show better compromise with spike created by the perforation of the second set of layers and the overall tests.

Figure 99 Figure 100 compare the allocated rates and the predicted rates to the total measured rates. The allocation shows good results for both

[2] A PETEX software

rates however the allocated rates based on uncertainty in measurements shows more consistent trend.

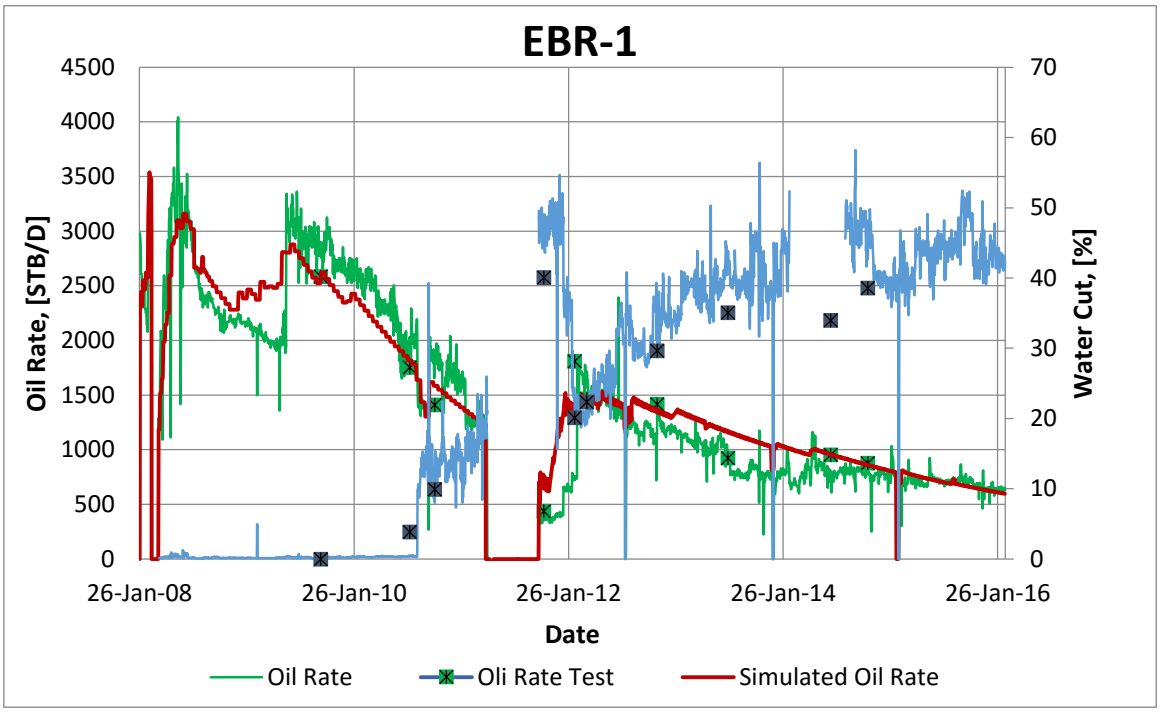

Figure 94. Simulated Rates of EBR-1 using Topaze

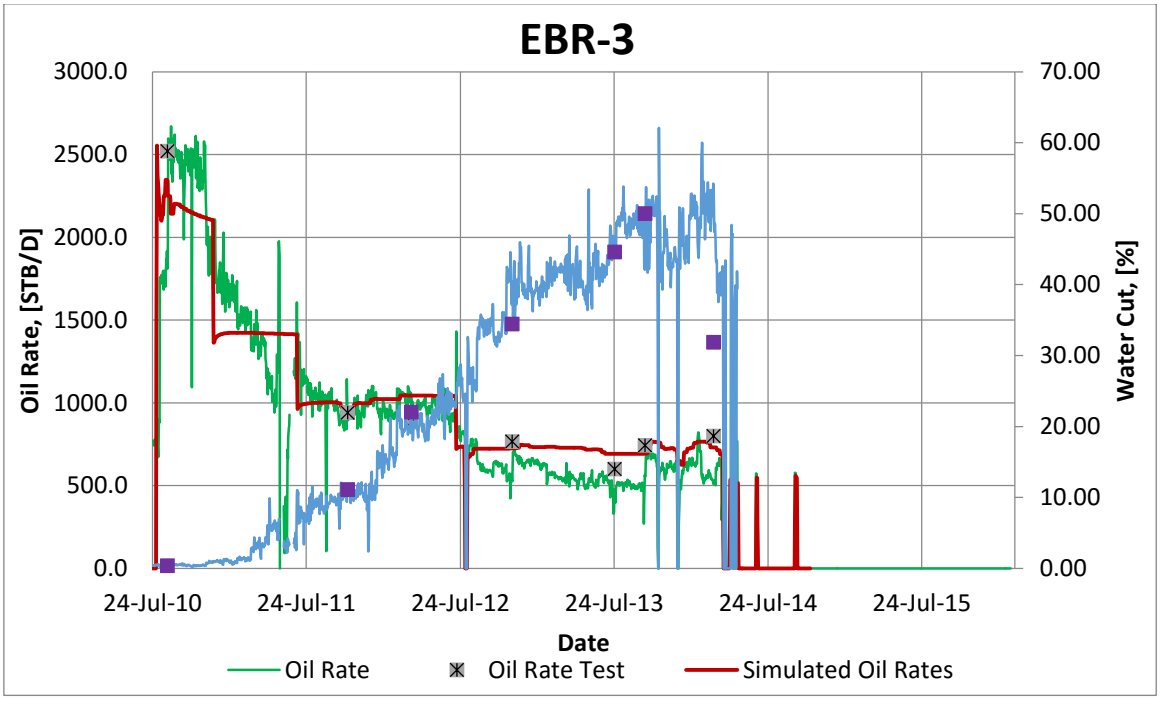

Figure 95. Simulated Rates of EBR-3 using Topaze

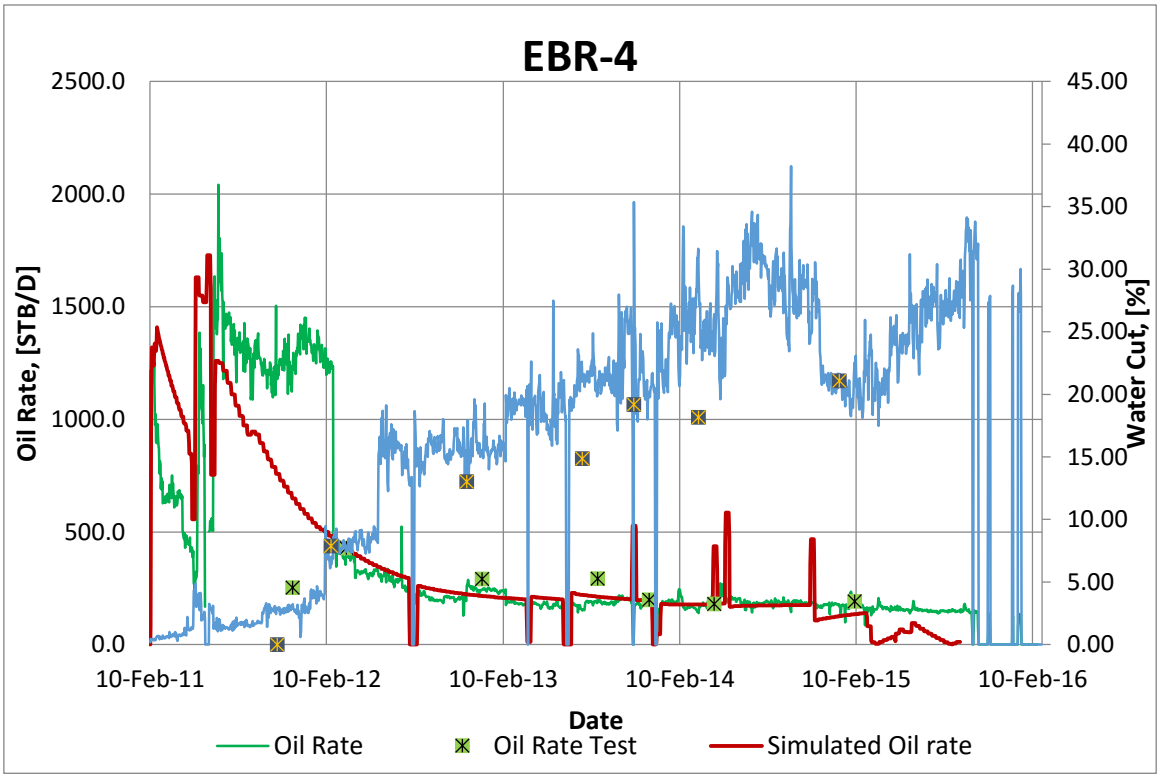

Figure 96. Simulated Rates of EBR-4 using Topaze

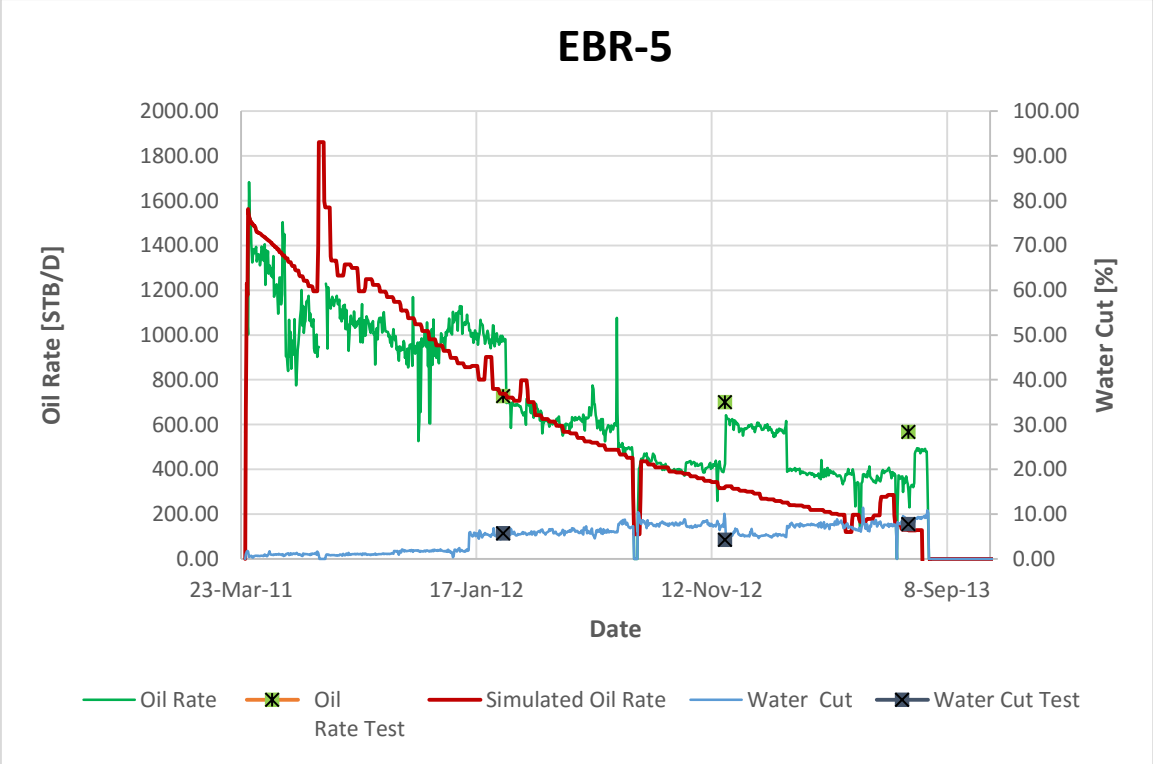

Figure 97. Simulated Rates of EBR-5 using Topaze

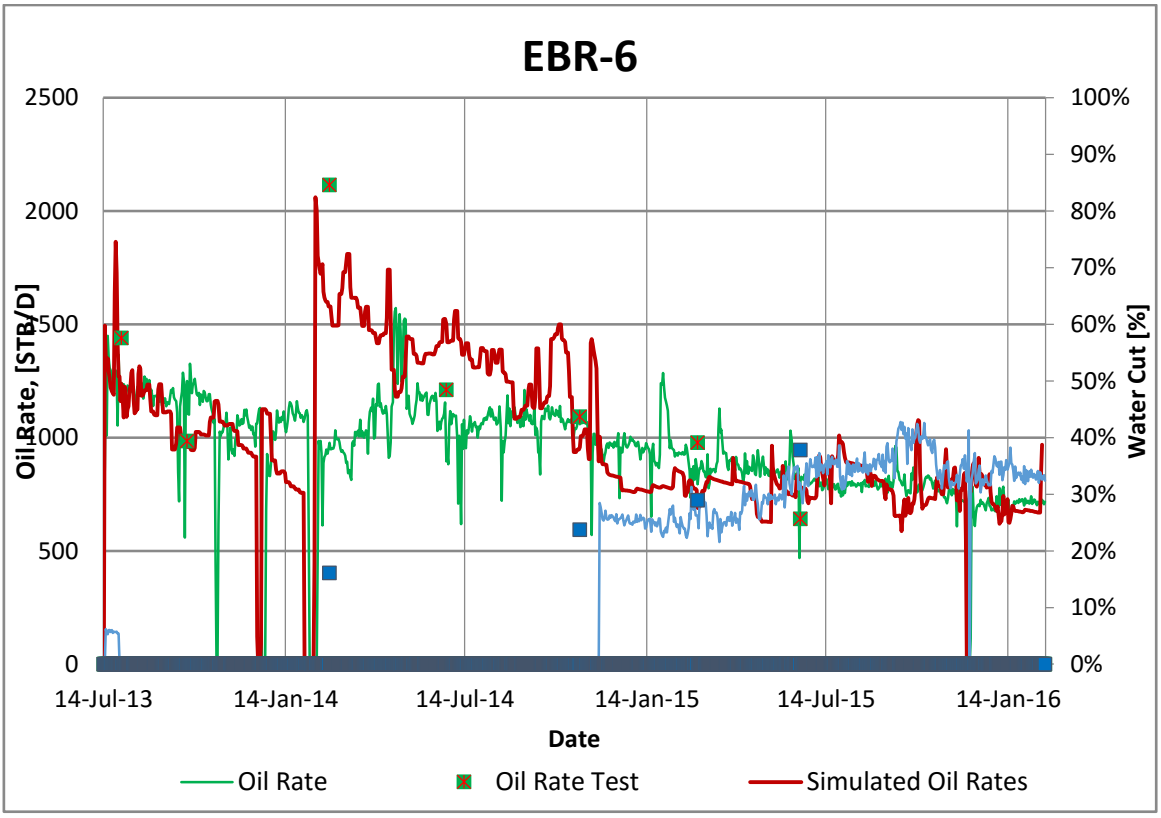

Figure 98. Simulated Rates of EBR-6 using Topaze

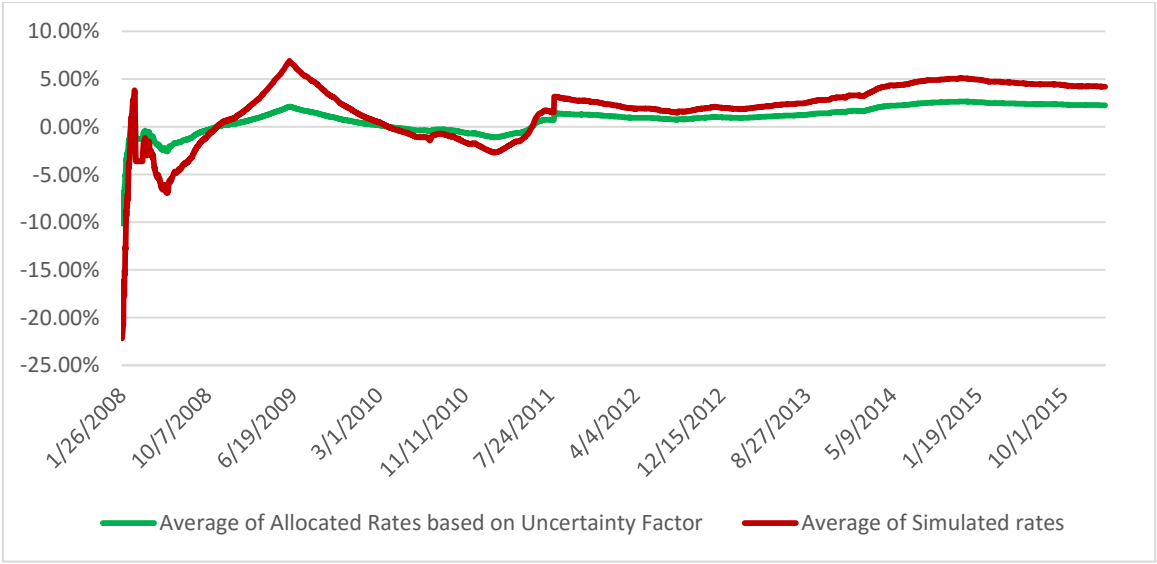

Figure 99. Relative Deviation of Predicted Rates and Uncertainty Factor Based Allocation

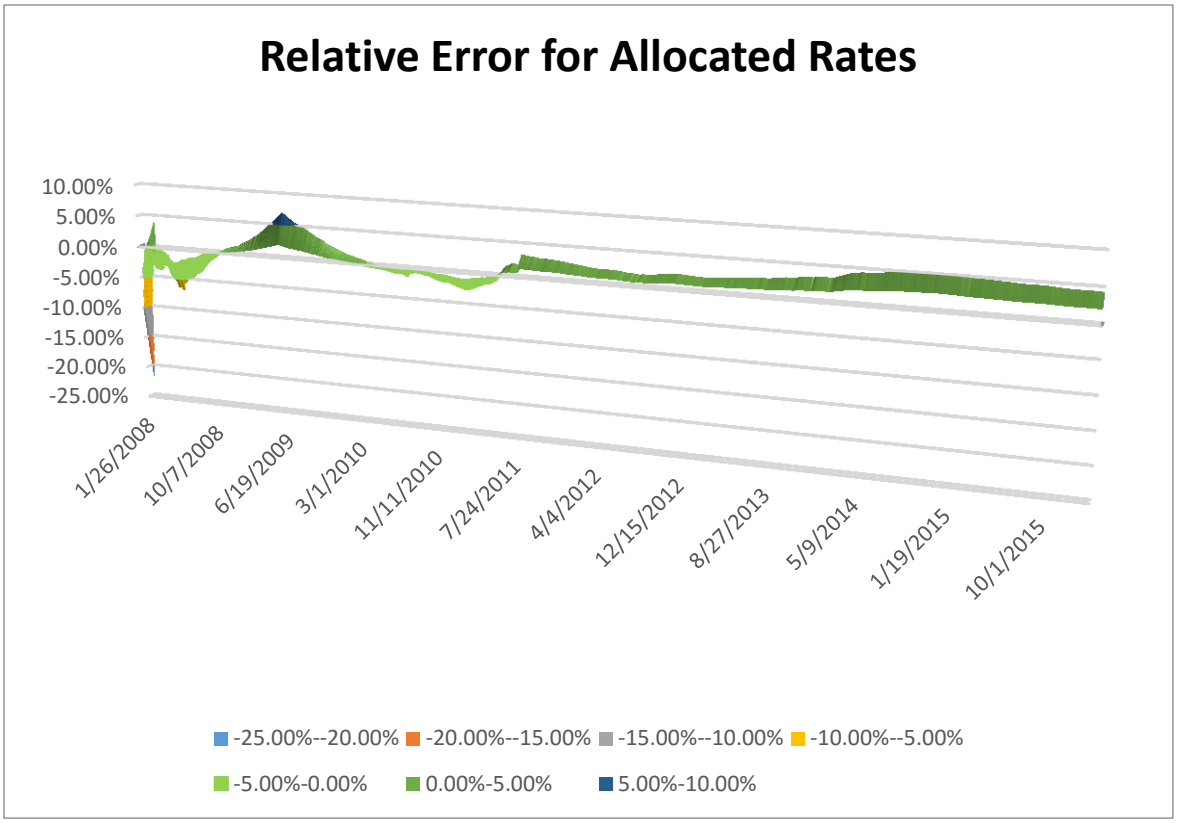

Figure 100.Relative Deviation of Allocated Rates versus the Measured Rates

5 Conclusions and Recommendations

5.1 Conclusions

We propose the following list of conclusions based on the study:

1- Re- evaluation of reserves using production analysis revealed that oil in place in the field is higher than that estimated by volumetrics. EBR-1 has highest connected pore volume with drainage raduis around 3000 ft and oil in place of more than 50 MMSTB. EBR-4 showed oil in place around 11 MMSTB and EBR-5 about 10 MMSTB, whereas EBR-3 and EBR-6 indicated inconsistent values due to the poor correlation between pressures and rates.

2- Under current circomstances,the total expected ultimate recovery from the field is between 6 and 9.6 MMSTB. Nevertheless, at least 1 MMSTB can not be recovered because of the watered wells (i.e. EBR-3 and EBR-5).

3- The water origin was evaluated using water oil ratio diagnostic plots. It is found that most of the water is coming from multilayer channeling.This channeling is supposed to be as result of an edge water aquifer coming from the north as EBR-3 and EBR-5 are firstly watered out.

4- The water produced in EBR-1 and EBR-4 is considered as good water and there is now way to avoid this water without loosing reserves.

5- A closing of the water producing SSD A in EBR-3 would eliminate the cross flow phenomena and will allow the well to resume production from from SSD B and C.Hence, Ultimate recovery of about 1 MMSTB of oil.

6- There is an immediate need to run a PLT in EBR-5 to evaluate layer pressures and their resepective contributions and a cased hole log to estimate the water saturation in the layers. This well can be turned to water injector to maintain pressure as it is the nearest to the aquifer.

7- The reservoir pressure is found near 3000 psi. the initial reservoir was above 5100 psi. this huge decline in pressure in conjunction with low recovery is typical solution gas drive mechanism. As the current reservoir pressure is approaching the bubble point pressure which is 1986 psi, pressure maintance projects must considered as soon as possible to enhance recovery.

8- In this work, pressure based rate allocation method was developped and implemented to all the well including those without downhole pressure monitoring. The method consists of building simple reservoir model based rate transient analysis and production diagnostic plots. Then using rate transient analysis to predict rates

based on the model created and bottom hole flowing pressures. The field included wells producing from stacked reservoirs and have commingled production in the weelbore. The approach used in rate allocation:

- Affords more consistent rates with the downhole pressures and on daily basis (i.e. higher frequency than periodic production well test).
- Consider relative pressure drawdown effects
- Can reduce the number of required surface well tests for allocation purposes and provide a method for allocating rates in wells producing from stacked reservoirs if individual downhole gauges are installed in each section.

5.2 RECOMMENDATIONS

The redevelopment of El Badr field can be extended to many other research area. We present a brief description of other possible area which can be associated to this study:

1- Reservoir Simulation: this study will provide more information highly required. Reservoir simulation can be carried out based on the allocated rates to develop a future management plan such pressure maintenance and/or infill drilling.
2- Nodal Analysis Re-evaluation: this study can benefit from the production data analysis brought values such as reservoir pressure and skin to optimize the future production.
3- Artificial lift: These methods can be discussed in details and optimized for the wells.
4- Intelligent Completions: Preceded by dynamic evaluation of the layers, these ICD/ICVs can improve the completion performance and extend the life of the wells. A detailed study including economical applicability can be carried out to the field.

6 APPENDICES

Appendix A: Wellbore Schematics

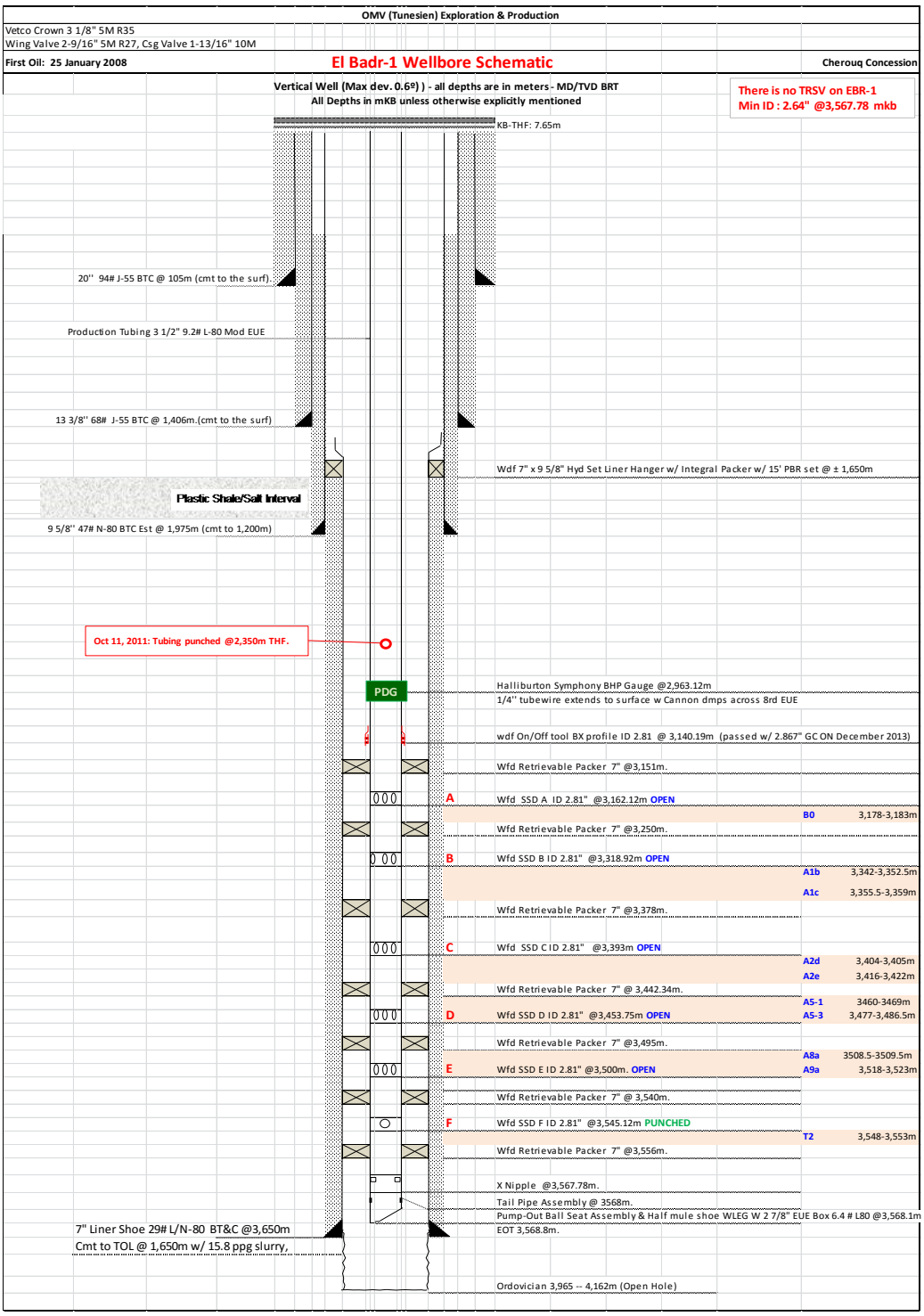

Figure 101. EBR-1 Wellbore Schematic

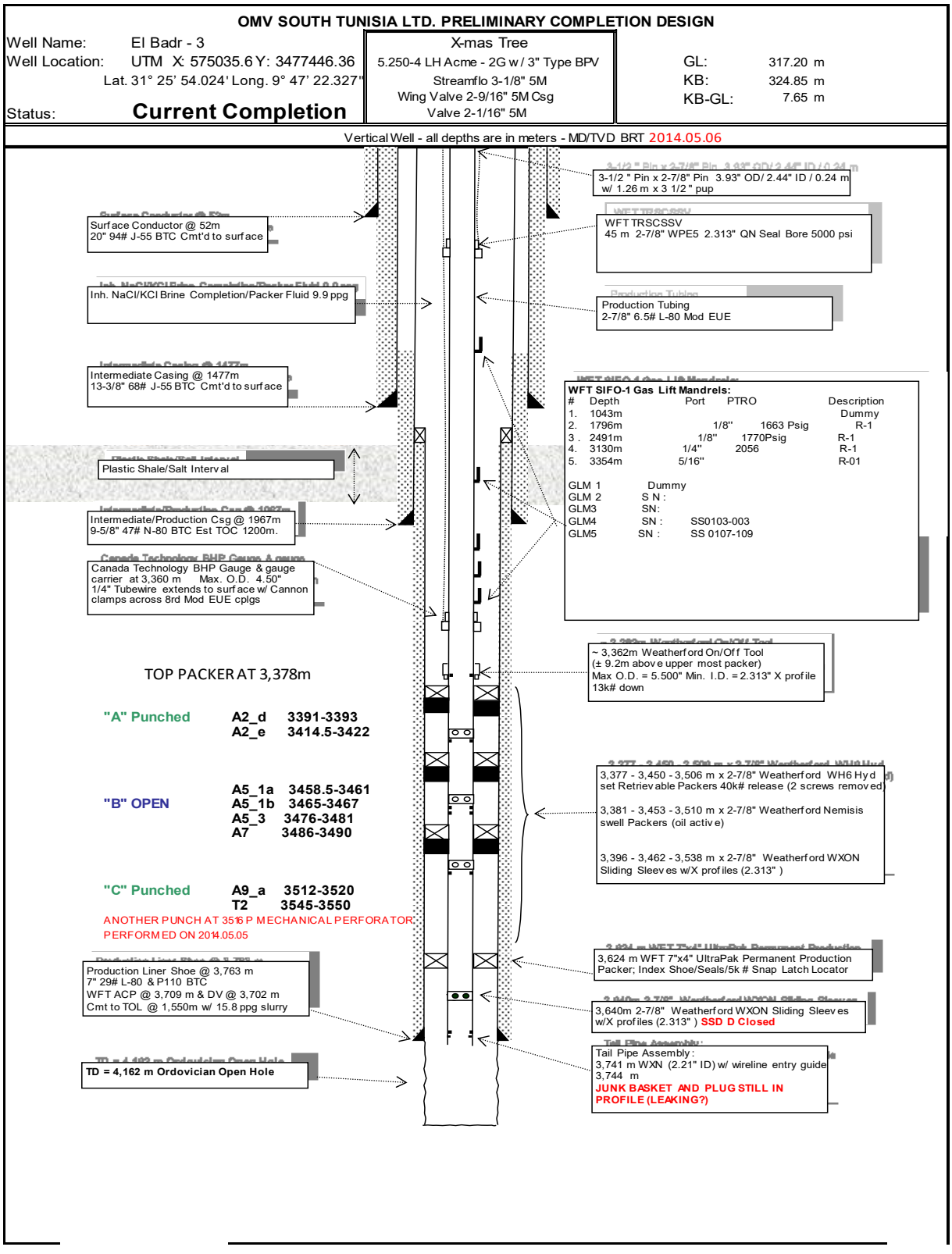

Figure 102. EBR-3 Wellbore Schematic

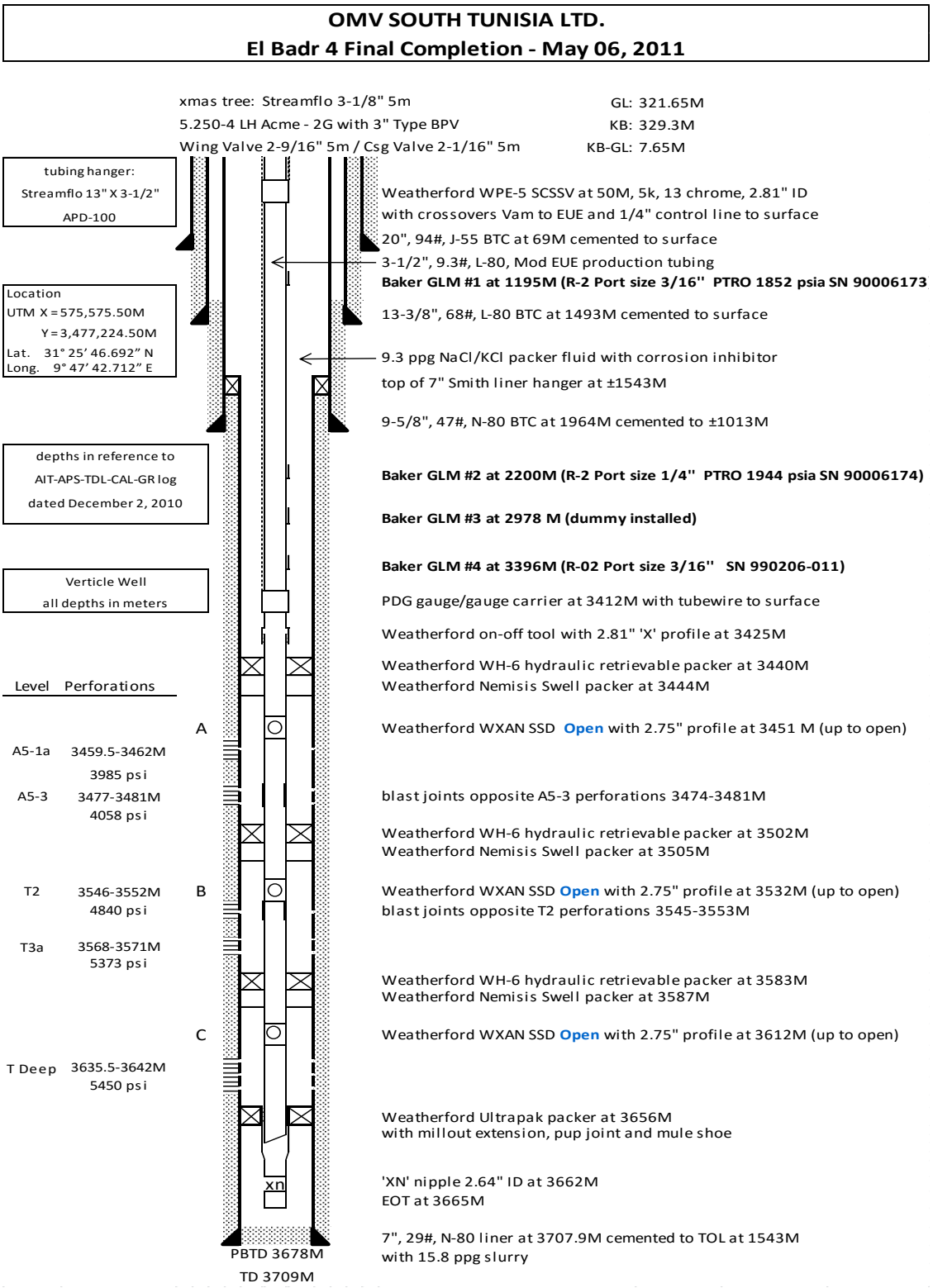

Figure 103. EBR-4 Wellbore Schematic

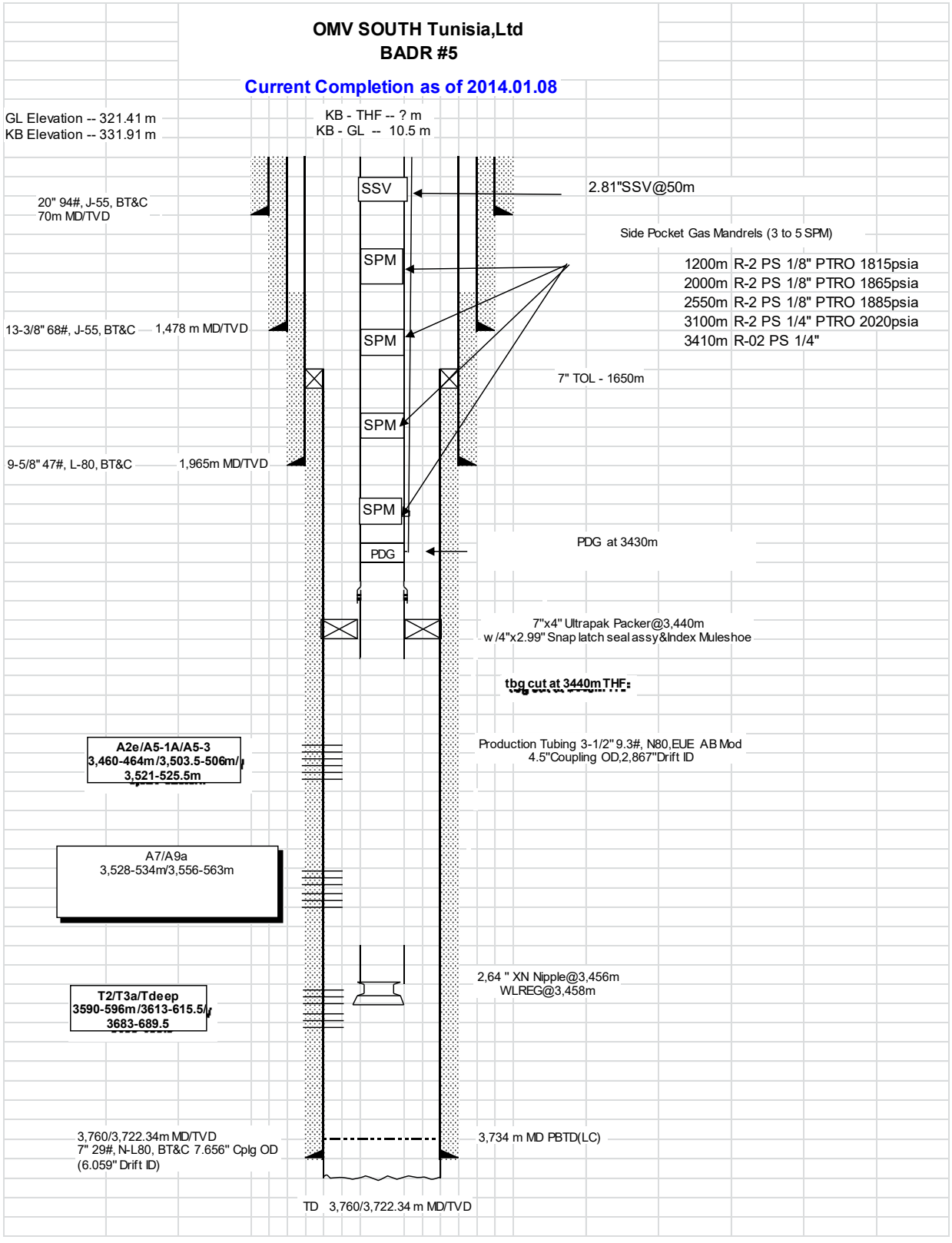

Figure 104. EBR-5 Wellbore Schematic

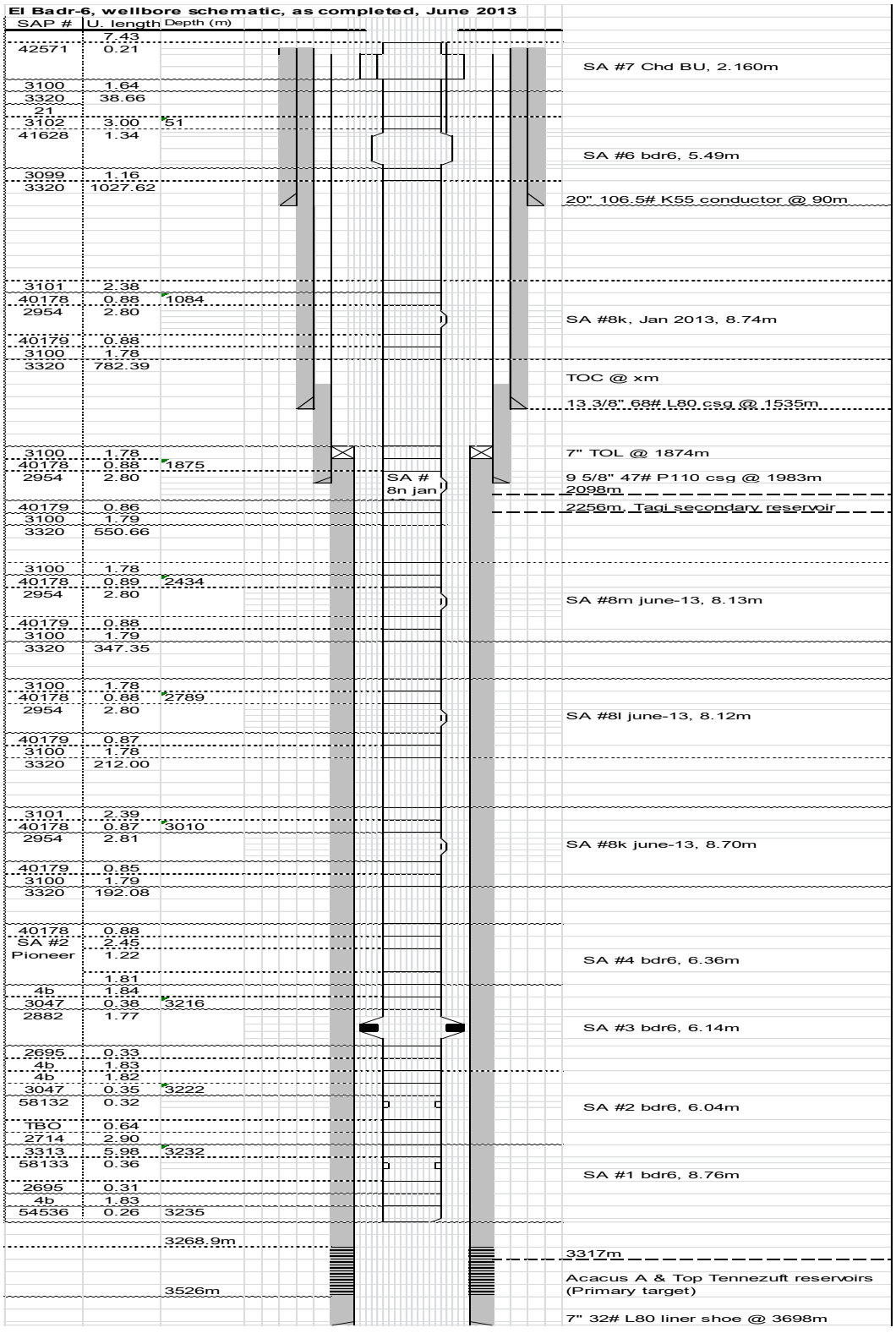

Figure 105.EBR-6 Wellbore Schematic

Appendix B: Example using uncertainty-based allocation

A system consist of a reference fiscal meter (Q_Z) that measures the oil-rate storage tank condition, and three individual wells measured by multiphase meters at the wellhead level. The well rates are converted also to stock tank condition.

$$Q_Z = 6000\,STB/D\ \pm 5\%$$
$$Q_1 = 1800\,STB/D\ \pm 10\%$$
$$Q_2 = 2950\,STB/D\ \pm 5\%$$
$$Q_3 = 900\,STB/D\ \pm 8\%$$

The system imbalance can be found as:

$$I = Q_Z - \sum_{i=1}^{N=4} Q_i$$
$$I = 6000 - (1800 + 2950 + 900) = 350\ STB/D$$

The variance of the different meters is:

$$\sigma_Z^2 = (Q_Z * 5\,\%)^2 = (6000 * 5\,\%)^2 = 90000\,(STB/D)^2$$
$$\sigma_1^2 = (Q_1 * 10\,\%)^2 = (1800 * 10\,\%)^2 = 32400\,(STB/D)^2$$
$$\sigma_2^2 = (Q_2 * 5\,\%)^2 = (2950 * 5\%)^2 = 21756.25\,(STB/D)^2$$
$$\sigma_3^2 = (Q_3 * 8\,\%)^2 = (900 * 8\%)^2 = 5184\,(STB/D)^2$$

The total uncertainty in throughput variance:

$$\sum_{j=1}^{N=4} \sigma_j^2 = 32400 + 21756.25 + 5184 = 59340.25\,(STB/D)^2$$

The allocations factors can then be found by using the following equation:

$$\alpha_i = \frac{\sigma_i^2}{\sigma_Z^2 + \sum_{j=1}^{N} \sigma_j^2} + \frac{Q_i}{\sum_{j=1}^{N} Q_j} * \frac{\sigma_Z^2}{\sigma_Z^2 + \sum_{j=1}^{N} \sigma_j^2}$$

$$\alpha_1 = \frac{32400}{90000 + 59340.25} + \frac{1800}{6000} * \frac{90000}{90000 + 59340.25} = 0.3969$$

$$\alpha_2 = \frac{21756.25}{90000 + 59340.25} + \frac{2950}{6000} * \frac{90000}{90000 + 59340.25} = 0.4406$$

$$\alpha_3 = \frac{5184}{90000 + 59340.25} + \frac{900}{6000} * \frac{90000}{90000 + 59340.25} = 0.1247$$

The adjusted rates for each well can then be calculated:

$$Q_1^{allocated} = Q_1 + I * \alpha_1 = 1800 + 350 * 0.3969 = 1938.915\,STB/D$$

$$Q_2^{allocated} = Q_1 + I * \alpha_2 = 2950 + 350 * 0.4406 = 3104.21\ STB/D$$
$$Q_3^{allocated} = Q_3 + I * \alpha_3 = 900 + 350 * 0.1247 = 943.645\ STB/D$$

And the sum of these allocated rates:

$$\sum_{i=1}^{N=4} Q_i^{allocated} = 2177.055 + 3368.57 + 1018.477 = 5986.77\ STB/D\ \cong Q_Z$$

REFERENCES

[1] R. O. Baker, H. W. Yarranton and J. L. Jensen, Practical Reservoir Engineering and Characterization, Oxford: Elsevier, 2015.

[2] T. Babadagli, "Mature Fields Development- A Review," in *EAGE Annual Conference*, madrid, 2005.

[3] D. Anderson and L. Mattar, "Practical Diagnostics Using Production Data and Flowing Pressures," in *SPE Annual Technical Conference and Exhibition*, Houston, 2004.

[4] P. N. ressources, "Cherouq Technical Report," Pioneer Natural Resources, Tunis, 2007.

[5] D. Ilk, L. Mattar and T. Blasingame, "Production Analysis- Future practices for Analysis and Interpretation," in *Canadian International Petroleum Conference(58th Annual Technical Meeting)*, Calgary, 2007.

[6] D. Anderson, L. Mattar, D. Ilk and T. Blasingame, "Production Data Analysis- Challegenges, Pitfalls, Diagnostics," in *SPE Annual Technical Conference and Exhibition*, San Antonio, 2006.

[7] L. Mattar and D. Anderson, "A Systematic and Comprehensive Methotodology for Advanced Analysis of Production Data," in *SPE Annual Technical conference and Exhibition*, Denver, Colorado, 2003.

[8] C. Kabir and B. Izgec, "Diagnosis of reservoir Bhavior From Reservoir Pressure/Rtae Data," in *SPE Gas Technology Symposuim*, Calgary, 2006.

[9] O. Houzé, D. Vitourat and O. S. Fjaere, Dynamic Data Handbook, Kappa Engineering, 2015.

[10] K. Chan, "Water Control Diagnostic Plots," in *SPE Annual Technical Conference and Exhibition*, Dallas, 1996.

[11] A. Hasan, C. Kabir and M. Sayarpour, "Simplified two-phase flow modeling in wellbores," *Journal of Petroleum Science and Engineering,* vol. 72, pp. 42-49, 2010.

[12] V. Bondar and T. Blasingame, "Analysis and Interpretation of Water Oil Ratio Performance," in *SPE Annual Technical Conference and Exhibition*, San Antonio, 2002.

[13] L. kappos, M. J. Economids and R. Buscaglia, "A Holistic Approach to Back Allocation of Well Production," in *SPE Reservoir Characterisation and Simulation Conference and Exhibition*, Abu Dhabi, 2011.

[14] M. McCracken and D. Chorneyko, "Rate Allocation Using Permanent Downhole Pressures," in *SPE Annual Technical Conference And Exhibition*, San Antonio, Texas, 2006.

[15] M. Hamad, S. Sudharman and A. Al-Mutairi, "Back Allocation System with Network Visualization," in *SPE International Petroleum Exhibition and Conference*, Abu Dhabi, 2004.

[16] H. Prabowo and M. Rinadi, "A production Allocation Method for Commingled Gas Completions," in *Internatiinal Meeting on Petroleum Engineering*, Beijing, 1995.

[17] M.Ibrahim, "Optimum Allcation Method for Gas Condensate Wells," in *SPE Annual Technical Conference and Exhibition*, Marrakech, 2008.

[18] N. Ezkewe, "Petroleum Reservoir Engineering Practice," in *Petroleum Reservoir Engineering Practice*, Boston, Pearson Education Inc, 2011.

[19] T. Ahmed, Reservoir Engineering Handbook, USA: Gulf Professional Publishing , 2006.

[20] J. W. Crafton, "Oil and Gas Well Evaluation Using the Reciprocal Productivity Index Method," in *Production Operations Symposuim*, Oklahoma, 1997.

[21] L. Mattar and D. Anderson, "A systematic and Comprehensive Methotodology for Advanced Analysis of Production Data," in *SPE Annual Technical Conference and Exhibition*, Denver, 2003.

[22] T. Unneland, Y. Manin and F. Kushuk, "Permanent Gaige Pressure and Rate measurments of Reservoir Desciption and Well monitoring: Field Cases," in *SPE Annual Technical Conference and Exhibition* , San Antonio, 1998.

[23] W.-C. Chu and J. Steckhan, "A practical Approach to Determine Low-Resistivity Pay in Clastic Reservoirs," in *SPE Annual Technical Confernce and Exhibition*, Denver, 2011.